

SEP 24 1968

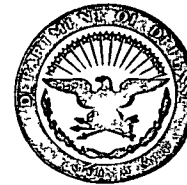
UNCLASSIFIED

AD 291783 ✓

Reproduced  
by the

MASTER

ARMED SERVICES TECHNICAL INFORMATION AGENCY  
ARLINGTON HALL STATION  
ARLINGTON 12, VIRGINIA



UNCLASSIFIED

## **DISCLAIMER**

**This report was prepared as an account of work sponsored by an agency of the United States Government. Neither the United States Government nor any agency Thereof, nor any of their employees, makes any warranty, express or implied, or assumes any legal liability or responsibility for the accuracy, completeness, or usefulness of any information, apparatus, product, or process disclosed, or represents that its use would not infringe privately owned rights. Reference herein to any specific commercial product, process, or service by trade name, trademark, manufacturer, or otherwise does not necessarily constitute or imply its endorsement, recommendation, or favoring by the United States Government or any agency thereof. The views and opinions of authors expressed herein do not necessarily state or reflect those of the United States Government or any agency thereof.**

## **DISCLAIMER**

**Portions of this document may be illegible in electronic image products. Images are produced from the best available original document.**

NOTICE: When government or other drawings, specifications or other data are used for any purpose other than in connection with a definitely related government procurement operation, the U. S. Government thereby incurs no responsibility, nor any obligation whatsoever; and the fact that the Government may have formulated, furnished, or in any way supplied the said drawings, specifications, or other data is not to be regarded by implication or otherwise as in any manner licensing the holder or any other person or corporation, or conveying any rights or permission to manufacture, use or sell any patented invention that may in any way be related thereto.

291 //83

TECHNICAL INFORMATION SERIES

CATALOGED BY ASTIA 291783  
AS IND 13

R62SD83

THERMODYNAMIC CONSIDERATIONS  
FOR MHD SPACE POWER SYSTEMS

S.I.FREEDMAN



SPACE SCIENCES LABORATORY

GENERAL  ELECTRIC

MISSILE AND SPACE DIVISION

# SPACE SCIENCES LABORATORY

## AEROPHYSICS OPERATION

### THERMODYNAMIC CONSIDERATIONS FOR MHD SPACE POWER SYSTEMS

by

**Steven I. Freedman, Consultant\***  
Magneto hydrodynamic Power Generation

This work was performed for the U. S. Office  
of Naval Research under Contract No. Nonr-3867( 00).  
Reproduction in whole or in part is permitted for any  
purpose of the United States Government.

R62SD83 - Class I  
September, 1962

\* Also Asst. Professor of Mechanical Engineering,  
Massachusetts Institute of Technology, Cambridge, Mass.

**MISSILE AND SPACE VEHICLE DEPARTMENT**

**GENERAL  ELECTRIC**

## ABSTRACT

Thermodynamic efficiencies and radiator sizes of Brayton Cycle MHD generator systems, with and without regenerators, were obtained. A new gas cycle, the Tri-Cycle, was synthesized. The Tri-Cycle has a radiator size as small as the regenerative Brayton Cycle, but a higher pressure ratio. A new cycle was discovered which operates on a dissociating chemical reaction and combines the advantages of a dry gas expansion, a liquid compression, and a Rankine Cycle size radiator.

Entropy generation in supersonic MHD generators was analyzed, the polytropic efficiency was related to the generator operating parameters.

Transient boil-off and refrigeration techniques were examined. Multiple radiation shield insulation thicknesses were computed. An optimum temperature ratio for heat rejection from an active refrigeration system was found for superconducting magnets.

# CONTENTS

	PAGE
Abstract	i
Table of Contents	ii
List of Figures	iii
GAS CYCLES	1
Brayton Cycle	1
Brayton Cycle with a Regenerator	5
Radiator and Regenerator Weights	9
Tri-Cycle Power Cycle	11
Isothermal Compression	11
Isothermal Expansion	13
The Possibility of Foam MHD Generators	16
Dissociation Cycle Description	17
Thermodynamics of the LiH Dissociation Cycle	20
ENTROPY INCREASE IN SUPERSONIC MHD GENERATORS	24
Generator Performance	24
The Entropy Gain in Subsonic and Supersonic Diffusers	26
The Overall Generator Efficiency	27
THERMAL INSULATION AND BOIL-OFF RATES FOR SUPERCONDUCTING MAGNET CRYOGENIC TANKS	30
Multiple Radiation Shields	30
Transient Boil-Off Protection Superinsulation	33
Multiple Radiation Shield Insulation	36
Active Refrigeration	37
Optimum Heat Rejection Temperature	38
THE INFLUENCE OF NON-CARNOT PERFORMANCE ON THE TEMPERATURE RATIO OF VAPOR CYCLES	41
Summary	44
Bibliography	46

## LIST OF FIGURES

<u>Figure No.</u>	<u>Title</u>
1	The Brayton (Gas Turbine) Cycle
2 (a), (b), (c), (d), (e)	Dimensionless Radiator Size Parameter as a Function of the Generator Temperature Ratio for the Direct Brayton Cycle . Lines of Constant Generator Efficiency and Compressor Inlet Temperature Ratio for Constant Compressor Efficiency.
3 (a), (b)	Dimensionless Radiator Size Parameter as a Function of the Generator Temperature Ratio for the Direct Brayton Cycle. Lines of Constant Compressor Efficiency and Compressor Inlet Temperature Ratio for Constant Generator Efficiency.
4	Dimensionless Radiator Size Parameter as a Function of Compressor Inlet to Turbine Inlet Temperature Ratio for the Direct Brayton Cycle . Lines of Constant Component Efficiency and Turbine Temperature Ratio.
5	Cycle Pressure Ratio as a Function of Turbine Temperature Ratio for Various Values of the Isentropic Exponent $\gamma = c_p/c_v$ .
6	The Regenerative Brayton (Gas Turbine) Cycle.
7 (a), (b)	Radiator Size Parameter of a Brayton Cycle with a Regenerator as a Function of the Turbine Temperature Ratio for Various Component Efficiencies.
8	Radiator Size Parameter of a Brayton Cycle with a Regenerator, as a Function of the Compressor Inlet to Turbine Inlet Temperature Ratio for Various Component Efficiencies.
9(a) 9(b)	The Stirling Cycle The Ericsson Cycle
10 (a)	Isothermal Compression Tri-Cycle
10 (b)	Isothermal Expansion Tri-Cycle
11	The Efficiency of a Reversible Isothermal Compression Tri-Cycle as a Function of the Temperature and Pressure Ratios.
12	The Radiator Parameter of a Reversible Tri-Cycle with Isothermal Compression as a Function of the Temperature and Pressure Ratios.

<u>Figure No.</u>	<u>Title</u>
13	Radiator Parameter of a Reversible Tri-Cycle with Isothermal Compression as a Function of the Thermodynamic Efficiency.
14	Pressure Ratio as a Function of Expansion Temperature Ratio.
15	Efficiency of an Isothermal Compression Tri-Cycle with 90% Efficient Components, as a Function of the Temperature and Pressure Ratios.
16	Radiator Parameter of an Isothermal Compression Tri-Cycle with 90% Efficient Components, as a Function of the Temperature and Pressure Ratios.
17	Radiator Parameter of an Isothermal Compression Tri-Cycle with 90% Efficient Components, as a Function of the Cycle Efficiency.
18	The Efficiency of a Reversible Tri-Cycle with Isothermal Expansion as a Function of the Temperature and Pressure Ratios.
19	The Radiator Parameter of a Reversible Tri-Cycle with Isothermal Expansion as a Function of the Temperature and Pressure Ratios.
20	The Radiator Parameter of a Reversible Tri-Cycle with Isothermal Expansion as a Function of the Cycle Efficiency.
21 (a), (b), (c), (d), (e), (f), (g)	The Efficiency of Irreversible Isothermal Expansion Tri-Cycles as a Function of the Temperature and Pressure Ratios.
22 (a), (b), (c), (d)	Radiator Parameter of Irreversible Isothermal Expansion Tri-Cycle as a Function of the Temperature and Pressure Ratios.
23 (a), (b), (c), (d)	Radiator Parameter of Irreversible Isothermal Expansion Tri-Cycle as a Function of the Cycle Efficiency.
24	LiH Dissociation Cycle
25	Stagnation and Local Temperature Described States in a MHD Generator.
26	Temperature-Entropy Triangle.

<u>Figure No.</u>	<u>Title</u>
27	Percent of Stagnation Pressure Lost in Compressible Flow Diffusers as a Function of the Diffuser Mach Number.
28	Overall Efficiency as a Function of Loading Factor for Various Mach Numbers and Temperature Ratios.
29	Radiative Heat Fluxes Between Parallel Planes
30 (a)	Ribbon Wound on Pins Type of Construction
30 (b)	Fiber Spacer Construction
31	Mechanical Refrigeration Efficiency as a Function of Temperature.
32	Temperature Ratio for Minimum Area Radiator as a Function of the Mechanical Efficiency of the Power Converter.
33	Thermodynamic Efficiency of a Power Cycle for Minimum Radiator Size as a Function of Mechanical Efficiency.
34	Radiator Size Parameter, $Z = \sigma T_{\max}^4 A/P$ , for Minimum Radiator Size as a Function of Mechanical Efficiency.
35	Radiator Size as a Function of $\theta$ for Two Values of the Mechanical Efficiency.

## GAS CYCLES

### Brayton Cycle

The basic gas cycle for steady flow power production is the Brayton Cycle<sup>(1)\*</sup>.

This cycle consists of an adiabatic compressor, a heat exchanger or combustion chamber in the case of an open cycle, an adiabatic turbine, and another heat exchanger. The MHD generator replaces the turbogenerator as is found in conventional closed cycle gas turbine power producers. Jet engines and open cycle gas turbines operate on this cycle; however, the heat rejection is replaced by the discharge of the hot exhaust gas into the atmosphere. Since the assumption of constant specific heat is valid for the monatomic gases which are likely to be used in nuclear reactor heated MHD generator closed gas cycles, the T-S diagram and the Mollier chart (H-S diagram) have identical form. The cycle is shown in Figure 1.

Process 0-3 represents the MHD generator: 0-1 is the supersonic nozzle, 1-2 the generator section, and 2-3 the diffuser. Process 3-4 is the heat rejection process, assumed at constant pressure. Process 4-5 is the adiabatic compressor and 5-0 is the heater. Primed states refer to states of the working fluid which would exist if the devices were reversible, and operated between the same pressures as the actual components.

---

\* Numbers in parentheses refer to items in the bibliography.

The efficiency of the cycle is obtained from the definition:

$$\eta = \frac{\text{Work}_{\text{net}}}{\text{Heat in}}$$

Since  $c_p$  is constant

$$\eta = \frac{(T_o - T_3) - (T_5 - T_4)}{T_o - T_5}$$

$$\eta = 1 - \frac{T_3 - T_4}{T_o - T_5}$$

The generator and compressor efficiencies are

$$\eta_g = \frac{T_o - T_3}{T_o - T_3'}$$

$$\eta_c = \frac{T_5' - T_4}{T_5 - T_4}$$

The pressure ratios across the compressor and turbine are assumed equal. Hence the isentropic temperature ratios are also equal.

$$\frac{T_5'}{T_4} = \frac{T_o}{T_3'}$$

The compressor temperature ratio becomes

$$\frac{T_5}{T_4} = \frac{(\eta_c - 1 + T_o/T_3')}{\eta_c}$$

The generator temperature ratio is

$$\frac{T_3'}{T_0} = \frac{(\eta_g - 1) + T_3/T_0}{\eta_g}$$

yielding

$$\frac{T_5}{T_4} = \frac{1}{\eta_c} \left( \eta_c - 1 + \frac{\eta_g}{\eta_g - 1 + T_3/T_0} \right)$$

The efficiency can now be evaluated as

$$\eta = 1 - \frac{\eta_c (T_3/T_4 - 1)}{\frac{\eta_c T_0/T_4 - \eta_c + 1 - \eta_g}{\eta_g - 1 + T_3/T_0}}$$

The power generated and the heat rejected are

$$P = \eta Q_{in}$$

$$Q_R = (1 - \eta) Q_{in} = \frac{(1 - \eta)}{\eta} P$$

The heat rejection radiates at a rate per unit of length

$$-\dot{m} c_p dT = \sigma \Phi \epsilon T^4 dA$$

It is assumed that the radiator is black and that there are no fins, hence  $\epsilon = \Phi = 1$ . Non-ideal emissivity and finite length fins result in the actual area exceeding the effective area. Since the emissivity is a surface property and  $\Phi$  is a geometric property, it is assumed that in the comparison of various cycles that the

values of  $\epsilon$  and  $\Phi$  will lie in a narrow range and that the effective area will be a valid criteria on which to judge radiator size and weight; that is,

$$A_{\text{effective}} = A = \Phi \epsilon A_{\text{actual}}$$

Integration of  $dA$  yields

$$\frac{1}{3} \left( \frac{1}{T_4}^3 - \frac{1}{T_3}^3 \right) = \frac{\sigma A}{\dot{m} c_p}$$

Referring the heat rejected to the thermal limited portion of the cycle establishes the top temperature as the appropriate variable in the dimensionless radiator size parameter,  $Z$ , given by:

$$Z = \frac{\sigma T_0^4 A}{P}$$

The heat rejected is

$$Q_R = \dot{m} c_p (T_3 - T_4)$$

The radiator parameter  $Z$  becomes

$$Z = \frac{\left( \frac{T_0}{T_4}^4 \right) \left( 1 - \left( \frac{T_4}{T_3}^3 \right) \right)}{\left( \frac{T_3}{T_4} - 1 \right)} \frac{(1 - \eta)}{3 \eta}$$

Plots of  $Z$  as a function of  $T_4/T_0$  and  $T_3/T_0$  for various values of  $\eta_c$  and  $\eta_g$  are shown in Figures 2, 3, and 4.

The resulting pressure ratios for various gases can be found from Fig. 5, which

shows the pressure ratio as a function of  $T_3/T_0$  for various values of  $\gamma$ , the ratio of the specific heats.

It is noted that typical component efficiencies,

$$\eta_g = \eta_c = 0.85$$

give a minimum value of  $Z$  of 80. A turbo-alternator generation system might have an efficiency of 90%, which would result in a  $Z$  of 70. A typical minimum value of  $Z$  can be selected of 75.

This value of  $Z$ , the dimensionless radiator size parameter of 75, is much higher than the value of 15 found for a Rankine Cycle. Equal radiator weights will occur when the top temperatures are in the ratio:

$$\frac{T_{\text{gas}}}{T_{\text{Rankine}}} = \left( \frac{Z_{\text{gas}}}{Z_{\text{Rankine}}} \right)^{1/4}$$

The ratio of the minimum  $Z$ 's is 5. The ratio of the top temperatures are then 1.495.

It is a materials evaluation question as to whether or not an inert (or other) gas can be heated in a nuclear reactor to an absolute temperature  $1 \frac{1}{2}$  times as large as that permissible for boiling a liquid metal.

#### Brayton Cycle With a Regenerator

A regenerative heat exchanger can be added to preheat the compressed gas using the hot exhaust gas. Such a cycle is shown in Fig. 6. General surveys of actual and predicted performance of Brayton Cycle power plants are in good agreement (2), (3), (4).

It is assumed that the temperature difference across the regenerator is small compared with temperature difference between the inlet and exit of either side of the regenerator. A  $50^{\circ}\text{F}$   $\Delta T$  across a regenerator is reasonable and  $1000^{\circ}\text{F}$  to  $1200^{\circ}\text{F}$  are typical changes in temperature accompanying the heating. The cycle radiator size is computed as follows:

$$\begin{aligned} Q_{in} &= T_0 - T_6 \\ Q_{out} &= T_7 - T_4 \\ T_6 &= T_3 - \Delta T_{\text{gas-gas}} \\ T_7 &= T_5 + \Delta T_{\text{gas-gas}} \end{aligned}$$

Assuming a regenerator effectiveness of unity,

$$\Delta T_{\text{gas-gas}} = 0$$

$$T_6 = T_3$$

$$T_7 = T_5$$

The net heat added is

$$Q_{\text{net}} = (T_0 - T_3) - (T_5 - T_4)$$

The net heat equals the net work. The efficiency is therefore

$$\eta = \frac{(\text{Work})_{\text{net}}}{Q_{in}}$$

$$\eta = \frac{(T_0 - T_3) - (T_5 - T_4)}{T_0 - T_3}$$

$$\eta = \frac{1 - T_5 - T_4}{T_0 - T_3}$$

The compressor and generator efficiencies are

$$\eta_c = \frac{T_5' - T_4}{T_5 - T_4}$$

$$\eta_g = \frac{T_o - T_3}{T_o - T_3'}$$

It is assumed that the pressure drop in the heat exchanger is small enough so that the pressure ratio is the same across the compressor and generator. Hence the isentropic temperature ratios are also equal.

$$\frac{T_5'}{T_4} = \frac{T_o}{T_3'}$$

The temperature ratio across the compressor becomes

$$\frac{T_5}{T_4} = \frac{1}{\eta_c} \left( \eta_c - 1 + \frac{T_o}{T_3'} \right)$$

and across the generator

$$\frac{T_3'}{T_o} = \frac{\eta_g - 1 + T_3/T_o}{\eta_g}$$

The efficiency can now be evaluated as

$$\eta = 1 - \frac{1 - T_3/T_o}{\left( \frac{\eta_g - 1 + T_3}{T_o} \right) \eta_c \left( \frac{T_o}{T_4} - \frac{T_3}{T_4} \right)}$$

The radiator area parameter  $Z$  is computed in the same manner as for the direct Brayton Cycle. Heat is only rejected between  $T_5$  and  $T_4$ .

$$\frac{1}{3} \left( \frac{1}{T_4^3} - \frac{1}{T_5^3} \right) = \frac{\sigma A}{\dot{m} c_p}$$

The radiator area parameter becomes

$$Z = \frac{\sigma A T_0^4}{P}$$

$$Z = \frac{T_0^4}{T_4} \frac{\left(1 - \left(\frac{T_4}{T_5}\right)^3\right)}{\left(\frac{T_5}{T_4} - 1\right)} \frac{(1 - \eta)}{3\eta}$$

Figures 7 and 8 show  $Z$  as a function of  $T_3/T_0$  and  $T_4/T_0$ . The minimum value of  $Z$  for the same typical component efficiencies as were chosen for the direct Brayton Cycle is 40. Thus it is seen that the regenerator essentially cuts the radiator in half. The reason why a larger savings is not made is because the cold part of the radiator is the largest, and the regenerator cannot cool the working fluid below the compressor discharge temperature. The compressor inlet temperature is again around 40% to 45% of the hottest temperature of the cycle. However, the component temperature ratios have come closer to unity, making the pressure ratio smaller.

Considering the difficulties of operating power generation equipment, especially MHD generators, on small pressure ratios, it is questionable as to the actual advantage of installing the regenerator.

### Radiator and Regenerator Weights

The relative weights of the regenerator and radiator can be estimated from the expected heat transfer rates and actual sizes. The weight-to-heat transfer ratio of the radiator is determined by the size of the meteor protection material. Typical sizes for aluminum tubes for megawatt generators range in size, with a typical value being 1/4 inch. The regenerator can be fabricated from thin tubes since the pressure difference across them is small and there is no meteor hazard. A typical tube wall size is assumed to be 0.025. The weights of the radiator and exchanger are proportional to the thickness of the wall and the wall area. The area is determined by the heat transfer coefficient and the temperature difference between the wall and the heat absorption medium. The weight of the radiator and exchanger for the same heat transfer is proportional to

$$\frac{\rho t}{h \Delta T}$$

where  $(h \Delta T)_R = h \Delta T_{\text{gas-wall}} = \frac{h \Delta T}{2} \text{ gas-gas}$

since

$$\sigma T^4 \gg h \Delta T$$

Thus the weight ratio is

$$\left( \frac{\rho t}{h \Delta T} \right)_R \quad \diagup \quad \left( \frac{\rho t}{h \Delta T} \right)_X$$

Numerical estimates of typical conditions are

$$\rho_{Al} = 170 \text{#/ft}^3$$

$$\rho_{st} = 490 \text{#/ft}^3$$

$$t_R = 1/4" = \frac{1}{48} \text{ ft.}$$

$$t_X = 1/40" = \frac{1}{480} \text{ ft.}$$

$$h \Delta T = (10)(50) = 500$$

$$\sigma T_R^4 = 0.171 \times 10^{-8} \times (1500)^4$$

$$= 8500 \text{ BTU/Hr Ft}^2 \rightarrow h \Delta T$$

therefore

$$\frac{W_R}{W_X} \approx 7$$

It is seen that the radiator weight per BTU transferred is 7 times that of the generator.

### Tri-Cycle Power Cycle

A novel power cycle is the Tri-Cycle. The unique features of the Tri-Cycle are the isothermal expansion or compression. The Stirling and Ericsson Cycles are cycles with both isothermal compression and expansion, at constant volume and pressure respectively, see Fig. 9. Both these cycles could have Carnot efficiency if all the component processes were reversible and if an ideal heat exchanger were used between the two constant temperature processes. These cycles are currently being examined elsewhere in conjunction with engine development for space power generation<sup>(5), (6)</sup>. The Tri-Cycle being considered here consists of only one isothermal process, the others being conventional isentropic and isobaric.

The isothermal compression of a gas is a highly desirable but very difficult process to accomplish in steady flow. The slow compression of a wet vapor can approach isothermal conditions. Gas turbines would perform much better if isothermal compression were possible. Even though no known method exists for isothermal compression, it is included here for the sake of completeness.

The thermodynamics of Tri-Cycles fall into two categories, isothermal expansion and compression. The ideal Tri-Cycles are shown in Fig. 10.

#### Isothermal Compression

The thermodynamics of the operation of isothermal compression Tri-Cycle is as follows. The heat added during the constant pressure heating is:

$$Q_{in} = c_p(T_h - T_c)$$

\* There is a slight possibility that an ejector using a wet vapor, with subsequent condensation of the vapor, could act as an isothermal compressor.

The work produced in the adiabatic expansion is

$$W = \eta_g c_p T_h (1 - 1/B)$$

where

$$B = T_h/T_{cs} = (p_h/p_l) \frac{\gamma-1}{\gamma}$$

The work consumed by the isothermal compression is

$$W = \frac{-RT_c \ln p_h/p_l}{\eta_c}$$

The thermodynamic cycle efficiency becomes

$$\eta = \frac{W_{net}}{Q_{in}}$$

$$\eta = 1 - \frac{\left(\frac{1}{\eta_g} - 1 + \frac{1}{B}\right) \ln B}{\eta_c \left(1 - \frac{1}{B}\right)}$$

The efficiency of the reversible Tri-Cycle with isothermal compression is

$$\eta = 1 - \frac{\ln B}{B-1}$$

The expression for Z for the reversible Tri-Cycle is

$$Z = \frac{B^4 \ln B}{B-1-\ln B}$$

The radiator area parameter, Z, for a Tri-Cycle with irreversible components is

$$Z = \frac{(1-\eta)}{\eta} B^4$$

Values of  $\eta$  and Z for the reversible Tri-Cycle with isothermal compression are shown

in Figs. 11, 12, and 13 as functions of the expansion temperature and pressure ratios.

Fig. 14 shows the pressure ratio is a function of the temperature ratio for values of 1.4 and 1.67. Figs. 15, 16, and 17 show the efficiency and radiator size parameter as functions of each other and of the temperature and pressure ratios for component efficiencies of 0.9. It is noted that component efficiencies about 0.87 and below result in negative efficiencies and hence cannot produce power.

### Isothermal Expansion

The thermodynamics of the isothermal expansion Tri-Cycle are as follows:

The heat added during the isothermal expansion is

$$Q_{in} = T_h \Delta S - (1 - \eta_g) c_p T_h \ln B$$

where  $\Delta S = -R \ln p_i / p_h$

$$\Delta S = c_p \ln B$$

where  $B$  is again the isentropic temperature ratio corresponding to the actual pressure ratio

$$B = \left( \frac{p_h}{p_i} \right)^{\frac{\gamma-1}{\gamma}}$$

The heat input then becomes

$$Q_{in} = \eta_g c_p T_h \ln B$$

The expansion work is

$$W = \eta_g R T_h \ln p_h / p_i$$

$$W = \eta_g c_p T_h \ln B$$

The work of compression is

$$W_c = c_p \frac{T_c(B-1)}{\eta_c}$$

$$W_c = \frac{c_p (B-1) T_h}{(B-1 + \eta_c)}$$

The efficiency becomes

$$\eta = \frac{W_{net}}{Q_{in}}$$

$$\eta = 1 - \frac{1}{\eta_g \ln B (1 + \frac{\eta_c}{B-1})}$$

The efficiency of the reversible Tri-Cycle becomes

$$\eta_R = 1 - \frac{B-1}{B \ln B}$$

The radiator parameter Z is evaluated in a manner similar to that used in the  
Brayton Cycle. Integrating the first law and black radiation rate results in

$$\begin{aligned} \frac{1}{T_c} - \frac{1}{T_n} &= \frac{3 \sigma A}{\dot{m} c_p} \\ &= \frac{3 \sigma A \eta (T_h - T_c)}{P (1 - \eta)} \end{aligned}$$

Evaluating Z yields

$$Z = \frac{\sigma T_h^4 A}{P}$$

$$Z = \frac{\frac{(1-\eta)}{3} \left( \left( \frac{T_h}{T_c} \right)^3 - 1 \right)}{\left( 1 - \frac{T_c}{T_h} \right)}$$

The temperature ratio is related to the pressure ratio by the isentropic relationship and the definition of the compressor efficiency.

$$\frac{T_h}{T_c} = \left( \frac{B-1}{\eta_c} \right) + 1$$

since

$$B = \frac{T_{hs}}{T_c} = \left( \frac{P_h}{P_l} \right)^{\frac{\gamma-1}{\gamma}}$$

and

$$\eta_c = \frac{T_{hs} - T_c}{T_h - T_c}$$

Therefore Z is

$$Z = \frac{\frac{(1-\eta)}{3\eta} \left( \left( \frac{B-1}{\eta_c} + 1 \right)^3 - 1 \right)}{(B-1)} (B-1 + \eta_c)$$

Figs. 18, 19, and 20 show the efficiency and radiator size of a reversible Tri-Cycle with isothermal expanding temperature and pressure ratios, and of each other. It is seen

that the radiator size is about half that of the radiator of the reversible compression Tri-Cycle, indicating a considerable weight saving.

Figs. 21, 22, and 23, the efficiency and radiator size of isothermal expansion Tri-cycles with irreversible components. It is seen that such cycles produced power even when the components have efficiencies as low as 70%, indicating the feasibility of such cycles. The radiator parameter at these values of component efficiencies is comparable with those of the Brayton Cycle. Foam MHD generators operating as isothermal expansion Tri-cycles are capable of favorable operation.

The higher efficiencies and lower values of  $Z$  are in part caused by the fact that all of the irreversibilities in the expansion process appear as reductions in the amount of heat which has to be added. This built-in reheat factor greatly enhances the isothermal expansion Tri-Cycle. It is to be noted that this cycle can be approximated by a foam MHD generator built internally in a nuclear reactor.

#### The Possibility of Foam MHD Generators

Before the advent of MHD power generation, isothermal expansion was as idealized a process as isothermal compression. It appears possible to build an isothermal expansion MHD generator by expanding a foamed liquid metal in a combined nuclear reactor and MHD generator. Such a device would utilize the high electrical and thermal conductivities of the continuous metallic matrix while still utilizing the compressibility of the gas. High velocities can be obtained by having only gas touch the walls, thereby avoiding the large viscous forces associated with condensed phases. Foams may be made in any of three ways.

One way to produce a foam is by the expansion of a saturated liquid to a lower pressure. The liquid would proceed to boil, with the bubbles hopefully uncoalesed. Expansion of a saturated vapor into the two-phase region is also possible, however, it is highly difficult to obtain a foam at the small percentages of moisture which would result.

A second method of foaming is by injecting a condensable vapor into a liquid metal. The vapor must be condensable in order to eventually pump the mixture (or separate substances), back up to the high pressure before expansion without an undue amount of work. Foam pumps are highly inefficient and extremely difficult to operate. The easiest way to compress the working substance in a foam MHD generator is to condense to vapor portion of the foam, separate the two fluids and then pump the resulting liquids. Simple two-fluid foamable and condensable pair of substances include the combination of mercury (with appropriate wetting agent) and water, or dow-therm, or organic liquids.

#### Dissociation Cycle Description

Space power conversion systems are faced with an additional thermal limitation besides those which confront ordinary ground based systems. This is the radiator size and weight. A one megawatt power generator operating on a Carnot cycle with a minimum size constant temperature black radiator will require 1250 ft.<sup>2</sup> of radiating area when the maximum temperature of the working fluid is 2000°R. Since non-isothermal fins will be used to reduce the radiator weight, power plants in the 10 to 20 MW range will have heat rejection radiators approaching a football field in size. Hence, engineers

have sought power cycles with high component efficiency, and high working fluid temperature levels. Most of these cycles have been based on the Rankine and Brayton cycles.

Metallic vapor Rankine cycles using vapor turbines suffer from the corrosive effects of the hot reactive metals and the wet vapor in the turbine, and the bearing problem. Brayton cycles suffer from the increased size of the radiator due to the variable temperature of heat rejection and the problems associated with hot rotating machinery. The use of a MHD generator in place of the turbo-alternator can eliminate the hotter rotating machine but still leaves the compressor problem. A more desirable cycle would have the compression portion of the cycle operate on a condensed phase, possibly an electrically conducting fluid which would permit the use of an electromagnetic pump with no moving parts, while still retaining a dry, and non-corrosive gas during the expansion portions of the cycle. Such a cycle has been found.

The cycle is based on the thermal decomposition of a metal hydride (LiH in particular). Metallic hydrides are electrical conductors in the molten phase, decompose to give off hydrogen, and recombine readily. A schematic diagram of a simple lithium hydride cycle is shown in Fig. 24.

The pressure of hydrogen over a Li-LiH mixture at  $1610^{\circ}\text{F}$  is one atmosphere (9). At this temperature a mixture of lithium and lithium hydride will change from a 25% to a 95% fraction of lithium to hydrogen atoms when heated. The difference in the hydrogen atoms percentage goes into gaseous hydrogen. At the melting point of LiH ( $1270^{\circ}\text{F}$ ), the dissociation pressure is 0.64 psia. A dissociation pressure of 1 psia occurs at

1310°F. Thus lithium hydride can be "boiled" at 1610°F and "condensed" at 1310°F with a pressure ratio of the hydrogen vapor of 14.7:1. Such a pressure ratio permits the use of either a gas turbine or a MHD generator. These temperatures appear feasible for a high performance high temperature alloy gas turbine. Considering that only a limited number of turbines (compared to jet engines) will be required for space flight, more expensive alloys may be allowable for the high temperature blades. While these temperatures may appear low for MHD generators, superheating the hydrogen above 1610°F to temperatures where the hydrogen (plus seeding material) becomes electrically conducting is more favorable than with corrosive metals and metallic vapors. Also, MHD generators may be operable with magnetically induced non-thermal conductivity at these low temperatures.

At 1610°F, 26,418 BTU/#H<sub>2</sub> will be required to decompose the lithium hydride. A 75% efficiency generator or turboalternator operating on a 14.7 pressure ratio on hydrogen entering at 1610°F produces 2961 BTU/#H<sub>2</sub> of work, assuming a constant  $\gamma$  of 1.4 and using the enthalpy change of the hydrogen based on spectroscopic measurements of the specific heat. The hydrogen emerges from the generator at 777°F. The 1610°F Li (with about 10% LiH) is taken from the separator following the boiler and flows into a combined condenser and radiator. This can be accomplished by a distributed injection of the hydrogen into the lithium as it passes through the radiator. The radiator will reject about 23,460 BTU/#H<sub>2</sub>. A 50% efficient EM pump will require 1.2 BTU/#H<sub>2</sub> to pump the LiH back up to atmospheric pressure. The 14.7 psia of the lithium entering the radiator is used to overcome viscous losses and to establish a low pressure by an

ejector configuration wherever the hydrogen enters the radiator.

The net efficiency of such a cycle is 11.2%. The radiator area parameter is

$$Z = \sigma T_h^4 A/P.$$

This value of Z is 16.28, comparable with the value of 16 for a Rankine Cycle, and is much better than the value of 75 which appears minimum for a Brayton Cycle with slightly optimistic components and 40 for a Brayton Cycle with similar components including a regenerator. It is to be noted that the radiators of a Rankine Cycle and a lithium hydride cycle will be the same when

$$\frac{T_{LiH}}{T_R} = \left( \frac{Z_{LiH}}{Z_R} \right)^{1/4}$$

The LiH cycle will have a top temperature only 15°F hotter than a Rankine Cycle having the same radiator area. This advantage of going to a dry vapor such as hydrogen should outweigh the 15°F temperature rise.

#### Thermodynamics of the LiH Dissociation Cycle

The enthalpy of formation of LiH (solid) from Li(solid) and H<sub>2</sub> (gas) at 298.16°K is -21.61 kcal/gm mole<sup>(7)</sup>. The decomposition of LiH at 77°F requires 38,900 BTU/#H<sub>2</sub> at 77°F. Calling solid LiH the reactant and the combination of solid Li and gaseous H<sub>2</sub> the product of dissociation, the change in latent heat of phase change is

$$\frac{dL}{dT} = (c_p)_p - (c_p)_R + \left[ (\mu c_p)_p - (\mu c_p)_R \right] \frac{dp}{dT}$$

where

$$\mu c_p = - \left( \frac{\partial h}{\partial p} \right) T$$

The hydrogen will always be at a pressure low enough (less than 1 atm.) so that it behaves as a perfect gas, hence the Joule-Thomson coefficient of the gas will be very near zero. The enthalpy of condensed phases have been assumed to be independent of the pressure.\* This latter assumption probably induces errors of up to 10% in changes in the latent heat of phase change, but requires additional accurate thermodynamic data in order to be properly computed. The change in the latent heat is therefore approximated by

$$\frac{dL}{dT} = (c_p)_p - (c_p)_R$$

Over the range from 77°F to 1610°F, we obtain

$$\frac{\Delta L}{\Delta T} = \Delta H_p - \Delta H_R$$

where  $\Delta H$  is the change in enthalpy excluding chemical change. The enthalpy changes between 77°F and 1610°F including the melting LiH are shown in Table I (8), (9).

TABLE I

<u>Substance</u>	<u><math>H</math>(BTU/#H<sub>2</sub>)</u>
H <sub>2</sub>	5,384
Li	11,930
LiH	28,796

Thus, it requires 26,418 BTU/#H<sub>2</sub> to decompose LiH at 1610°F, which is supplied in the

\* For liquid water between 200°F and 300°F  $\mu c_p$  dp/dT is 0.168 BTU/#, which is 25% of  $\mu c_p$ .

boiler.

The hydrogen expands in the generator at an (assumed) polytropic efficiency of 75%. The temperature difference assuming a constant ratio specific heat of 1.4 is

$$\Delta T = \eta_g T_{in} \left( 1 - \left( \frac{1}{P} \right)^{\frac{\gamma-1}{\gamma}} \right)$$

where  $P$  is the pressure ratio, 14.7 in this case. For these conditions  $\Delta T = 833^{\circ}\text{F}$ .

The generator then discharges hydrogen at  $777^{\circ}\text{F}$ . The net work produced is 2961 BTU/#H<sub>2</sub>.

Since the radiator discharges the LiH at  $1270^{\circ}\text{F}$  the LiH must be heated to  $1610^{\circ}\text{F}$ .

It is possible to partially accomplish this by use of a regenerator using the molten lithium emerging from the separator, however, the additional piping may not become justified on a weight basis. The enthalpy to be added to the feed LiH by a preheater operating between  $1270$  and  $1610^{\circ}\text{F}$  is 5046 BTU/#H<sub>2</sub>. The preheater operating with a  $20^{\circ}\text{F}$  temperature difference regenerator would save 2221 BTU/#H<sub>2</sub>. The pump work is  $\Delta p / \eta_p$ , which is 1.2 BTU/#H<sub>2</sub> for a 50% efficient pump.

The thermodynamic efficiency becomes

$$\eta = \frac{2960}{26,418 + 5046} = 0.112$$

The radiator area parameter  $Z$  is

$$Z = \sigma T_h^4 A/P$$

$$Z = (1 - \eta) / \eta \theta^4$$

where  $\theta$  is the temperature ratio

$$\theta = T_c/T_h$$

The numerical value of  $Z$  is 16.28.

## ENTROPY INCREASE IN SUPERSONIC MHD GENERATORS

### Generator Performance

There are three sources of entropy increase in supersonic MHD generators, joule heating, diffuser losses, and boundary layer phenomena. It is assumed that the MHD interaction parameter is much larger than the friction factor and Stanton number so that boundary layer phenomena can be neglected compared with the other sources of irreversibilities.

The loading factor  $K$ , which is the ratio of the voltage across the electrodes to the open circuit voltage, is the local efficiency of the MHD generator as seen by an observer moving with the gas. The usual thermodynamic definition of efficiency is based on the work obtained during processes between stagnation states. Since the complete MHD generator includes the nozzle and diffuser, the thermodynamic definition can be applied.

The nozzle is assumed to be isentropic, the generator is characterized by its efficiency,  $K$ , which is defined as:

$$K = \frac{h_b - h_c}{h_b - h_{cs}}$$

for constant specific heat  $K$  becomes

$$K = \frac{T_b - T_c}{T_b - T_{cs}}$$

The irreversibility appears as the temperature rise,  $T_{cs} - T_c$ , which is the result of the induced joule heating. Assuming that the temperature changes are small in com-

parison with the temperatures themselves permits the use of the Maxwell relationships to compute the temperature change due to entropy production, see Figs. 25 and 26.

$$\frac{\partial S}{\partial T}_p = \frac{c_p}{T}$$

hence  $\Delta S = \frac{c_p}{T} \Delta T$

and  $\Delta T = \frac{T}{c_p} \Delta S$

therefore since

$$K = \frac{\Delta T_{bc}}{\Delta T_{bc} + T_{ccs}}$$

$$\Delta T_{ccs} = \Delta T_{bc} (1-K)/K$$

$$\Delta S = c_p \Delta T_{bc} (1-K)/KT$$

The polytropic stage efficiency of the generator is

$$\eta_p = \frac{\Delta T_{ad}}{\Delta T_{ads}}$$

The power extracted is

$$c_p \Delta T_{ad} = c_p \Delta T_{bc}$$

hence  $\Delta T_{ad} = \Delta T_{bc} = \Delta T$

therefore

$$\eta_p = \frac{\Delta T}{\Delta T + \Delta T_{dds}}$$

since

$$T_{dds} = T_0 \Delta S/c_p$$

$$\eta_p = \frac{1}{1 + T_0 \frac{(1-K)}{KT}}$$

where  $T_0$  is the stagnation temperature,

$$\frac{T_0}{T} = 1 + \frac{\gamma-1}{2} M^2$$

yielding

$$\eta_p = \frac{1}{1 + (1 + \frac{\gamma-1}{2} M^2)(1-K)/K}$$

$$\eta_p = \frac{K}{1 + \frac{\gamma-1}{2} M^2 (1-K)}$$

$$\eta_p = \frac{K}{1 + \frac{\sqrt{2} (1-K)}{2c_p T}}$$

#### The Entropy Gain in Subsonic and Supersonic Diffusers

The percent of stagnation pressure loss in subsonic and supersonic diffusers was plotted as a function of Mach number<sup>(10), (11)</sup>, see Fig. 27. Best values were chosen from the reported data available. The data are represented to within 10% by the equation

$$P = 0.056M^{1.83}$$

where  $P$  is the percent of the initial stagnation pressure lost in the diffuser.

The entropy production accompanying an adiabatic pressure decrease is

$$\Delta S = -R \ln \frac{p_{\text{final}}}{p_{\text{initial}}}$$

The stagnation pressure ratio is

$$\frac{p_{\text{final}}}{p_{\text{initial}}} = 1 - 0.056M^{1.83}$$

Linearizing the logarithm of the pressure ratio gives

$$\frac{\Delta S}{R} = 0.056M^{1.83}$$

The entropy production can also be written as

$$T_0 \Delta S = c_p T_D (1 - \eta_D)$$

where

$$\eta_D = \frac{2 c_p \Delta T \text{ isentropic}}{v^2}$$

#### The Overall Generator Efficiency

It has been shown that

$$\Delta S_{\text{gen}} = \frac{c_p (1-K)}{K} \frac{\Delta T}{T}$$

and

$$\Delta S_{\text{diff.}} = R(0.056M^{1.83})$$

The overall efficiency is

$$\eta = \frac{\Delta T}{\Delta T + \frac{T}{c_p} \Delta S}$$

$$\eta = \frac{\Delta T}{\frac{\Delta T + T_o(1-K)}{T} \frac{\Delta T + RT_o(0.056M^{1.83})}{K}}$$

$$\eta = \frac{K}{K + \left(1 + \frac{\gamma-1}{2} M^2\right) (1-K) + \frac{KRT}{c_p \Delta T} (0.056M^{1.83})}$$

$$\eta = \frac{K}{1 + \left(\frac{\gamma-1}{2} M^2 (1-K) + \frac{KT_o(\gamma-1)}{\Delta T \gamma} (0.056M^{1.83})\right)}$$

The polytropic stage efficiency is related to the overall efficiency of the generator by the following set of relationships:

$$T_o \Delta S_{gen} = c_p \Delta T_{gen} (1 - \eta) / \eta$$

since the dissipation

$$\Phi = T_o \Delta S$$

equals  $c_p \Delta T_{IR} = c_p \Delta T_{gen} (1 - \eta) / \eta$

hence

$$\eta_{overall} = \frac{\Delta T}{\Delta T + \Phi / c_p}$$

$$\Phi = T_o (\Delta S_{gen} + \Delta S_{diffuser})$$

$$= T_o (c_p \Delta T (1 - \eta_p) / (\eta_p T_o) + R \ln \frac{p_o \text{out}}{p_o \text{in}})$$

$$\eta_{\text{overall}} = \frac{1}{1 + \Phi / c_p \Delta T}$$

$$\eta_{\text{overall}} = \frac{1}{1 + \frac{(\gamma - 1)}{\eta_p} \frac{T_o}{\gamma \Delta T} \ln \frac{p_o \text{out}}{p_o \text{in}}}$$

The loading factor,  $K$ , is shown in Fig. 28 as a function of the overall device efficiency for various Mach numbers and temperature ratios.

An alternative description of the diffuser irreversibility is the thermodynamic efficiency of the diffuser (12)

$$\eta_D = \frac{c_p \Delta T_D}{V^2/2} = \frac{(1 + \frac{\gamma-1}{2} M^2) \left( \frac{p_o \text{out}}{p_o \text{in}} \right)^{\frac{\gamma-1}{\gamma}} - 1}{\frac{\gamma-1}{2} M^2}$$

The overall generator plus diffuser efficiency is then

$$\eta_{\text{overall}} = \frac{1}{\frac{1}{\eta_g} + (1 - \eta_D) \frac{\Delta T_{\text{diffuser}}}{\Delta T_{\text{gen}}}}$$

Both figures of merit, efficiencies and percent loss of stagnation pressure are used to describe the performance of supersonic diffusers. Since the reported values are based on the same original data, either description can be used.

## THERMAL INSULATION AND BOIL-OFF RATES FOR SUPERCONDUCTING MAGNET CRYOGENIC TANKS

### Multiple Radiation Shields

It is apparent that superconducting magnets will be needed for MHD generators for space application. Ordinary temperature air core copper magnets and cryogenic air-core aluminum and sodium magnets weigh an order of magnitude more than superconducting magnets in the size of interest<sup>(13)</sup>. Large superconducting magnets have not actually operated to date, but every expectation is that superconducting magnets producing 20 to 80 kilogauss over a volume of several cubic feet will be available concurrently with the other components of MHD generators<sup>(14)</sup>.

The particular insulation scheme under consideration is that of multiple radiation shields. Consider a number of parallel evacuated gaps, each enclosed on both sides by surfaces of low thermal emissivity, see Fig. 29. Since the incoming and outgoing radiation are from similar surfaces whose temperatures differ only slightly then the emissivity and absorbtivity will be equal.

Between each pair of surfaces the radiant flux, which is the only energy flux, is given by:

$$\frac{q}{A} = \frac{\sigma \Delta T^4}{\frac{1}{\epsilon_a} + \frac{1}{\epsilon_b} - 1}$$

In this case it is assumed that

$$\epsilon_a = \epsilon_b = \epsilon$$

and that the material has been chosen such that

$$\epsilon \ll 1$$

therefore the interchange factor

$$\left( \frac{2}{\epsilon} - 1 \right)^{-1}$$

is best approximated by

$$\frac{\epsilon}{2}$$

For gold or silver plating  $\epsilon = 0.01$  to  $0.02$ . For  $\epsilon = 0.02$

$$\left( \frac{2}{\epsilon} - 1 \right)^{-1} = \frac{1}{99} = .010101$$

Which is within 1% of  $\epsilon/2$ .

It is to be noted that for large  $\epsilon$

$$\left( \frac{2}{\epsilon} - 1 \right)^{-1} \rightarrow \epsilon^2$$

and when  $\epsilon \rightarrow 1.0$

$$\left( \frac{2}{\epsilon} - 1 \right)^{-1} \rightarrow 2\epsilon - 1$$

and  $\epsilon^2 \rightarrow 2\epsilon - 1$

These other approximations are quoted here in order to relate the present approximation to others, which are valid in other regimes, with which the reader may have more familiarity.

The net heat transfer is then

$$\frac{q}{A} = \frac{\sigma \epsilon}{2} \Delta T^4$$

In the steady state all of the heat fluxes are equal. Adding the  $T^4$ 's yields

$$T_h^4 - T_3^4 = \frac{2}{\sigma \epsilon} \frac{A}{q}$$

$$T_3^4 - T_2^4 = \frac{2}{\sigma \epsilon} \frac{A}{q}$$

$$T_2^4 - T_1^4 = \frac{2}{\sigma \epsilon} \frac{A}{q}$$

$$T_1^4 - T_c^4 = \frac{2}{\sigma \epsilon} \frac{A}{q}$$

$$\overline{T_h^4 - T_c^4} = \overline{N \left( \frac{2}{\sigma \epsilon} \frac{A}{q} \right)}$$

where  $N = 4$ , the number of spaces. In general then

$$\frac{q}{A} = \sigma \left( \epsilon / 2 \right) \frac{\Delta T^4}{N}$$

For an area of 6 ft.<sup>2</sup> to be insulated with a multiple radiation shield of low emissivity  $\epsilon = 0.02$ , the heat transfer per year ( $10^4$  hours) is

$$Q(\text{BTU}) = 10^{-6} \frac{\Delta T^4}{N} (\text{°R}^4)$$

### Transient Boil-Off Protection

A hydrogen dewar surrounding the helium bottle with only one radiation gap results in a heat transfer rate per year of:

$$Q = 1.68 \text{ BTU/Year}$$

enough to boil 0.15#He. Conduction heat leaks in the structure will also be of this order of magnitude, hence the helium boil-off rate of a pound or so per mission can easily be maintained by use of a hydrogen dewar.

The hydrogen dewar can be surrounded by an oxygen dewar at 90°K. The heat transfer to the hydrogen, for a 6 ft.<sup>2</sup> dewar, is 687 BTU for 1 year with only one radiation gap. The evaporation rate of hydrogen will be 3.45#/year, which appears tolerable. Allowing for conduction heat leaks in the structure of the same order of magnitude still permits favorable weight loss per year of operation.

The liquid oxygen can, in a like manner, be protected by a water jacket. Here the heat transfer rate without added radiation shields is large, 62,500 BTU/year under the same conditions as above. 694# of oxygen would boil off in a year. Six radiation shields would reduce this to 116#/year, which may be tolerable. This oxygen may also be used to condense some of the water evaporated in the water jacket.

### Superinsulation

Linde Superinsulation SI-4 has an apparent thermal conductivity in vacuum of  $2 \times 10^{-5}$  BTU/Hr.FT°F (15) between room and liquid hydrogen temperatures. One-tenth of a foot (1.2") of SI-4 will result in about 920 BTU/year being conducted to a hydrogen dewar from a water jacket. This heat flux through a conduction cross section of 6 ft<sup>2</sup>

will result in 27.5# of  $H_2$  being boiled off per year. SI-4 insulation then appears preferable to other insulation techniques.

Due to structure, SI-4 can be considered as a close packing of radiation shields. Equating the two methods of computation of heat transfer, shielded radiation and conduction gives

$$\frac{k \Delta T}{X} = \frac{\sigma \epsilon}{2} \frac{\Delta T^4}{N}$$

Assuming equally spaced shields,

$$X = aN$$

$$a = \frac{2k \Delta T}{\sigma \epsilon \Delta T^4}$$

$$= 10^{-2} \text{ ft.}$$

for  $\epsilon = 0.02$ .

Thus SI-4 is equivalent to radiation shields placed  $1/100$  of a foot apart.

Assuming that an insulating material can be built for which this relation holds above room temperature to say,  $1500^{\circ}\text{R}$ , 6" of it will contain 50 shields, and will permit a heat transfer of  $10^5$  BTU/year for 6 square feet of exposed surface. This heat is sufficient to evaporate 108# of water per year, an acceptable amount.

The power cycles being considered have the working fluid emerging from the pump or compressor at temperatures around  $1500^{\circ}\text{R}$ . It appears possible then to use the hot walls of the generator as a preheater for the working fluid so that temperatures of the order of  $1500^{\circ}\text{R}$  ( $2000^{\circ}\text{R}$  maximum) appear as the hot temperature which the helium, which is keeping the magnet superconducting, must be protected from.

This analysis has shown that an insulation construction of

1. Vacuum space (gold plated).
2. Liquid hydrogen container.
3. 1.2 inches of SI-4.
4. Water jacker (40°F).
5. 6 inches of SI-4, or 50 radiation shields.
6. Condensate preheater.

is sufficient to maintain the superconducting property of the magnet. The boil-off rate per year for six feet of area of heat path is:

108 #water

0.6# H<sub>2</sub>

.35# He

which appears tolerable. These evaporation rates will probably be less than the evaporation losses due to conduction through the structure, however, using them as a guide indicates that for missions of duration of 1 year, and for one to ten megawatt MHD generators, transient boil-off appears as a feasible mode of operation.

### Multiple Radiation Shield Insulation

The heat transfer rate in an evacuated multiple radiation shield configuration, such as shown in Fig. 30, is

$$\frac{q}{A} = \frac{\sigma \epsilon}{2N} \Delta (T^4)$$

Assuming  $10^{-3}$  ft. (.012 inches) as the minimum thickness of a foil that will withstand the severe mechanical conditions at launch, and  $10^{-3}$  ft. as the minimum allowable spacing, considering the possibility of the foils touching, the insulation will have 500 gaps/ft. An average emissivity of gold is 0.02. Allowing 2 inches of insulation between the hot (assumed  $2500^{\circ}$ R) MHD generator surface and a liquid water heat sink at  $500^{\circ}$ R the heat transfer rate for a 5 ft.<sup>2</sup> section is 390,000 BTU/yr; enough to boil 430 lbs. of water/year.

In order to reduce this amount of boil-off the water vapor can be passed through a passage in the layered insulation which is at  $2000^{\circ}$ R. Placing 50 radiation gaps between the  $2500^{\circ}$ R heat source and the  $2000^{\circ}$ R layer results in a heat flux of 384,000 BTU/yr. between the MHD generator and the passageway at  $2000^{\circ}$ R. The 50 gaps will occupy 1.20 inches. Allowing 160 lbs. of water/yr. to evaporate results in a heat sink of  $\dot{m} c_p \Delta T$  in the passageway. The heat transfer rate out of the water vapor passageway will be  $\dot{m} c_p \Delta T$ (240,000 BTU/yr.) less than the rate in. Thus, 144,000 BTU/year will be transferred to the water jacket, which will boil the water at the rate of 160 lbs., which is required. Ninety gaps are required between the  $2000^{\circ}$ R passageway and the  $500^{\circ}$ R water jacket, occupying 2.16 inches.

The heat transfer rate to the hydrogen container will be of the order of the uncertainties in the above calculation and has been omitted from the analysis of the water boil-off rate. Ten radiation gaps are sufficient to reduce the hydrogen boil-off rate to 6 lbs/year if regenerative cooling is used where the hydrogen gas passes on the cool side of the water jacket, and 40 lbs/yr. if the hydrogen boils and is jettisoned directly. The ten gaps would occupy 0.24 inches.

The heat transfer from the hydrogen tank to the helium reservoir across a single gold plated vacuum gap would be 1.5 BTU/yr., a negligible amount.

Thus it is seen that the use of 3.4 inches of vacuum-foil sandwiches will result in the evaporation of 160 lbs/yr. of water, 6 lbs/yr. of hydrogen, and a negligible amount of helium. In addition to the heat fluxes calculated here, there will be heat fluxes due to conduction along supporting structure. This conduction through the structure, which must bear the force induced on the magnet by the generator, is difficult to estimate. If the heat leak by the structure is (340,000 BTU/yr.) between the 500°R section and the hydrogen vessel then an additional 20 lbs/yr. of hydrogen will be consumed. The total weight loss will be less than 200 lbs/yr.

#### Active Refrigeration

It is worthwhile noting that the power required to remove one watt from liquid hydrogen temperature to room temperature (300°K) is about 100 watts<sup>(16)</sup>. Such a cryostate would weigh about 30 lbs/watt, and the weight penalty of 5 lbs/kw<sup>(17)</sup> for the power generated would be 1/2 lb./watt of cooling. A 100 watt radiator operating at 540°R would weight about 8 lbs. Allowing additional weight for plumbing, valving,

etc. it appears that 10 lbs/watt is the order of the weight penalty for removing heat from liquid hydrogen temperature and rejecting heat at 300°K. A 50 watt "heat leak" would only cost 500 lbs. of additional equipment. A hybrid system combining both transient boil-off (needed during launch and until the MHD system starts operating) and refrigeration might prove worthwhile. Additional work is needed here.

### Optimum Heat Rejection Temperature

The mechanical efficiency of a refrigeration cycle can be defined as the ratio of the reversible work required divided by the actual work required by the refrigerator:

$$M = W_{\text{rev}}/W_{\text{actual}}$$

Fig. 31 shows a plot of  $M$  as a function of the refrigeration temperature for systems which reject heat to room temperature reservoirs<sup>(16)</sup>. The data can be represented by the line

$$M = \theta^{1.07}$$

where

$$\theta = T_{\text{reject}}/T_{\text{refrigeration}}$$

A reasonable approximation is

$$M = \theta$$

where

$$\theta = T_{\text{hot}}/T_{\text{cold}}$$

The coefficient of performance is

$$COP = -Q_{\text{in}}/\text{Work}$$

The refrigerator work becomes

$$W = M W_{\text{rev}}$$

or

$$\frac{W}{Q_{in}} = \theta(1-\theta)$$

The heat rejected at the hot temperature becomes

$$\frac{Q_{rej}}{Q_{in}} = 1 + \frac{W}{Q_{in}} = 1 + \theta - \theta^2$$

which for large  $\theta$ , can be approximated as  $\theta(1-\theta)$ , the work input.

Radiator weights for refrigeration systems cooling at  $36^{\circ}\text{R}$  (liquid  $\text{H}_2$  temperature) should weigh about

$$\frac{1000(\theta-1)}{\theta^3} \text{ #/watt of cooling}$$

which is  $10^3/\theta^2$  for large  $\theta$ . This shows that the radiator area diminishes as  $\theta^{-2}$  since the heat transfer area varies as  $\theta^{-4}$  while the heat transfer varies like  $\theta^2$ .

The weight of the radiator plus extra power supply, at 5#/kwe (14), is

$$\frac{wt}{Q_{in}} = \frac{\theta^3}{\theta^3} (\theta-1) + 5 \times 10^{-3} (\theta-1)$$

The weight per watt of cooling has a minimum at

$$\frac{dwt. / Q_{in}}{d\theta} = 0$$

which is at

$$0 = 10^6 \left(2 - \frac{3}{\theta}\right) + 5(1 - 2\theta)$$

For large  $\theta$  the term  $3/\theta$  is small compared with 2 and  $2\theta$  is much larger than unity,

hence

$$\theta^{-4} = 2 \times 10^5$$

and

$$\theta = 21$$

justifying  $2 > 0.14$  and  $42 > 1$ .

The hydrogen refrigerator should then reject heat at  $756^{\circ}\text{R}$ , with a weight of  $.45\text{#/watt}$  of cooling. A 50 watt heat transfer rate will require 225 lbs. of power supply and radiator, a tolerable amount.

THE INFLUENCE OF NON-CARNOT PERFORMANCE ON THE TEMPERATURE RATIO  
OF VAPOR CYCLES

It is known that the requirement of minimum radiator area per net power output determines that the temperature of heat rejection of a Carnot heat engine is three-fourths of the temperature of heat admission. Rankine Cycle performance can be closely approximate as being proportional to that of a Carnot Cycle. Defining the proportionability factor as

$$N = \eta / \eta_c$$

The efficiency of the Rankine Cycle is

$$= N(1 - T_c / T_h)$$

The heat rejected is

$$Q_r = P(1 - \eta) / \eta$$

where  $P$  is the net power produced by the cycle. Since the weight per unit of heat transfer is inversely proportional to  $T_c^4$  (18), the minimum weight of the system requires that

$$\frac{Q_r}{T_c^4}$$

be a minimum.

Defining a dimensionless radiator area parameter as

$$Z = \sigma T_h^4 A / P$$

one obtains for a thermally black radiator

$$Z = \left( \frac{T_h}{T_c} \right)^4 \frac{(1-\eta)}{\eta}$$

Calling the temperature ratio  $\theta$

one obtains

$$\theta = T_c/T_h$$

$$Z = (1/N - 1/\theta)/(1-\theta)\theta^4$$

The requirement of that  $Z$  be a minimum for a given  $N$  is

$$\left( \frac{\partial Z}{\partial \theta} \right)_N = 0$$

Which results in the quadratic equation

$$\theta^2 + \theta(5/4N - 2) + 1 - 1/N = 0$$

with roots

$$\theta = \frac{8N - 5 \pm \sqrt{25 - 16N}}{8N}$$

as was shown by Pitkin (19).

The positive roots of this equation are shown in Fig. 32.

The asymptotic values of  $\theta$  are  $3/4$  at  $N = 1$  (Carnot Cycle) and  $4/5$  at  $N = 0$ .

The thermodynamic efficiency at optimum  $\theta$  is

$$\eta_{opt.} = (5 - \sqrt{25 - 16N})/8$$

and is shown in Fig. 33. Fig. 34 shows the value of  $Z$  corresponding to the optimum temperature ratios.  $Z$  has an asymptote of 9.481 at  $N = 1$ .

Metallic vapor Rankine Cycles whose efficiency lies between 70% and 90% of the Carnot efficiency corresponding to the boiling and condensing temperatures of the Rankine Cycle will have values of  $Z$  between 15 and 10 respectively. The corresponding values of  $\theta$  lie between 0.77 and 0.76, thus a  $\theta$  of 3/4, which corresponds to a Carnot Cycle is an adequate preliminary design point for actual systems.

Fig. 35 shows how the radiation parameter,  $Z$ , depends on  $\theta$  for various values of  $N$ . It is seen that the  $Z$  possesses a fairly flat minimum with respect to  $\theta$ , and that this minimum increases slowly with decreasing  $N$ .

## SUMMARY

The thermodynamic performance of gas power cycles is analyzed in terms of the temperature limited components and the radiator size. Optimum Brayton Cycles with and without regenerators were found to require radiators 3 to 5 times as large as Rankine Cycles with the same maximum temperature of the working fluid. A new cycle, the Tri-Cycle, was synthesized. An optimum Tri-Cycle with 80% component efficiency, will only require a radiator which is  $2\frac{1}{4}$  times as large as a Rankine Cycle with the same top temperature. Equal radiator areas result when the maximum temperature of the working fluid is raised according to the fourth root of the equal-temperature condition radiator area ratio.

A new cycle was discovered which operates using a chemical reaction which produces gas. Using such a reaction, a completely dry vapor expansion can be obtained while still retaining a condensed phase in the compression process. Using lithium hydride dissociating at  $1610^{\circ}\text{F}$  and recombining at  $1310^{\circ}\text{F}$ , results in an 11% thermodynamic cycle efficiency. The radiator area is only a few per-cent larger than that of the optimum Rankine Cycle operating with the boiler at the same temperature. Such a cycle is useful for gas turbines as well as for MHD power generation techniques.

Entropy generation in MHD generators and supersonic diffusers were analyzed. Expressions for obtaining the overall polytropic efficiency of the MHD generator in terms of the Mach Number, temperature drop of the gas, pressure ratio, and loading factors were obtained. Under typical conditions the loading factor is greater than the device polytropic efficiency by one sixth.

Various means of thermally insulating the superconducting magnet from the hot MHD generator were examined. Both transient boil-off and active refrigeration systems were analyzed. Refrigeration power and radiator weight were used to minimize the weight penalty of active refrigeration. Since the helium boil-off rate due to heat transfer from an enclosing hydrogen dewar is so small active refrigeration of liquid hydrogen was considered. The optimum temperature to reject heat at is about 300°F, with a weight penalty of 4.5#/watt of cooling at 36°R.

## BIBLIOGRAPHY

1. Sorenson, H. A., *Gas Turbines*, Ronald Press, 1951.
2. Keenan, J. H., and Kaye, J., *A Survey of the Calculated Efficiencies of Jet Power Plants*, J. A. S. 14, pgs. 437-450, August 1947.
3. Keller, C., *The Escher Wyss-AK Closed-Cycle Turbine, Its Actual Development and Future Prospects*, Trans. A.S.M.E. November 1946.
4. Streid, D. D., *Gas Turbine Fundamentals*, Mech. Eng. Feb. 1946.
5. Snyder, N. W., Editor, *Energy Conversion for Space Power* Academic Press, 1961, pg. 541.
6. Stephinson, J. M., *Gas Turbine Engines with Heat Transfer During the Compression and Expansion*, ARS Journal, Feb., 1962, pg. 266.
7. NBS Circular 500, *Selected Values of Chemical Thermodynamic Properties, Part I*, page 431, March 31, 1950.
8. Keenan, J. H., and Kaye, J., *Gas Tables*, John Wiley & Sons, Inc. New York, 1954.
9. Weatherford, W. D., Jr., Tyler, J. C., and Ku, P. M., "Properties of Inorganic Energy Conversion and Heat-Transfer Fluids for Space Applications", WADD TR 61-96, November, 1961.
10. Neumann, E. P., and Lastwerk, F., *High-Efficiency Supersonic Diffusers*, J. A. S., 51, 6, 1951, pg. 369.
11. Hermann, R., *Supersonic Inlet Diffusers and Introduction to Internal Aerodynamics*, Minneapolis-Honeywell Regulator Co., Minneapolis, Minnesota, 1956.
12. Shapiro, A. H., *The Dynamics and Thermodynamics of Compressible Fluid Flow*, Ronald Press, 1953.
13. Rosa, R. J., *Magnetohydrodynamic Generators and Nuclear Propulsion*, ARS Journal, August 1962, pg. 1221, see also Reference 14.

14. Kolm, H., Lax, B., Bitter, F., and Mills, R., Editors, *High Magnetic Fields*, M. I. T. Technology Press and John Wiley and Sons, 1962, see also, Avco SC-500, *Superconducting Coil Bulletin*, Avco-Everett Research Lab.
15. *Advances in Cryogenic Engineering*, Vol. 6, 1960, pg. 20.
16. Fleming, R. B., *Private Communication*
17. Hodgson, A. G., *Joule Cycle for Space Power*, A. R. S. Journal, Vol. 32, No. 4, page 639, April 1962.
18. Mackay, D. B., and Bacha, C. P., *Space Radiator Analysis and Design*, North American Aviation, Inc., Space and Information Systems Division, October 1961, ASTIA-269587, page 48.
19. Pitkin, E. T., *Optimum Radiator Temperature for Space Power Systems*, ARS Journal, 29, p. 596 (1959).

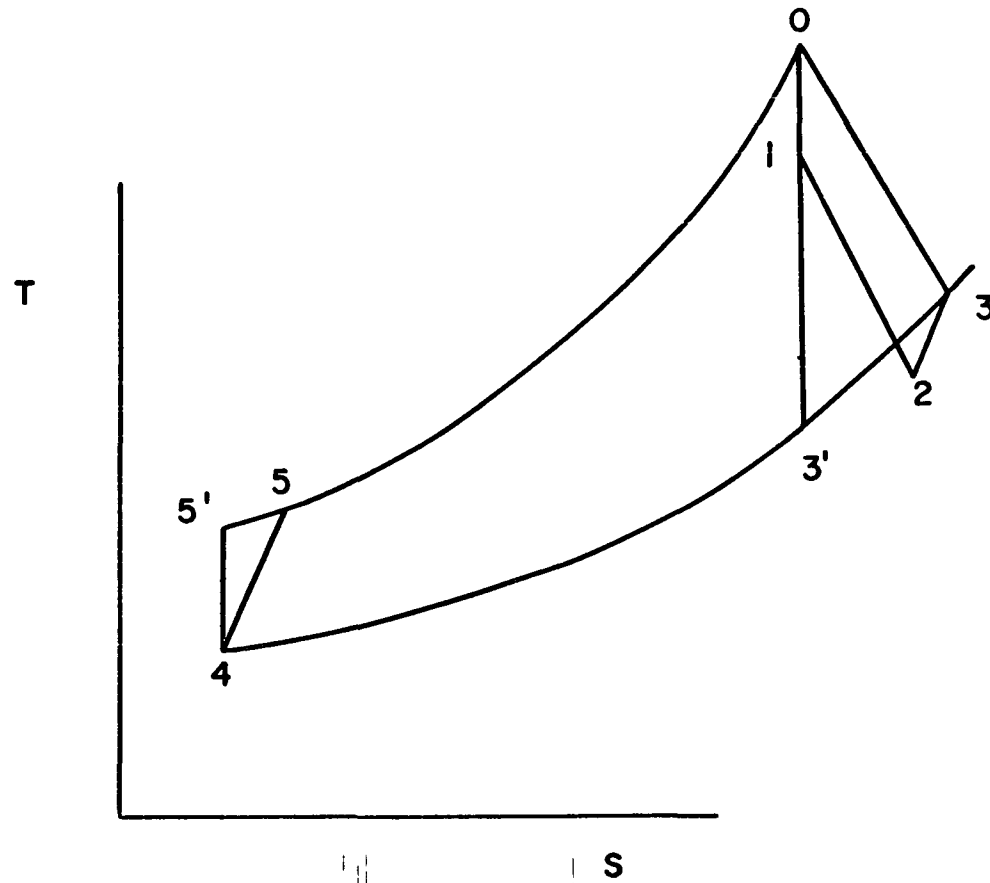
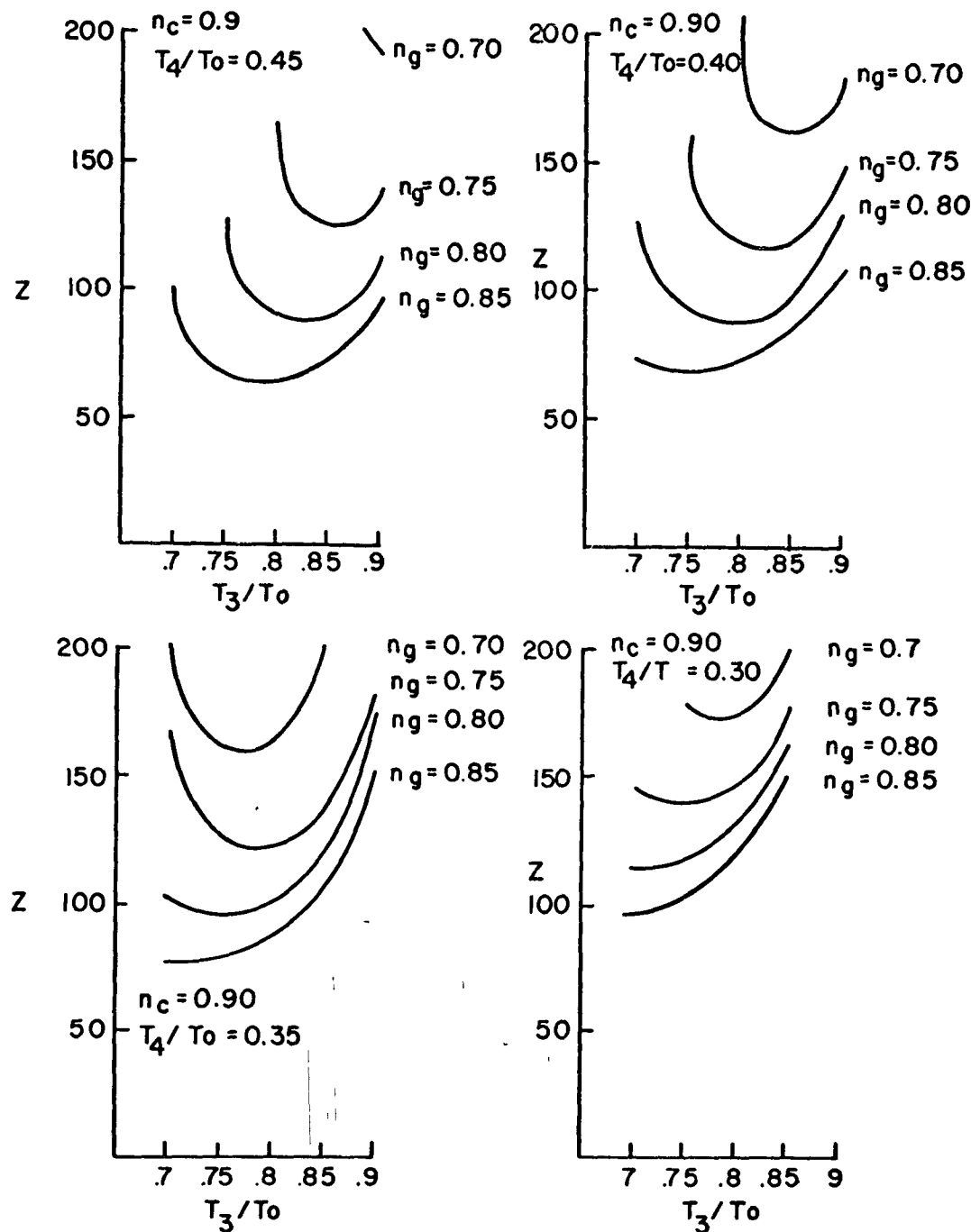
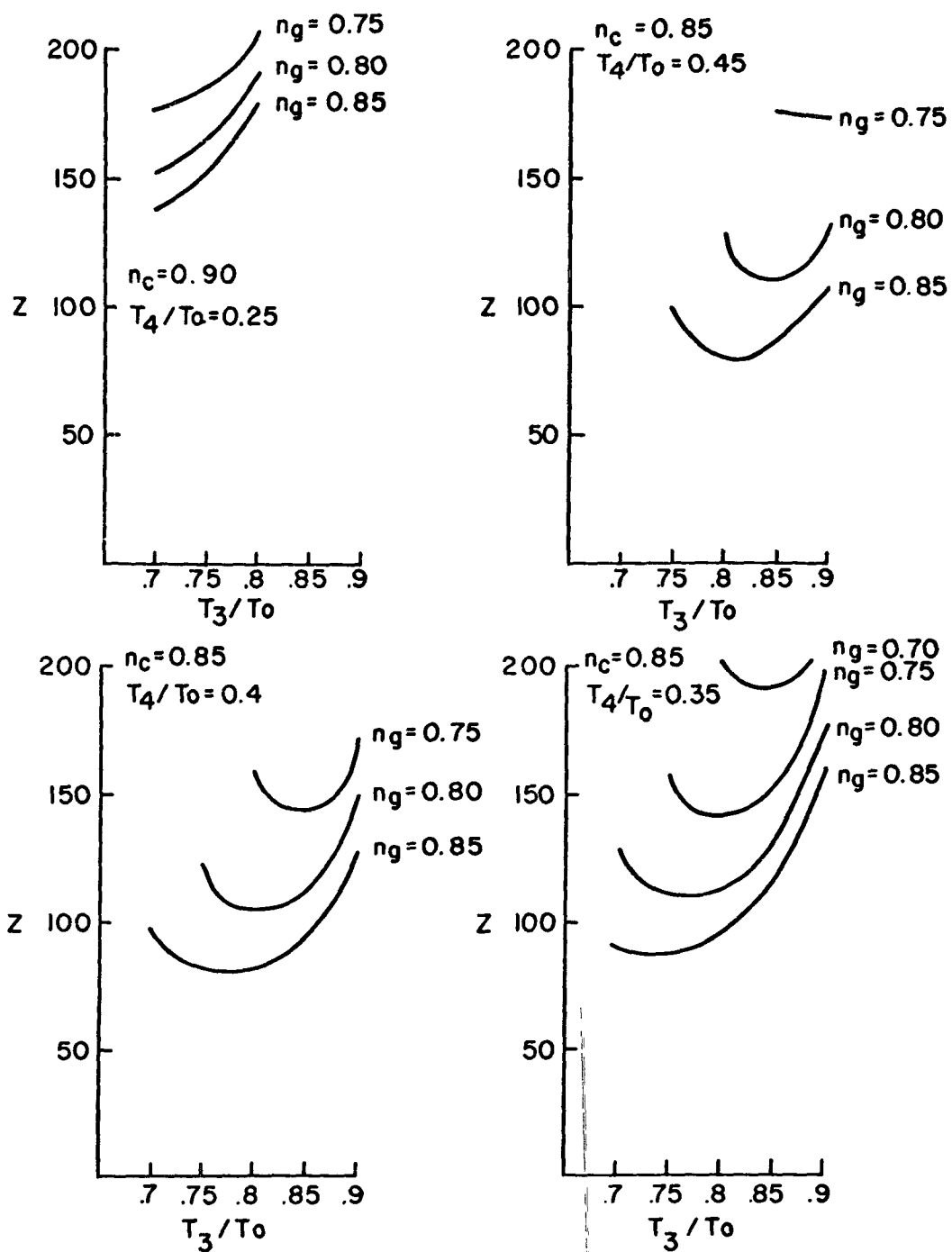


Figure 1. The Brayton Gas Turbine Cycle.



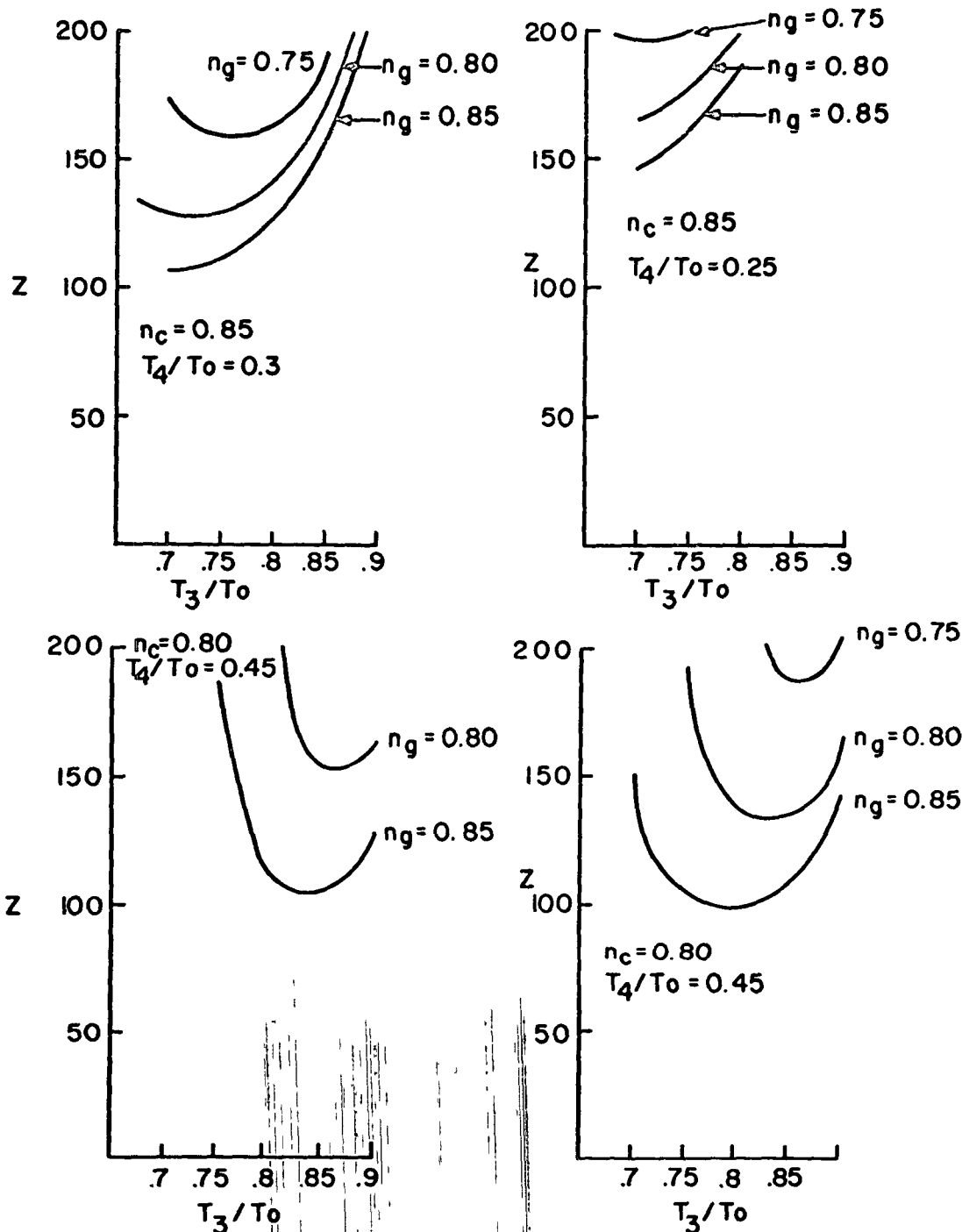
(a)

Figure 2. Dimensionless radiator size parameter as a function of the generator temperature ratio for the direct Brayton cycle. Lines of constant generator efficiency and compressor inlet temperature ratio for constant compressor efficiency.



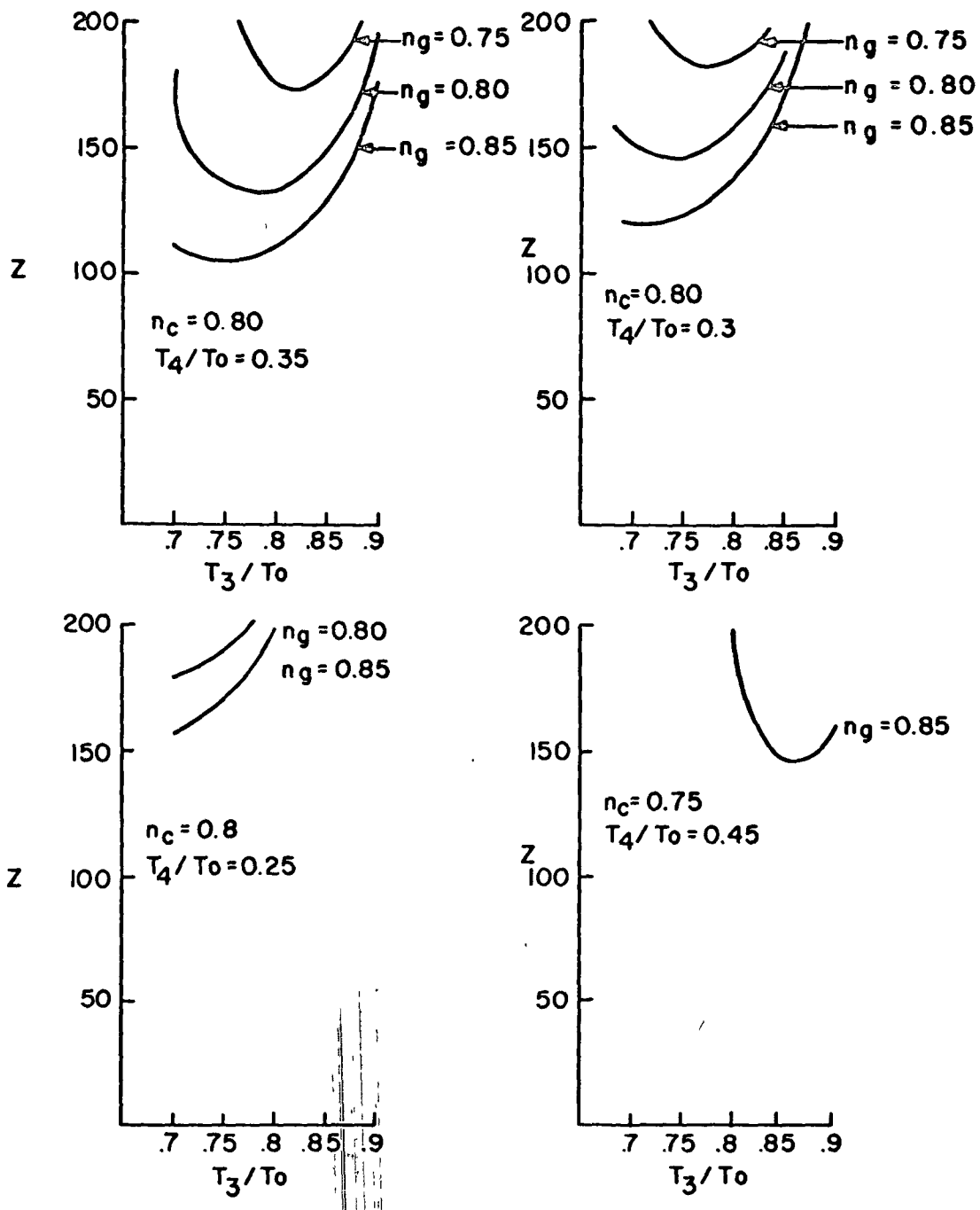
(b)

**Figure 2.** Dimensionless radiator size parameter as a function of the generator temperature ratio for the direct Brayton cycle. Lines of constant generator efficiency and compressor inlet temperature ratio for constant compressor efficiency.



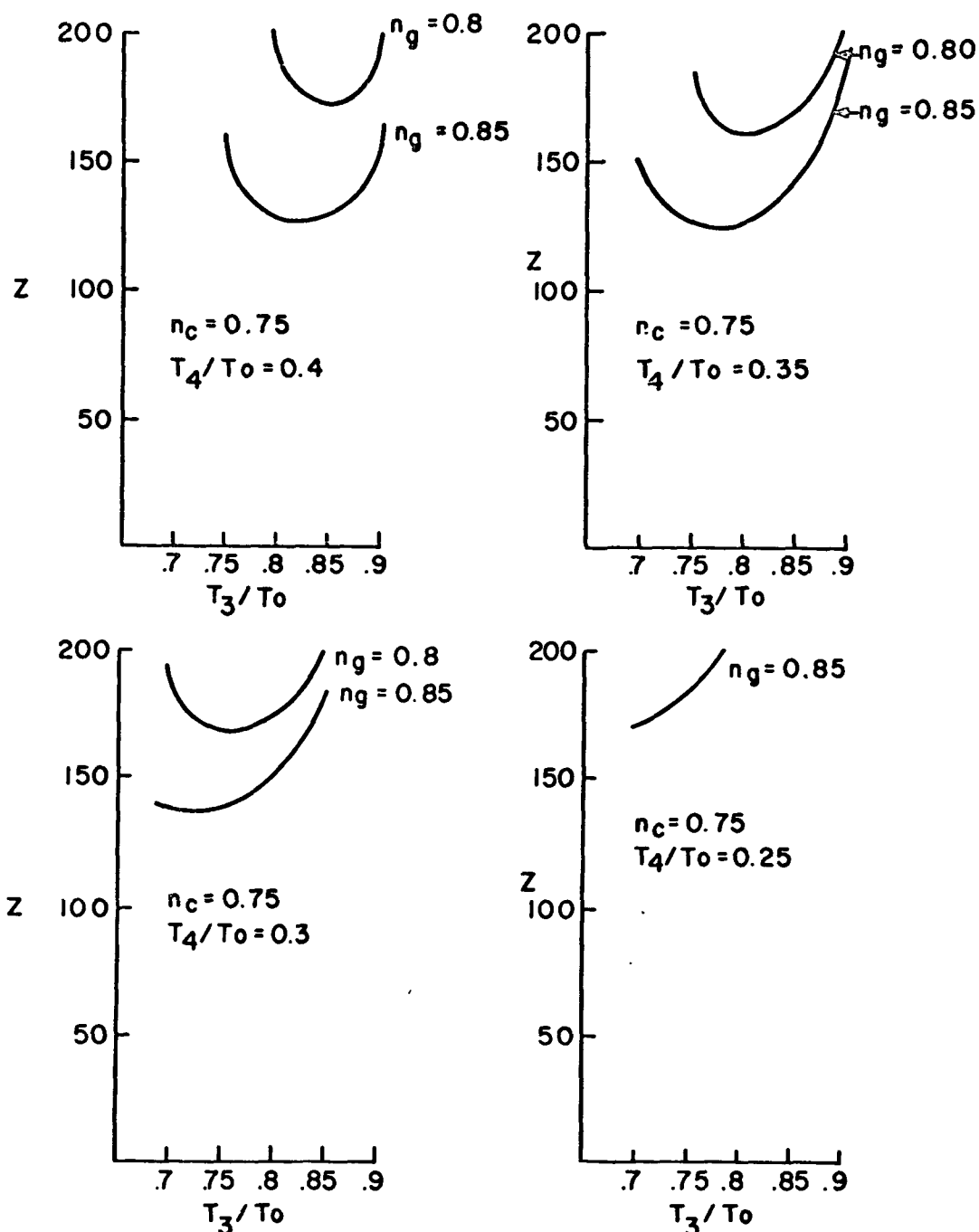
(c)

Figure 2. Dimensionless radiator size parameter as a function of the generator temperature ratio for the direct Brayton cycle. Lines of constant generator efficiency and compressor inlet temperature ratio for constant compressor efficiency.



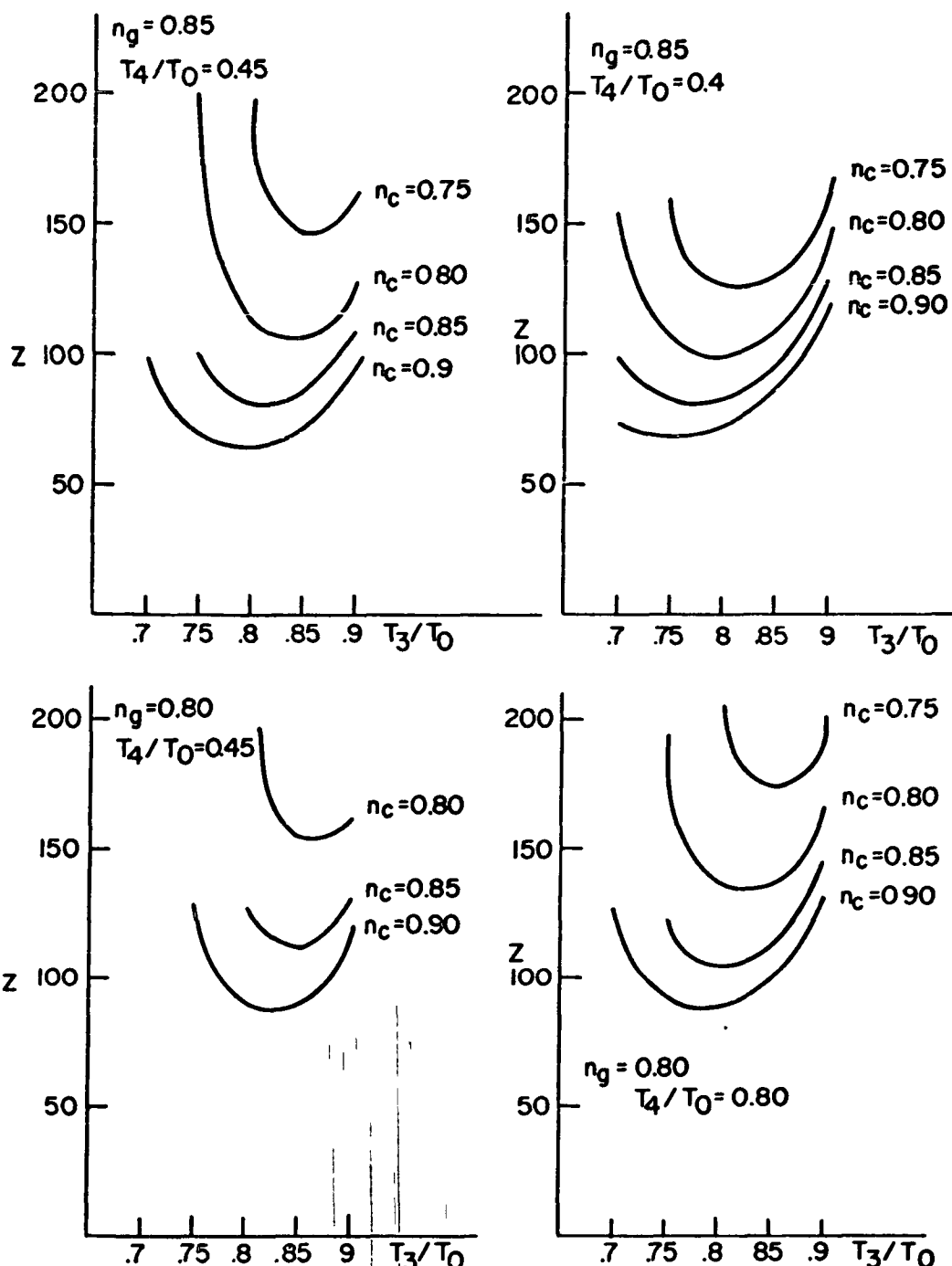
(d)

**Figure 2.** Dimensionless radiator size parameter as a function of the generator temperature ratio for the direct Brayton cycle. Lines of constant compressor efficiency and compressor inlet temperature ratio for constant compressor efficiency.



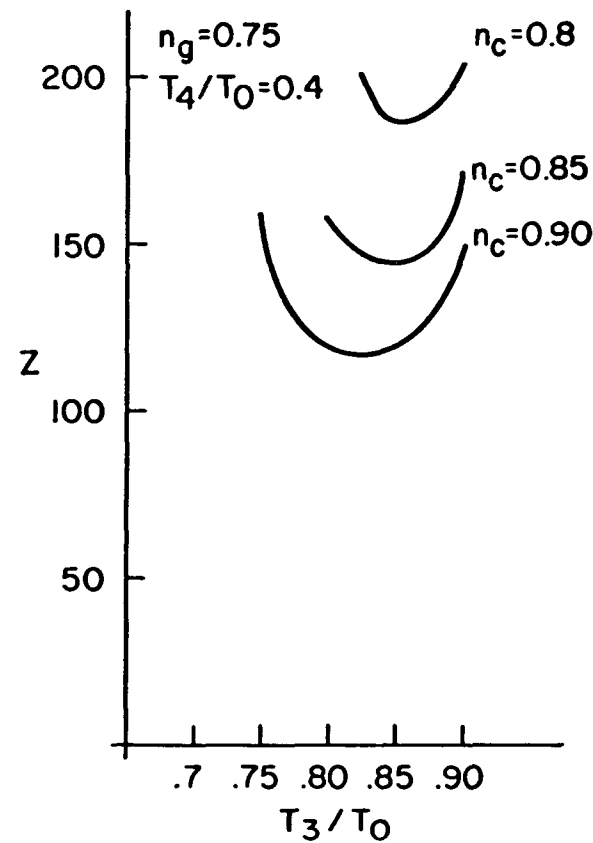
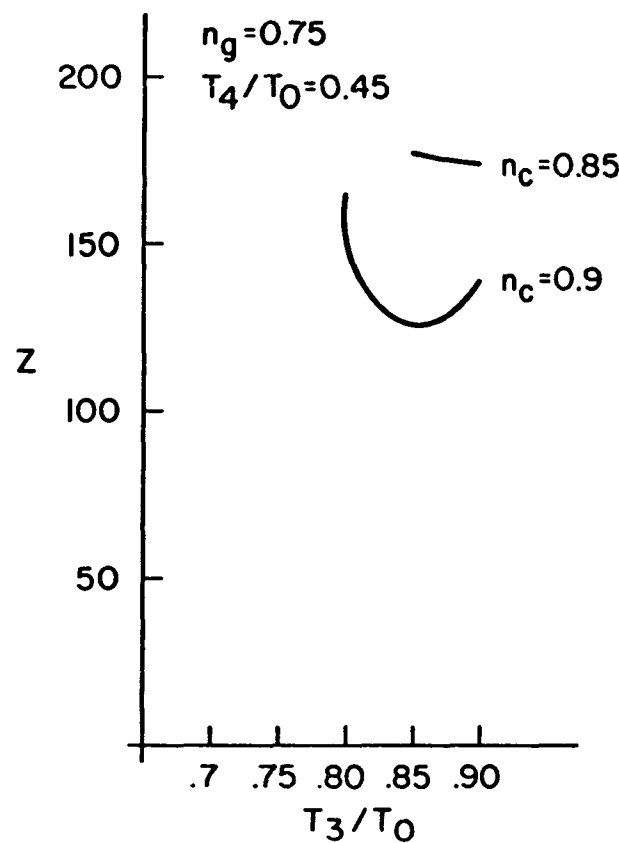
(e)

Figure 2. Dimensionless radiator size parameter as a function of the generator temperature ratio for the direct Brayton cycle. Lines of constant generator efficiency and compressor inlet temperature ratio for constant compressor efficiency.



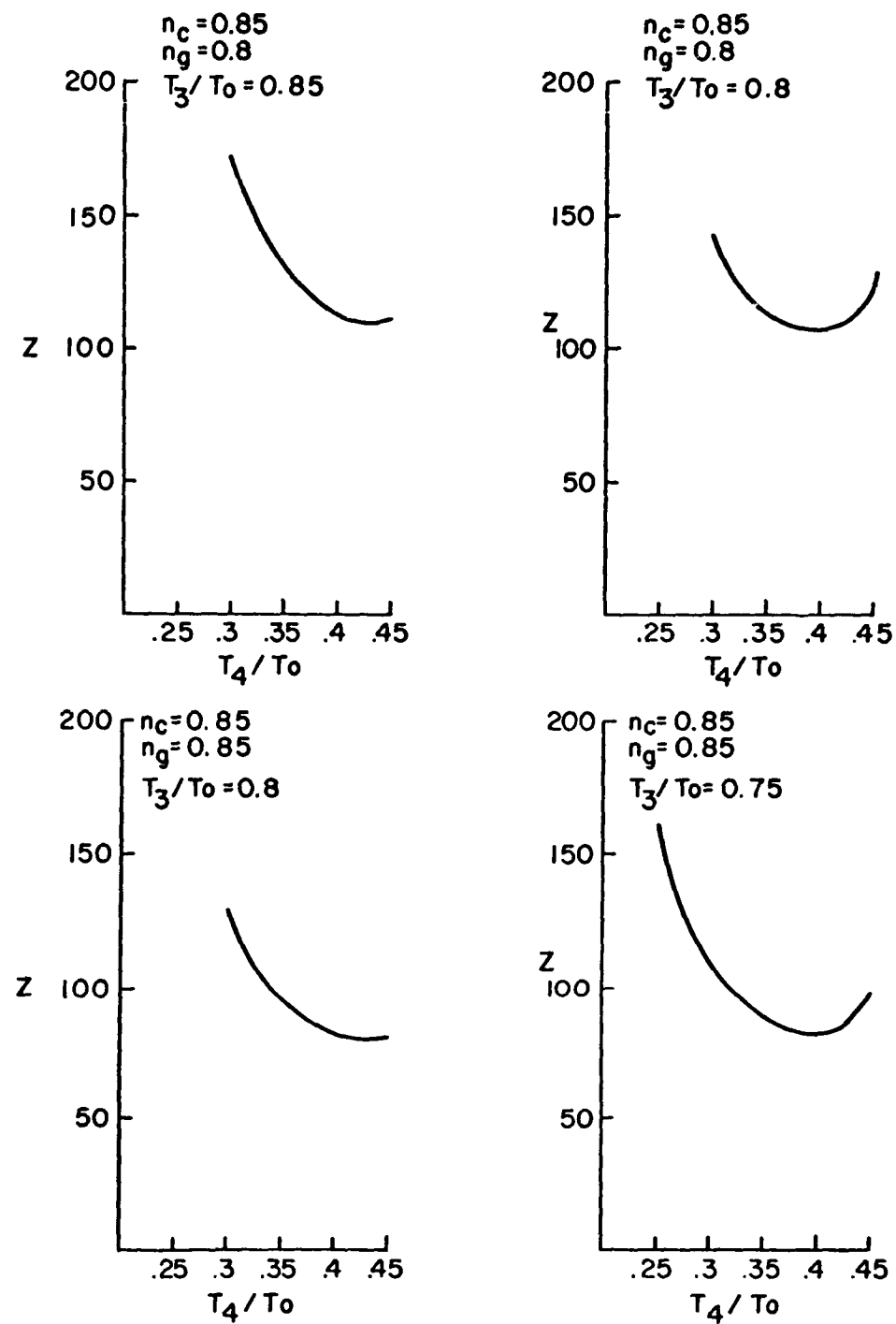
(a)

Figure 3. Dimensionless radiator size parameter as a function of the generator temperature ratio for the direct Brayton cycle. Lines of constant compressor efficiency and compressor inlet temperature ratio for constant generator efficiency.



(b)

**Figure 3.** Dimensionless radiator size parameter as a function of the generator temperature ratio for the direct Brayton cycle. Lines of constant compressor efficiency and compressor inlet temperature ratio for constant generator efficiency.



**Figure 4.** Dimensionless radiator size parameter as a function of compressor inlet to turbine inlet temperature ratio for the direct Brayton cycle. Lines of constant component efficiency and turbine temperature ratio.

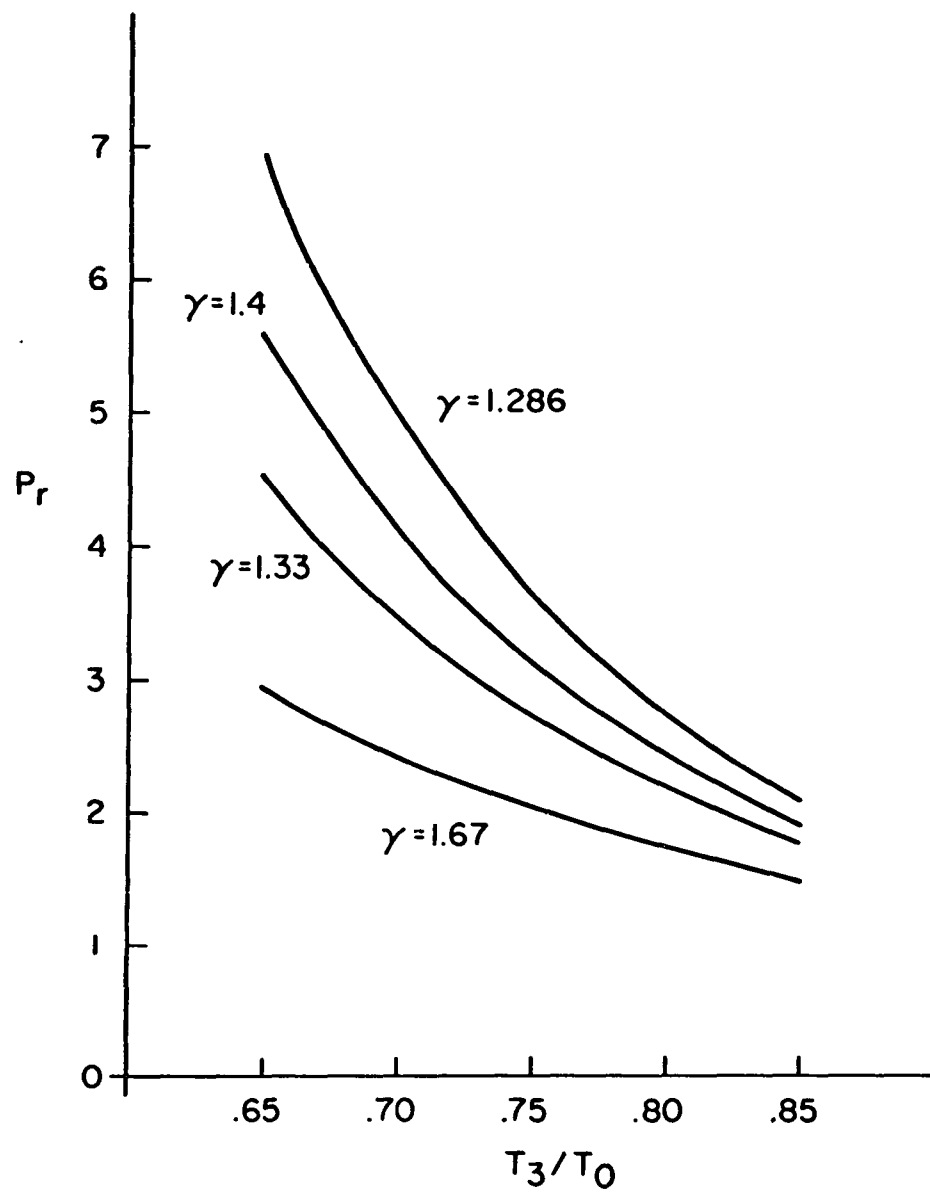


Figure 5. Cycle pressure ratio as a function of turbine temperature ratio for various values of the isentropic exponent  $= c_p/2v$ .

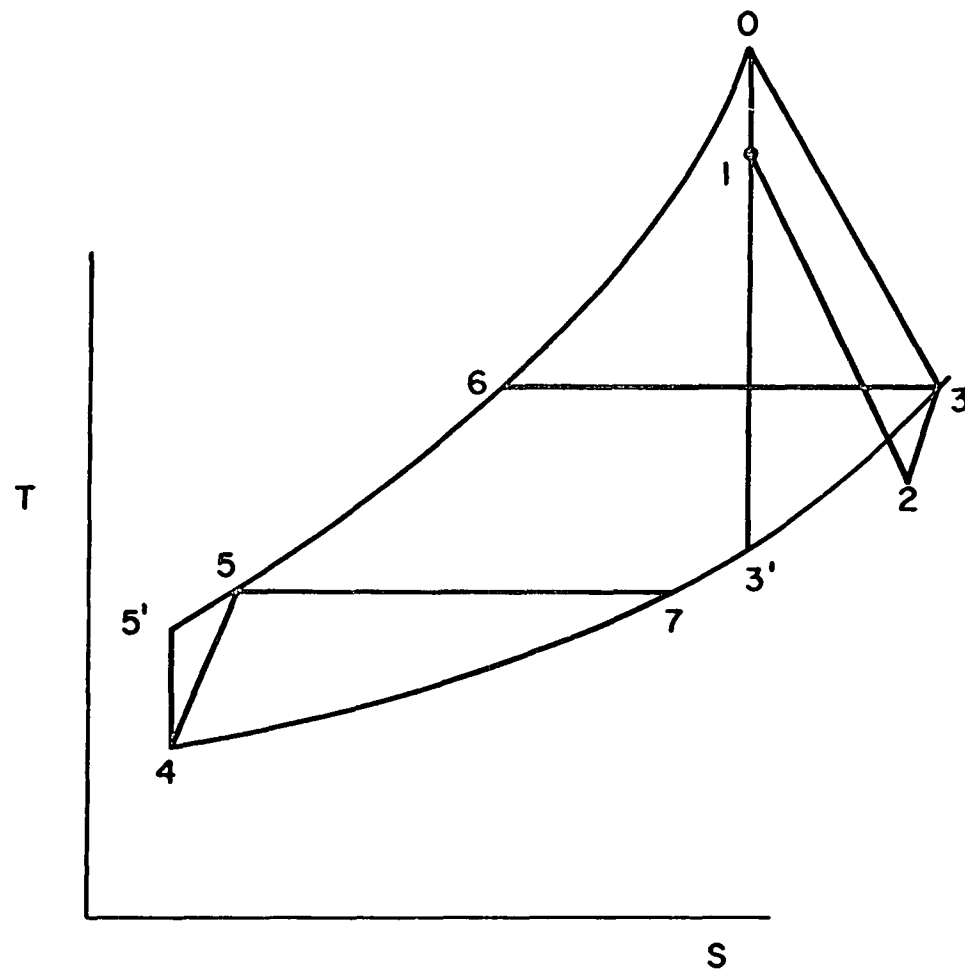
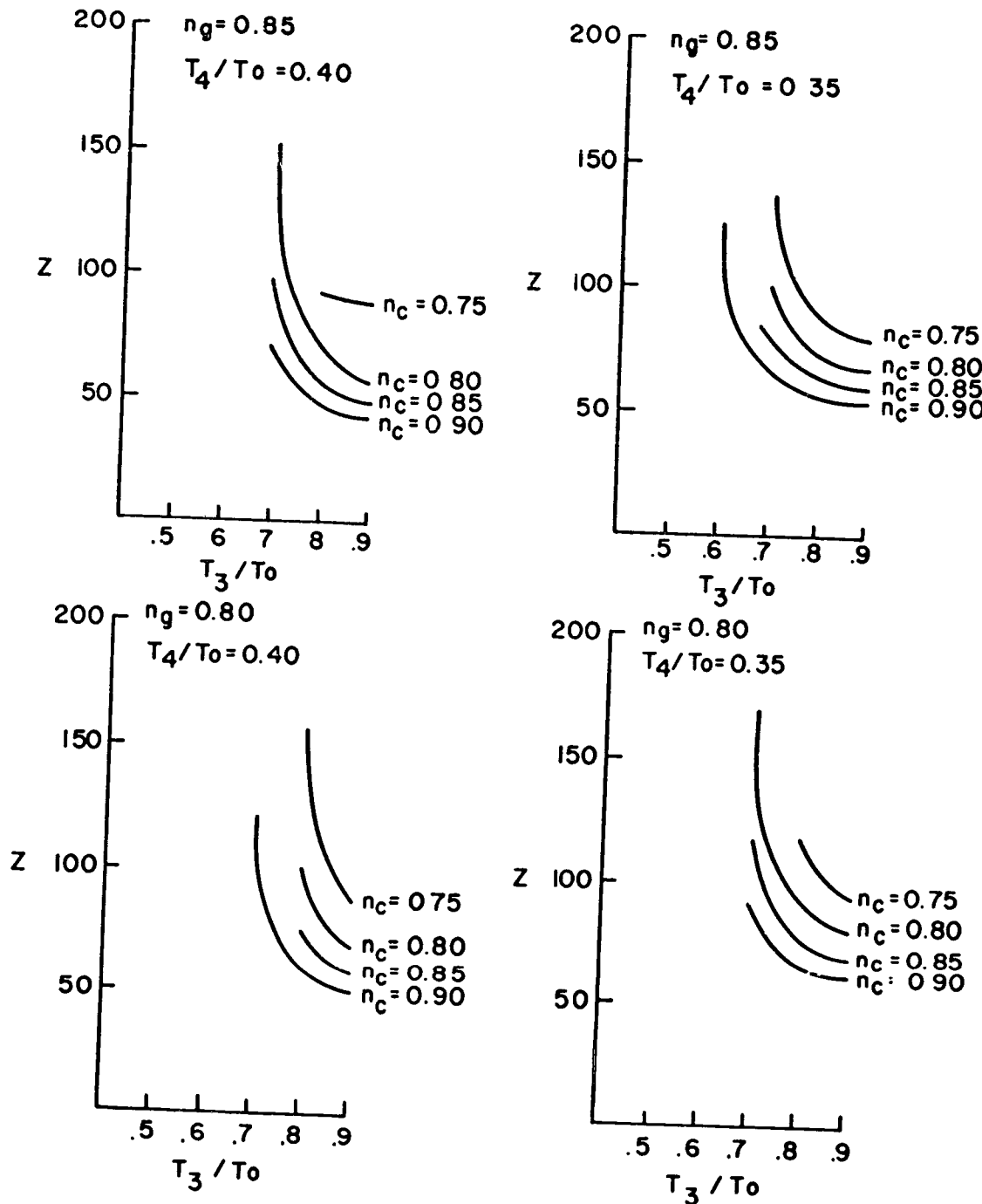
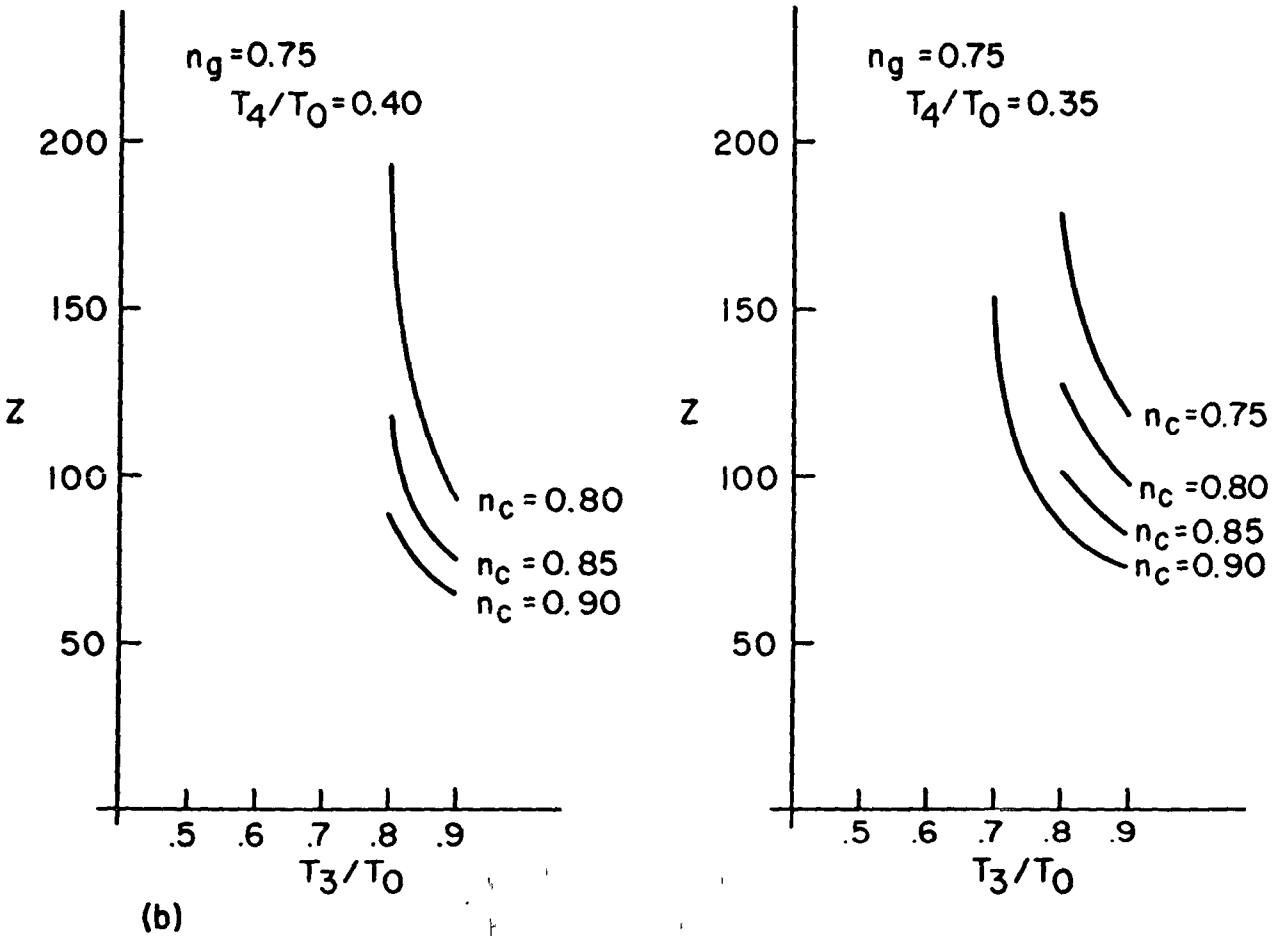


Figure 6. The regenerative Brayton (Gas Turbine) cycle.



(a)

Figure 7. Dimensionless radiator size parameter as a function of the generator temperature ratio for the Brayton cycle with an ideal regenerator. Lines of constant component efficiencies and compressor inlet temperature ratios.



**Figure 7.** Dimensionless radiator size parameter as a function of the generator temperature ratio for the Brayton cycle with an ideal regenerator. Lines of constant component efficiencies and compressor inlet temperature ratios.

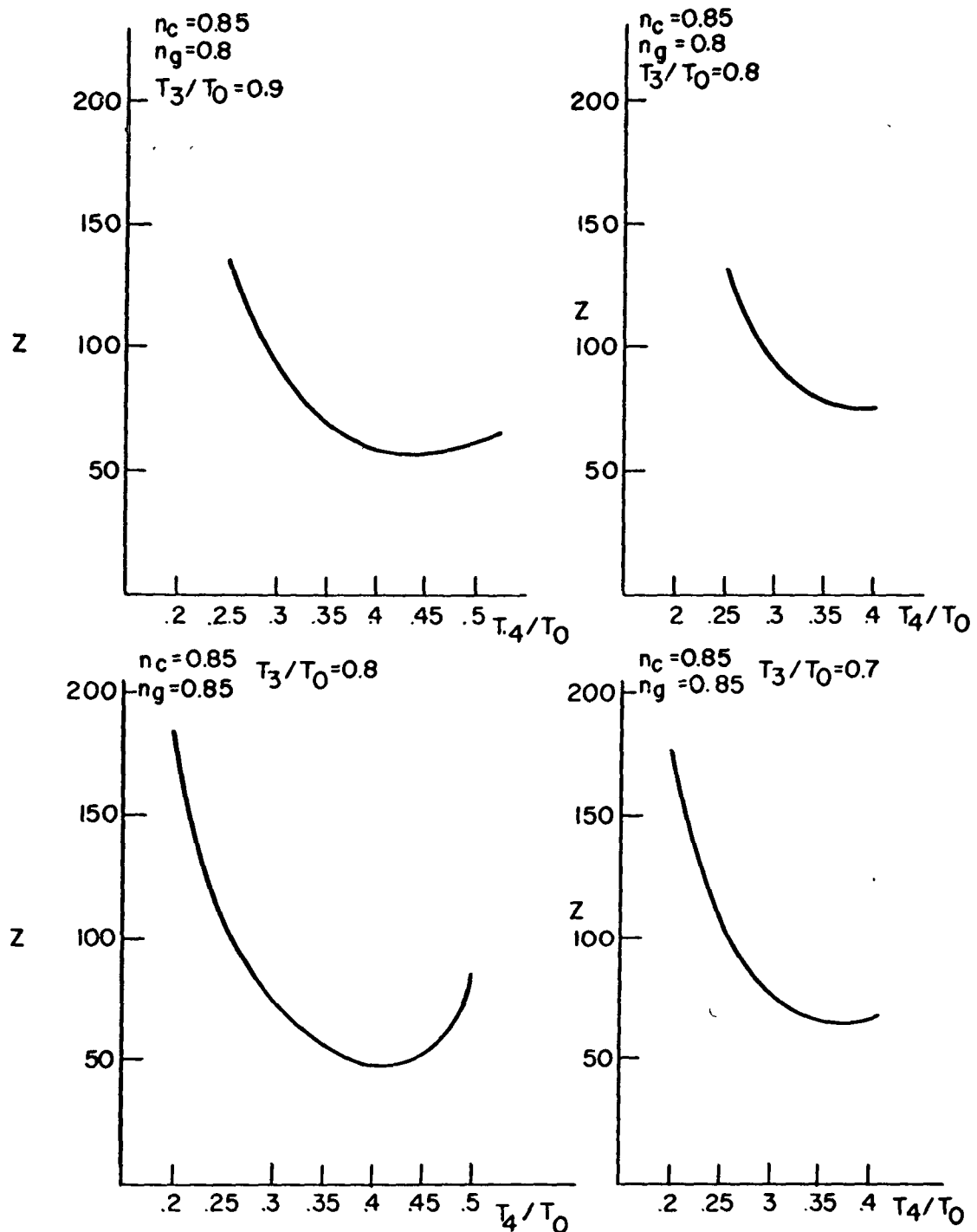
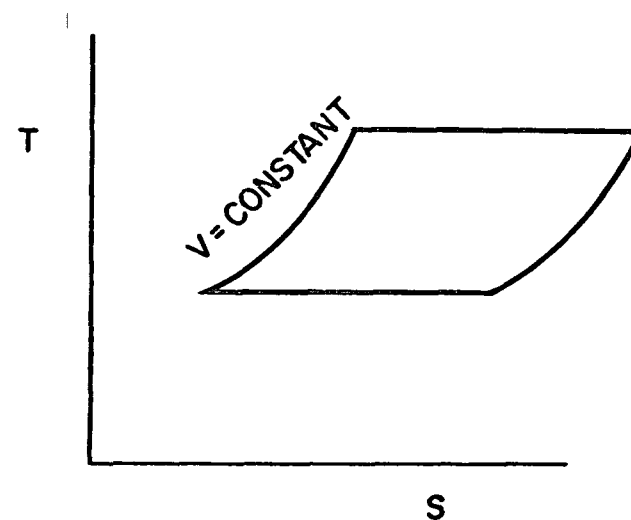
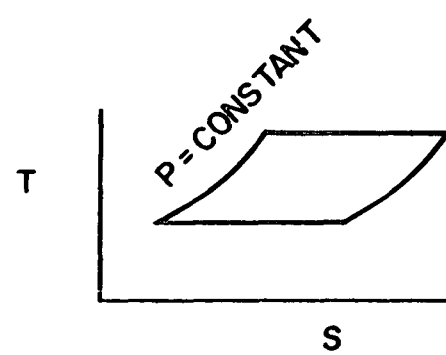


Figure 8. Dimensionless radiator size parameter as a function of the component temperature ratio for the Brayton cycle with an ideal regenerator. Lines of constant generator efficiencies and compressor inlet temperature ratios.

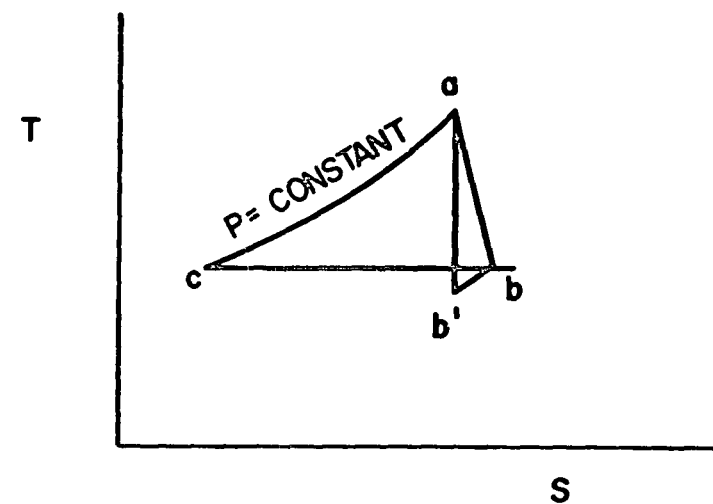


(a)

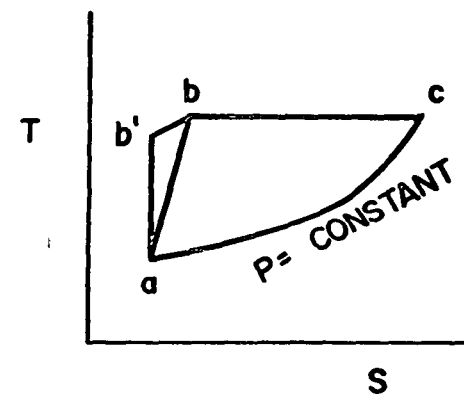


(b)

Figure 9. (a) The Stirling cycle; (b) The Ericsson cycle.



(a)



(b)

Figure 10. (a) Iso-thermal compression tri-cycle.  
(b) Iso-thermal expansion tri-cycle.

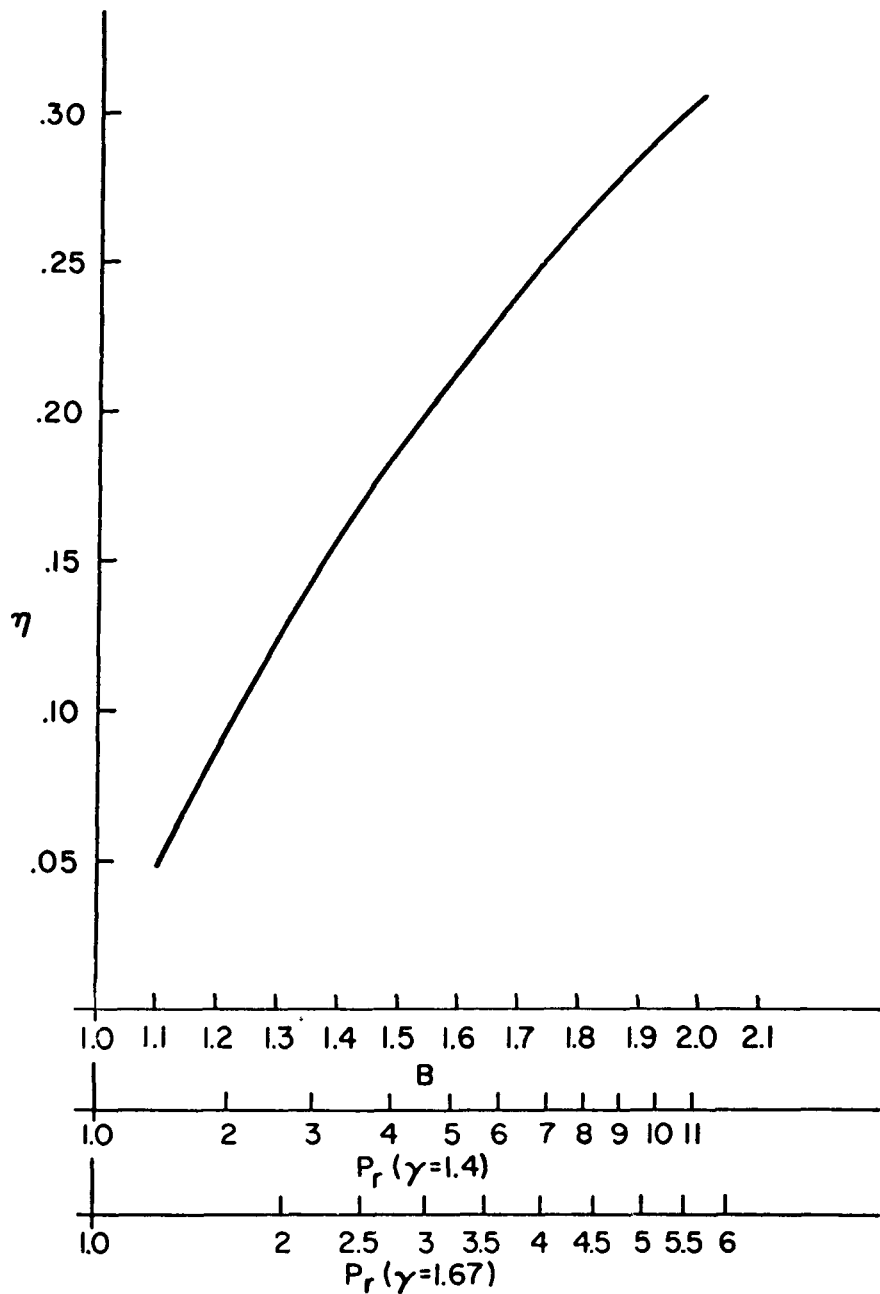


Figure 11. The efficiency of a reversible tri-cycle as a function of the temperature and pressure ratios.

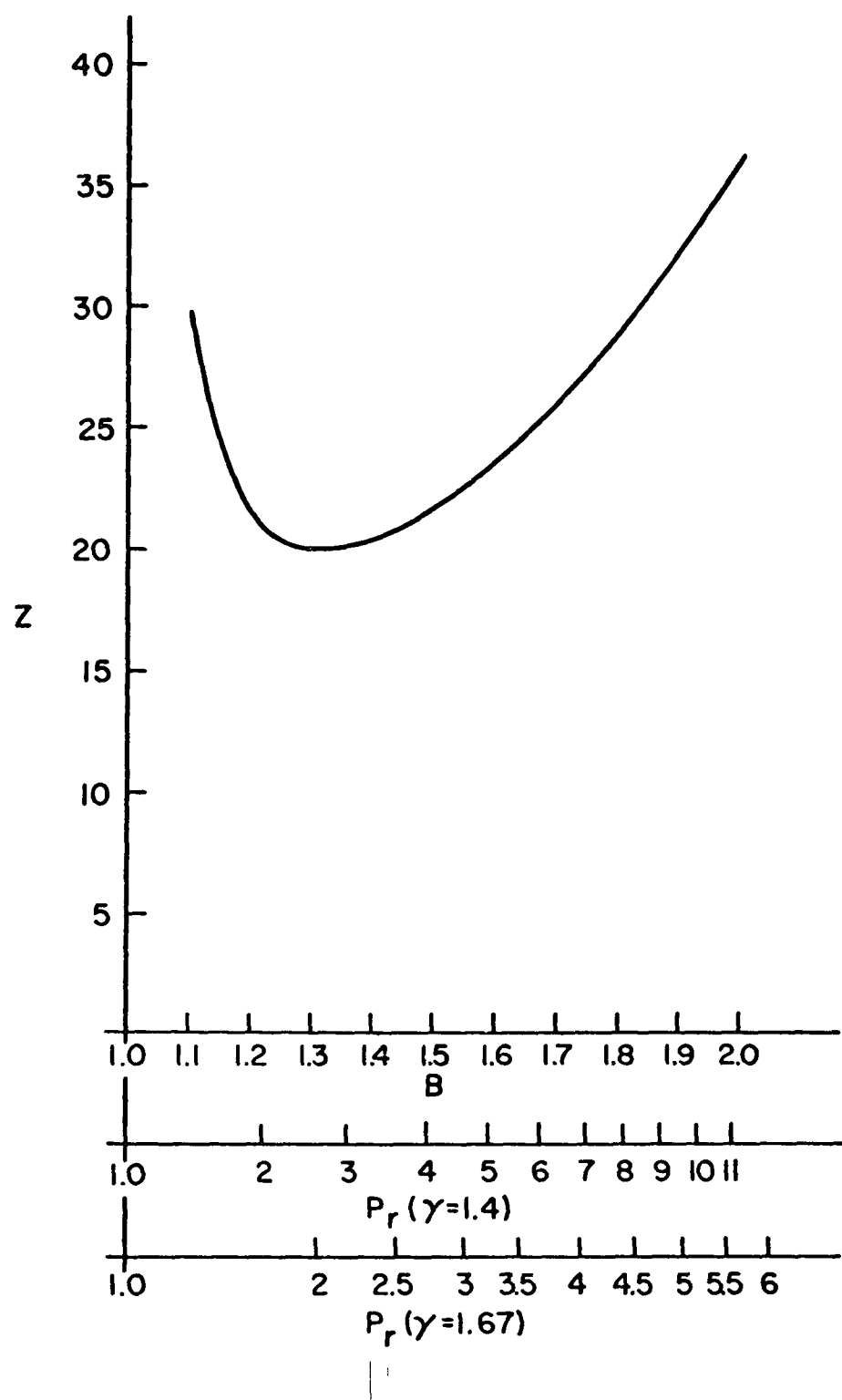


Figure 12. The radiator parameter of a reversible tri-cycle with isothermal compression as a function of the temperature and pressure ratios.

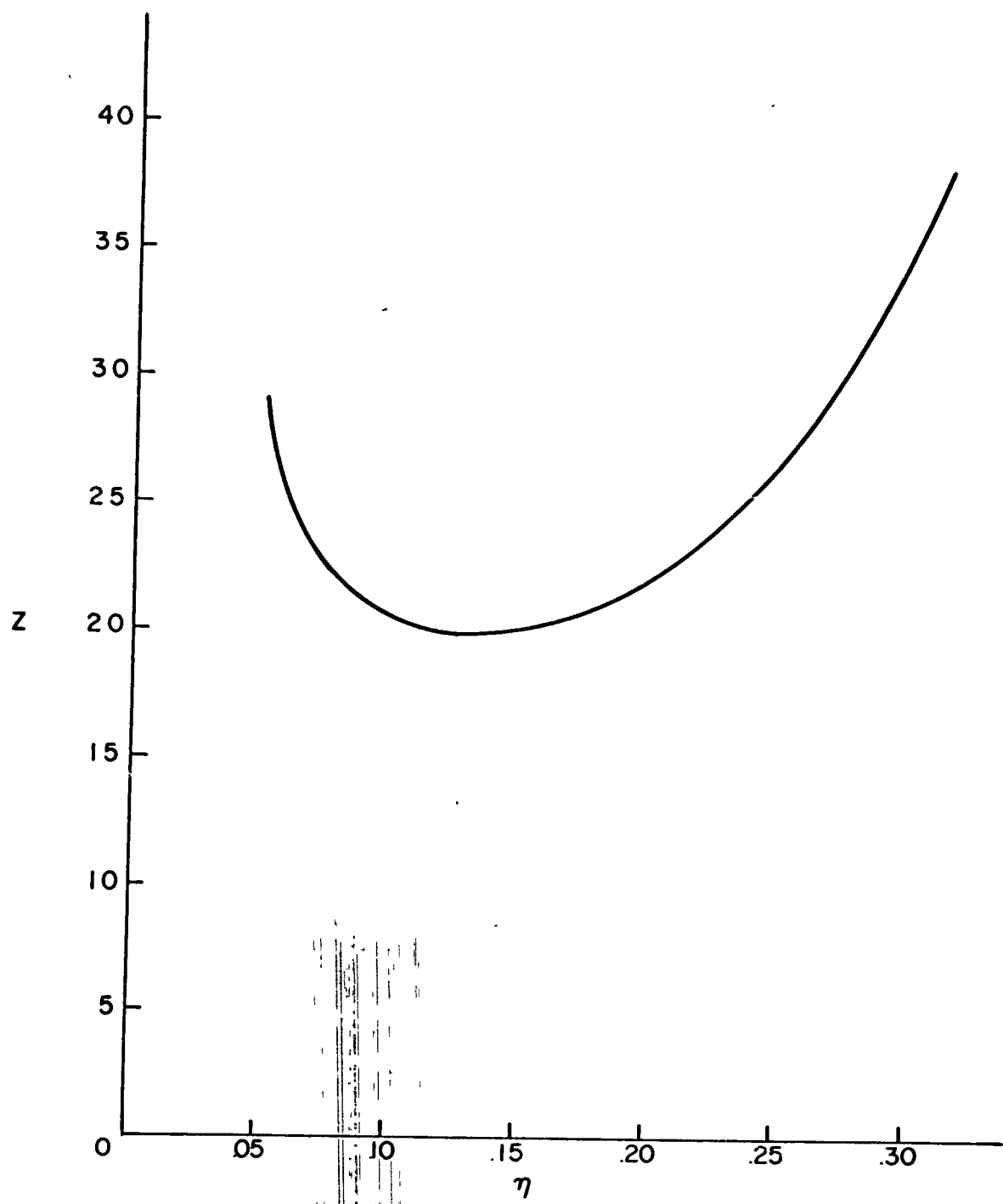


Figure 13. Radiator parameter of a reversible tri-cycle with isothermal expansion as a function of the thermodynamic efficiency.

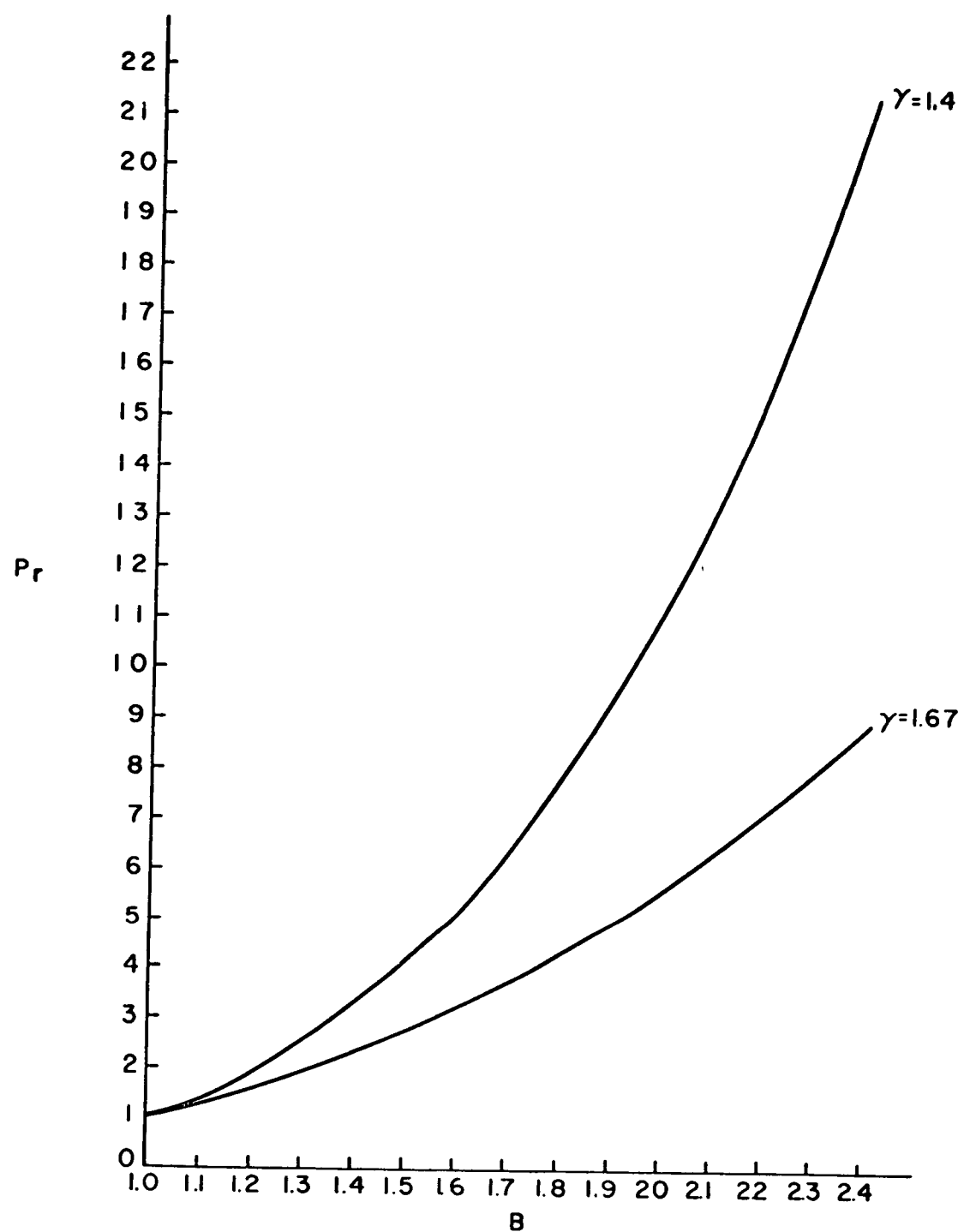


Figure 14. Pressure ratio as a function of expansion temperature ratio.

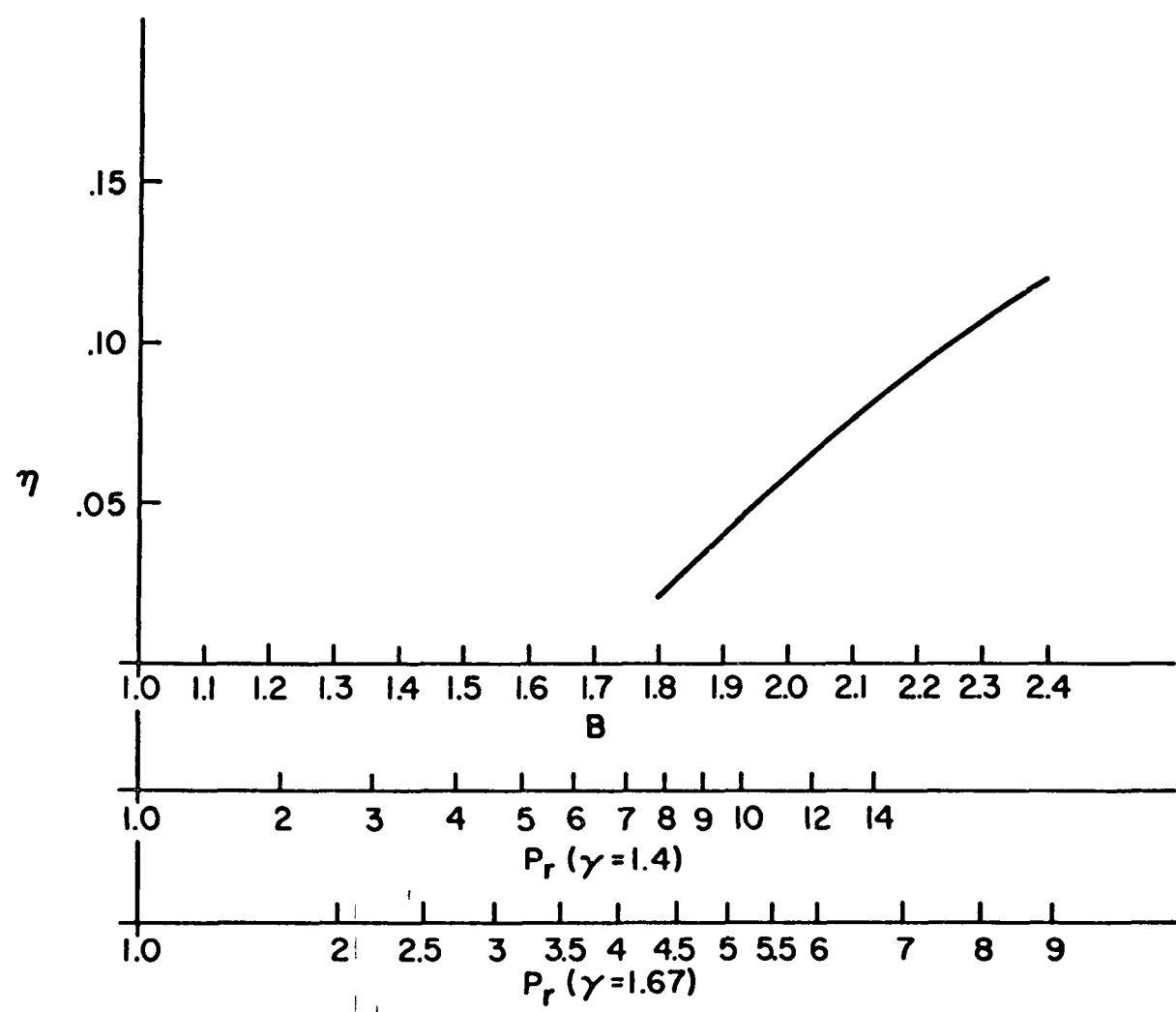


Figure 15. Efficiency of an isothermal compressor tri-cycle with 90% efficient components as a function of the temperature and pressure ratios.

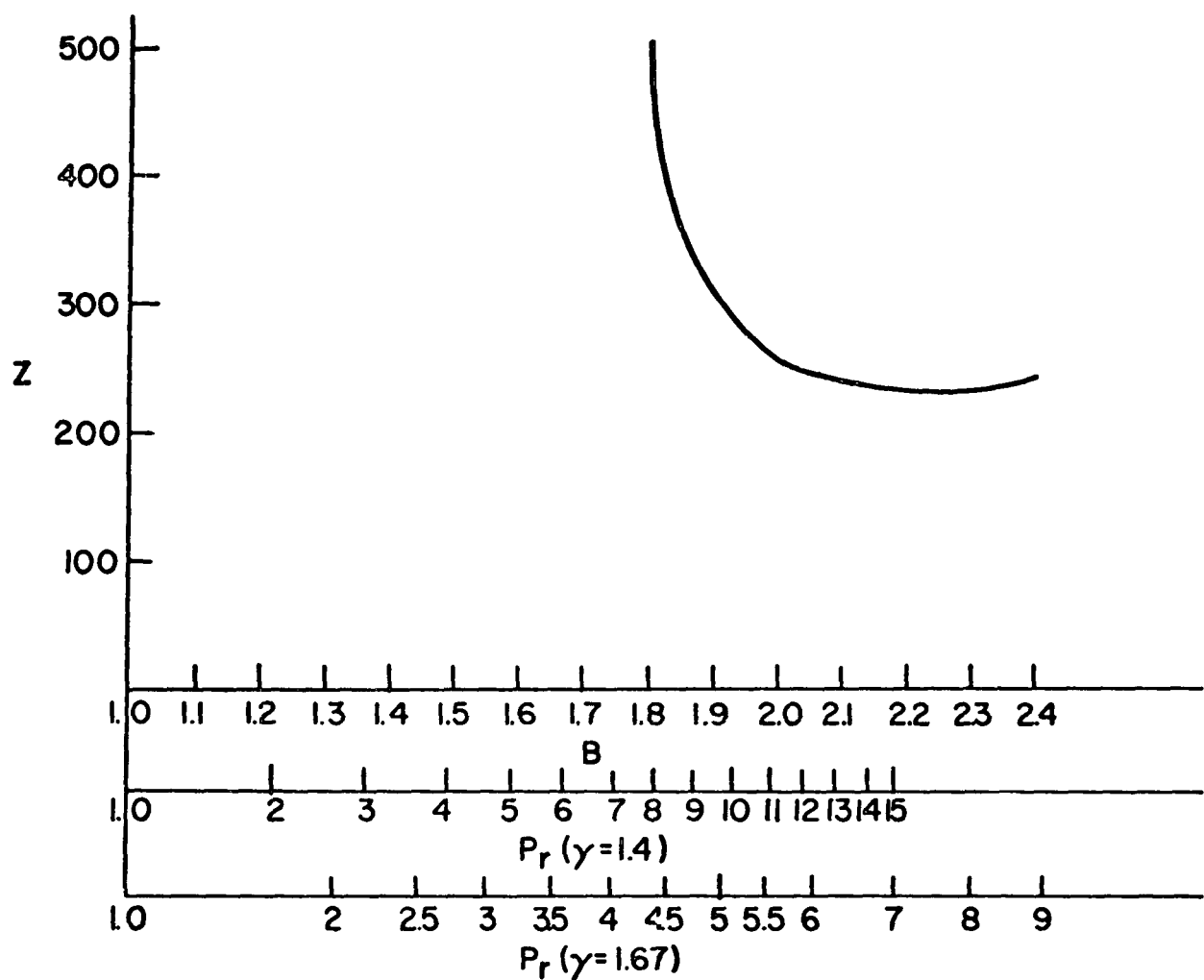


Figure 16. Radiator parameter of an iso-thermal compression tri-cycle with 90% efficient components as a function of the temperature and pressure ratios.

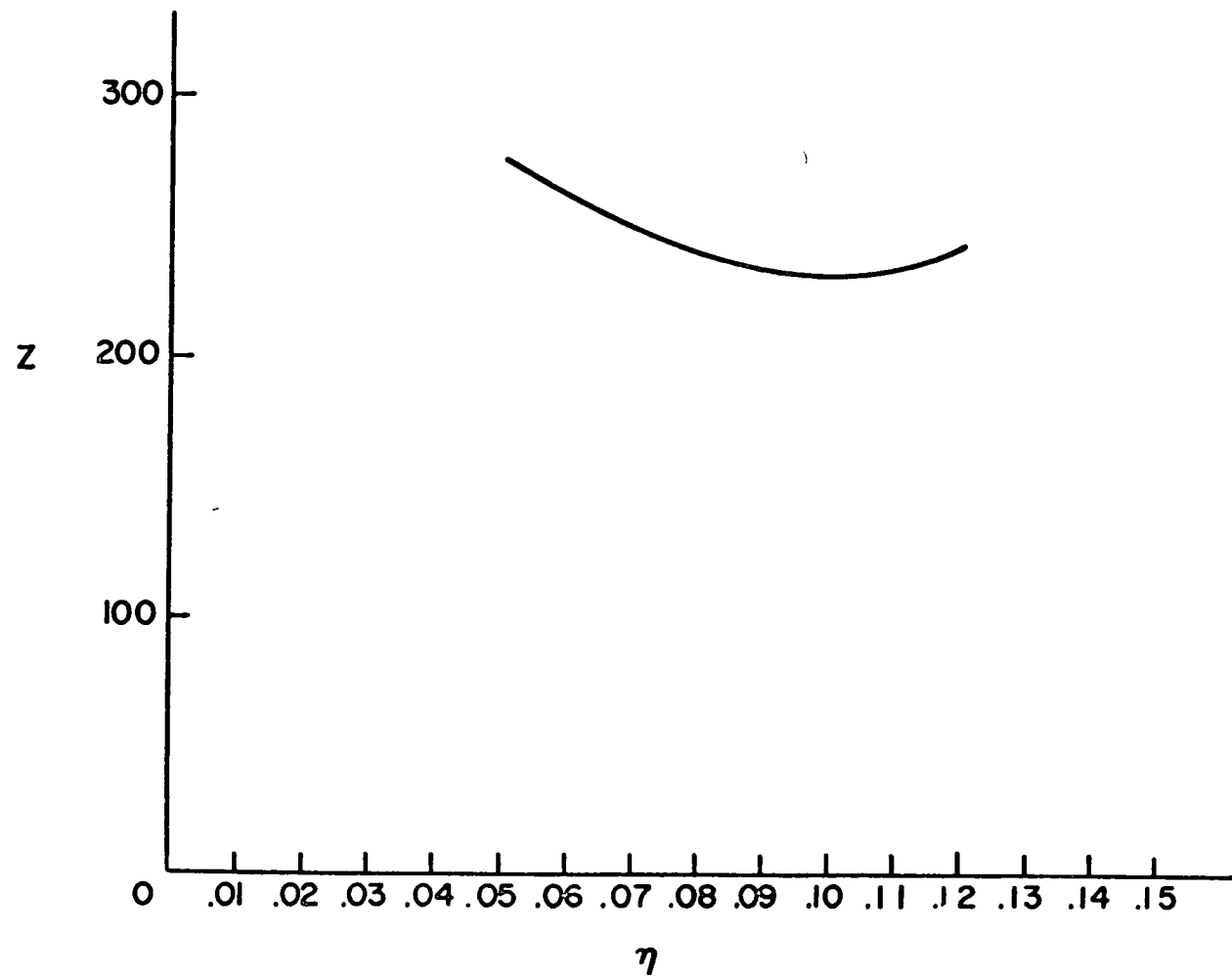


Figure 17. Radiator parameter of an isothermal compression tri-cycles with 90% efficient components, as a function of the cycle efficiency.

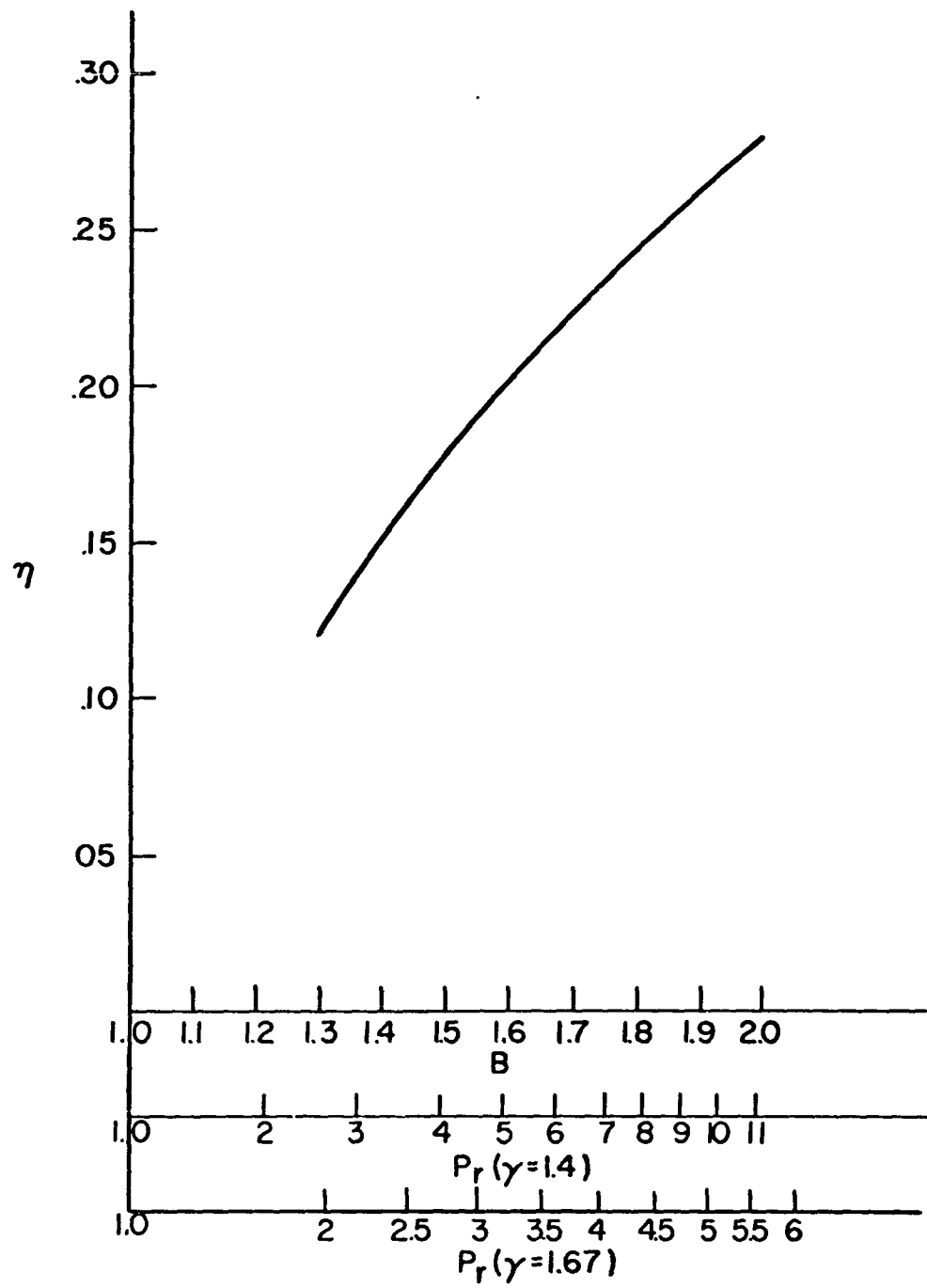


Figure 18. The efficiency of a reversible tri-cycle with isothermal expansion as a function of the temperature and pressure ratios.

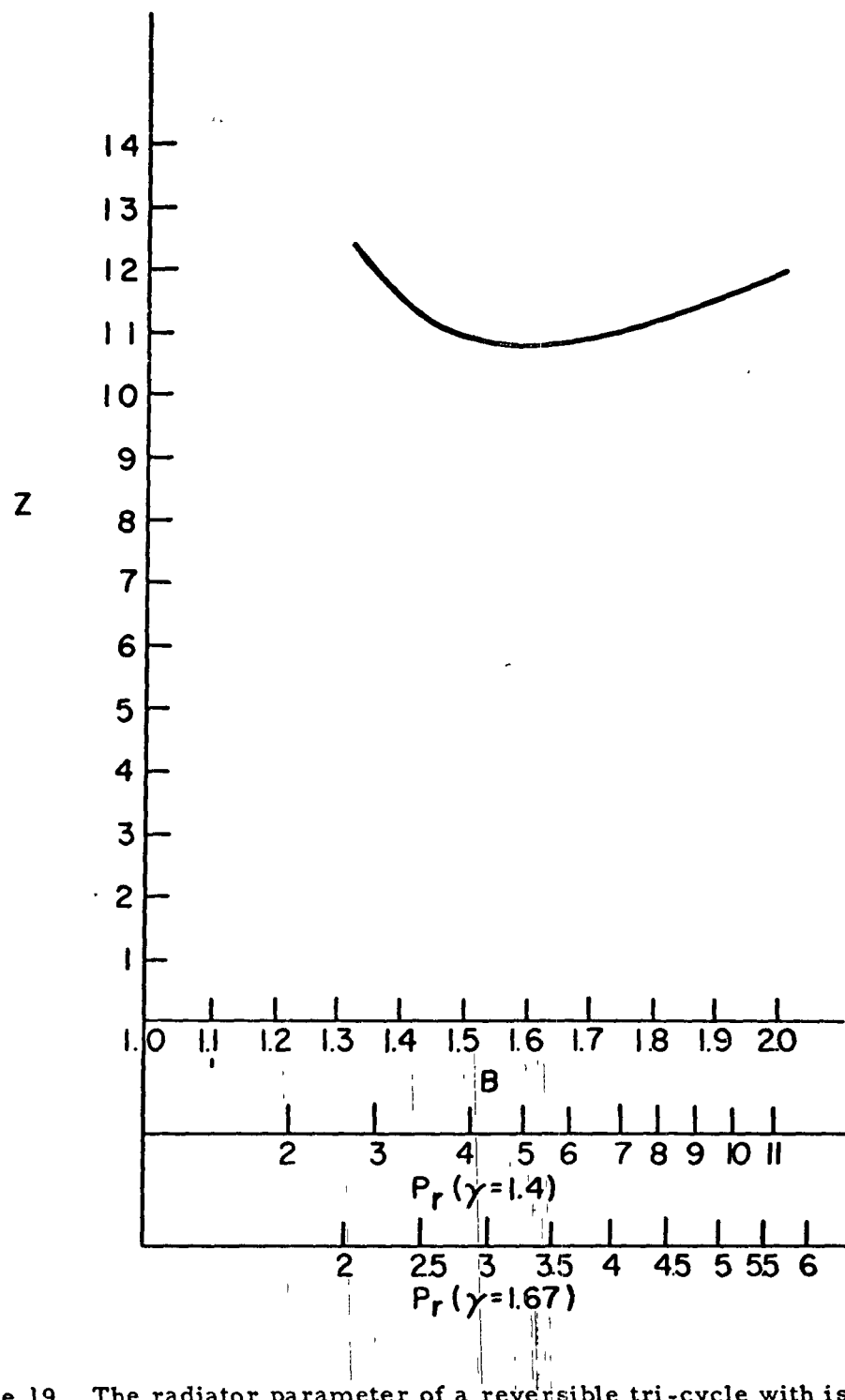


Figure 19. The radiator parameter of a reversible tri-cycle with isothermal expansion as a function of the temperature and pressure ratios.

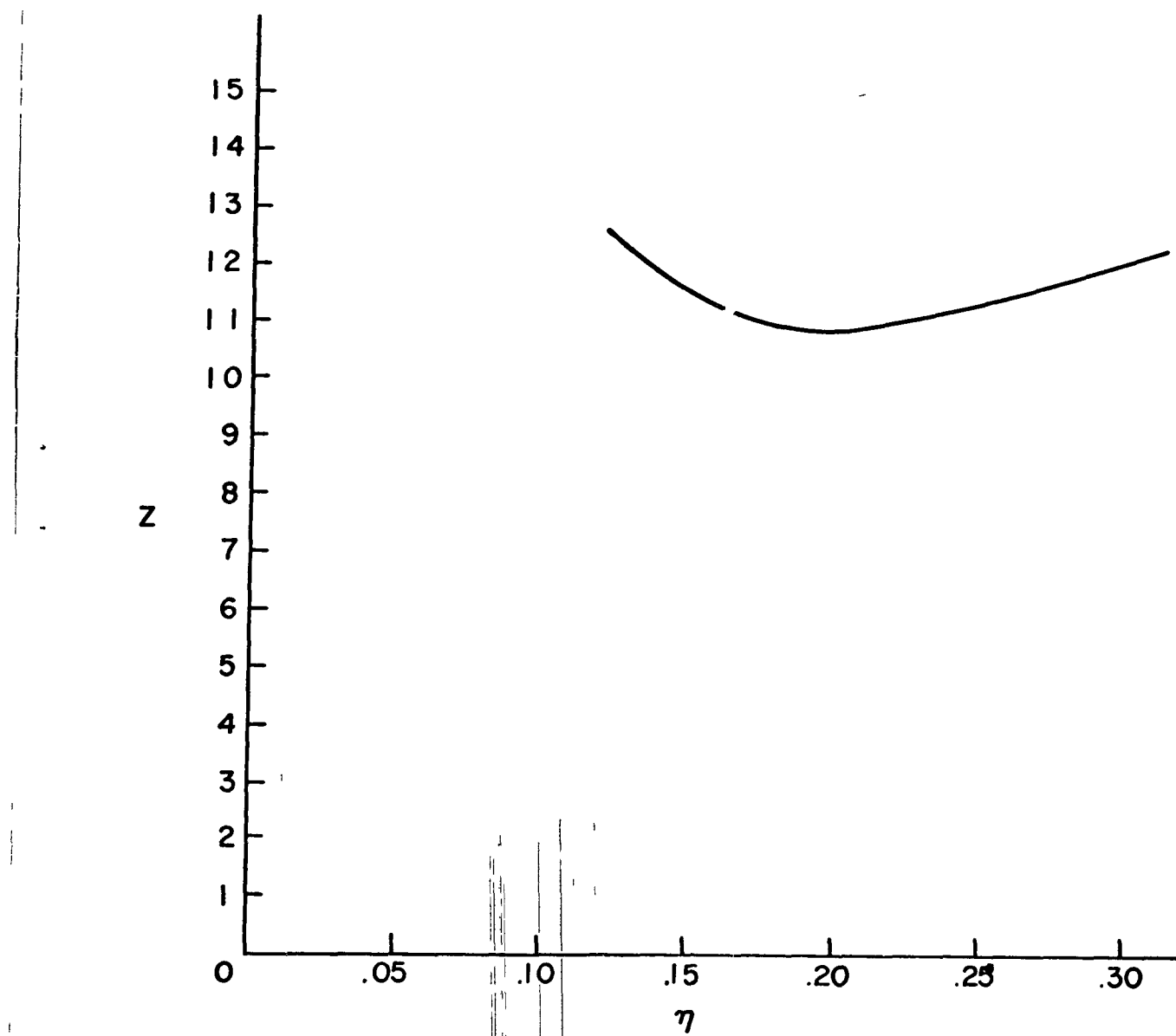
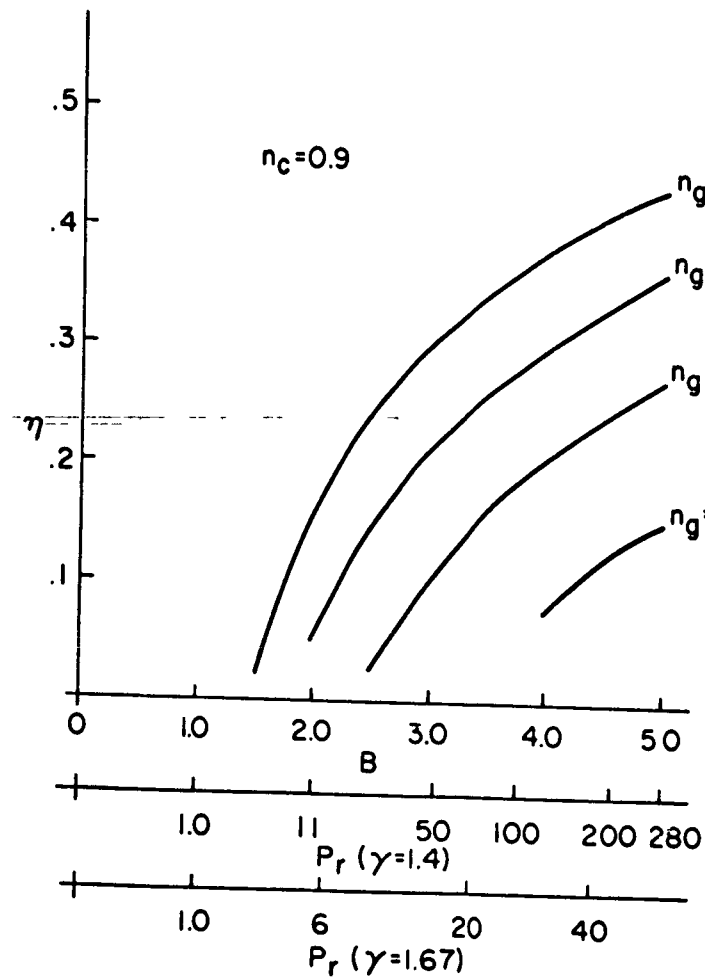
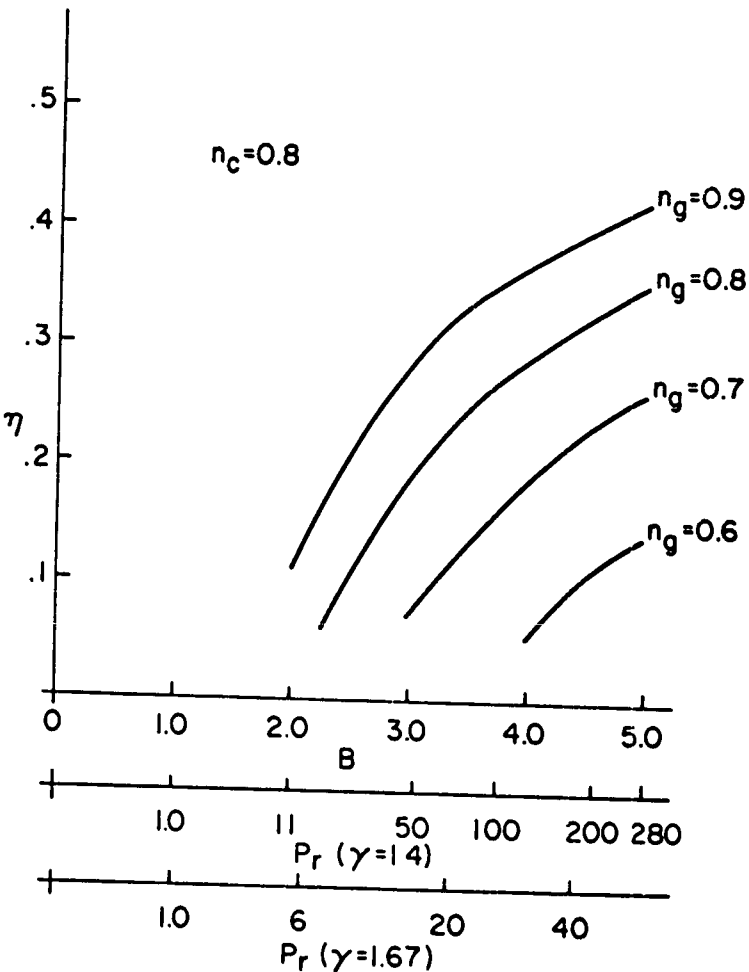


Figure 20. The radiator parameter of a reversible tri-cycle with isothermal expansion as a function of the cycle efficiency.

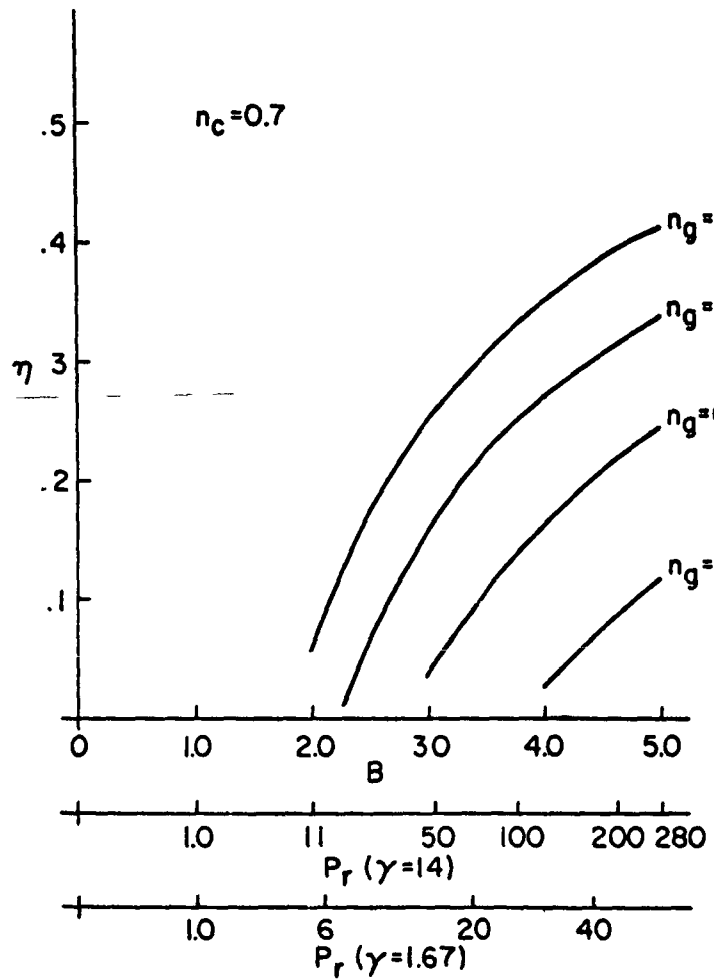


(a)

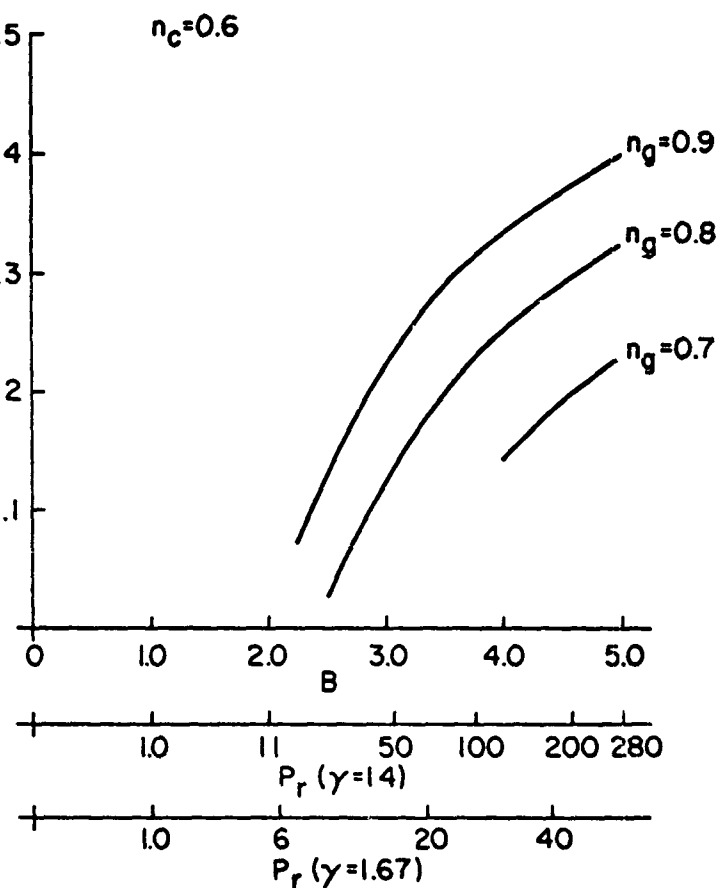


(b)

Figure 21. The efficiency of irreversible isothermal expansion tri-cycles as a function of the temperature and pressure ratios.



(c)



(d)

Figure 21. The efficiency of irreversible isothermal expansion tri-cycles as a function of the temperature and pressure ratios.

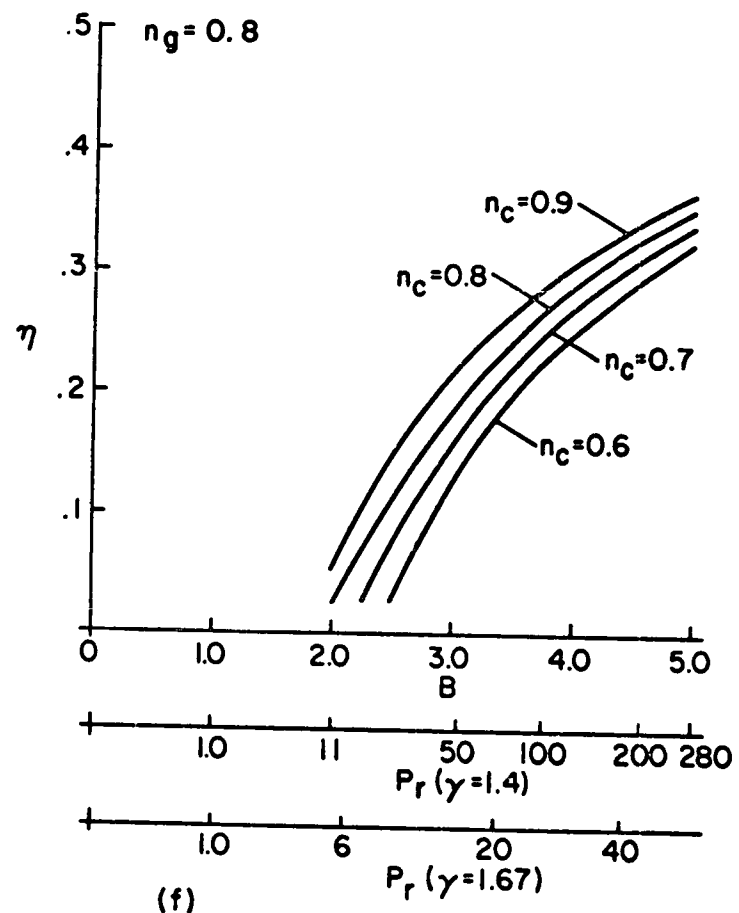
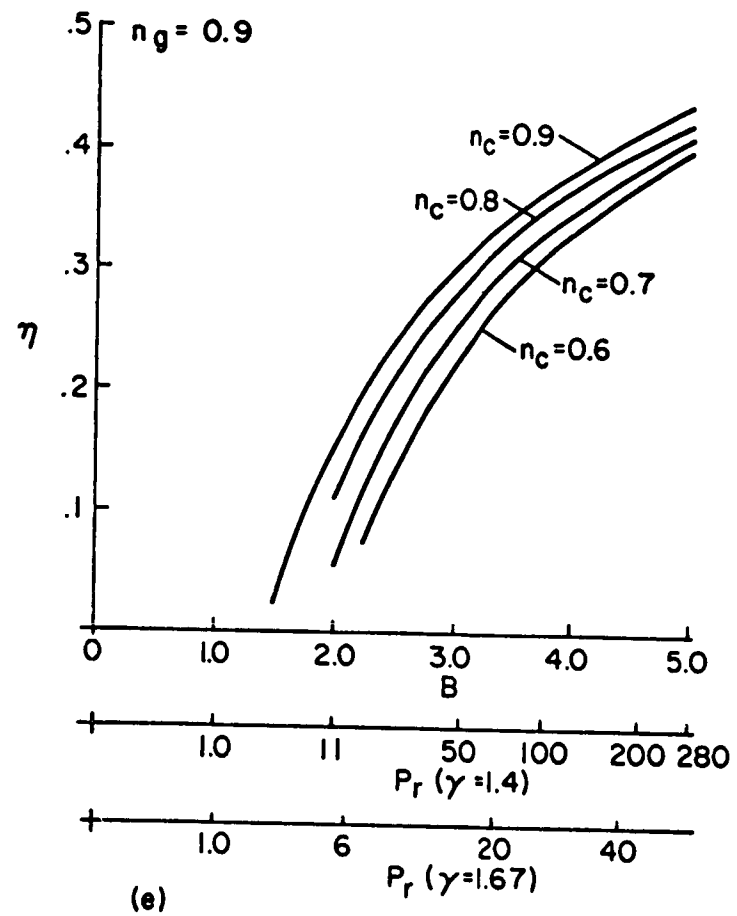
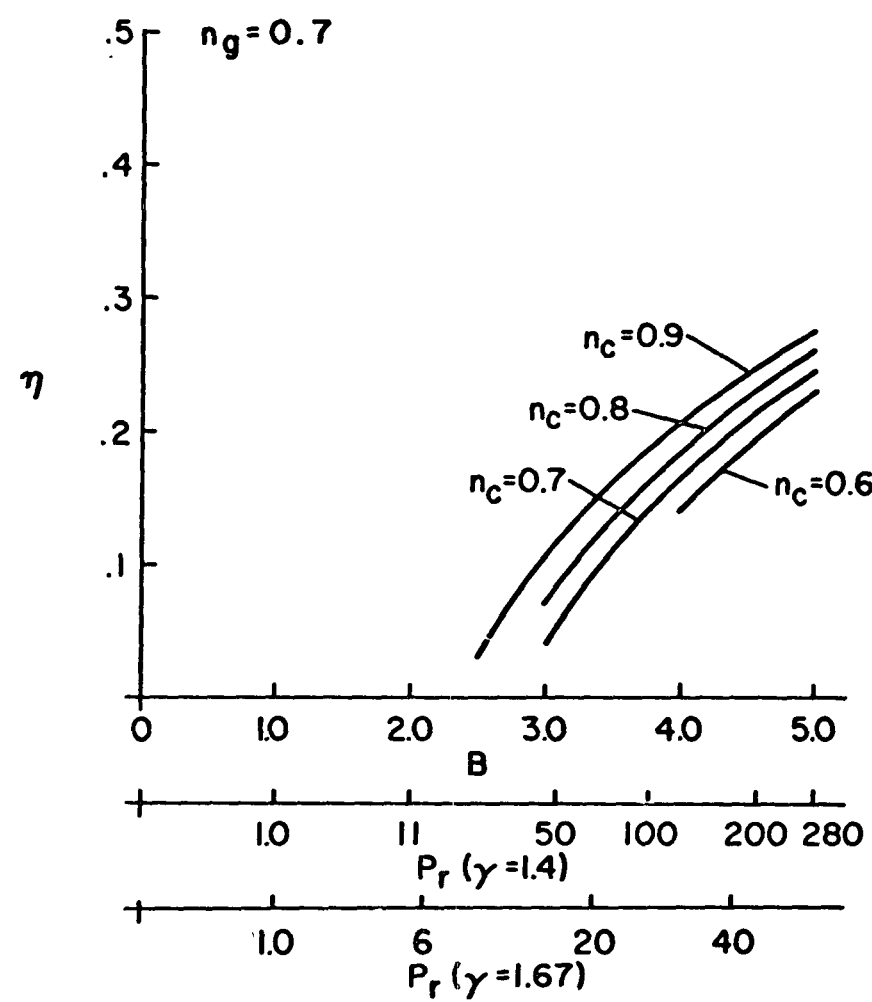
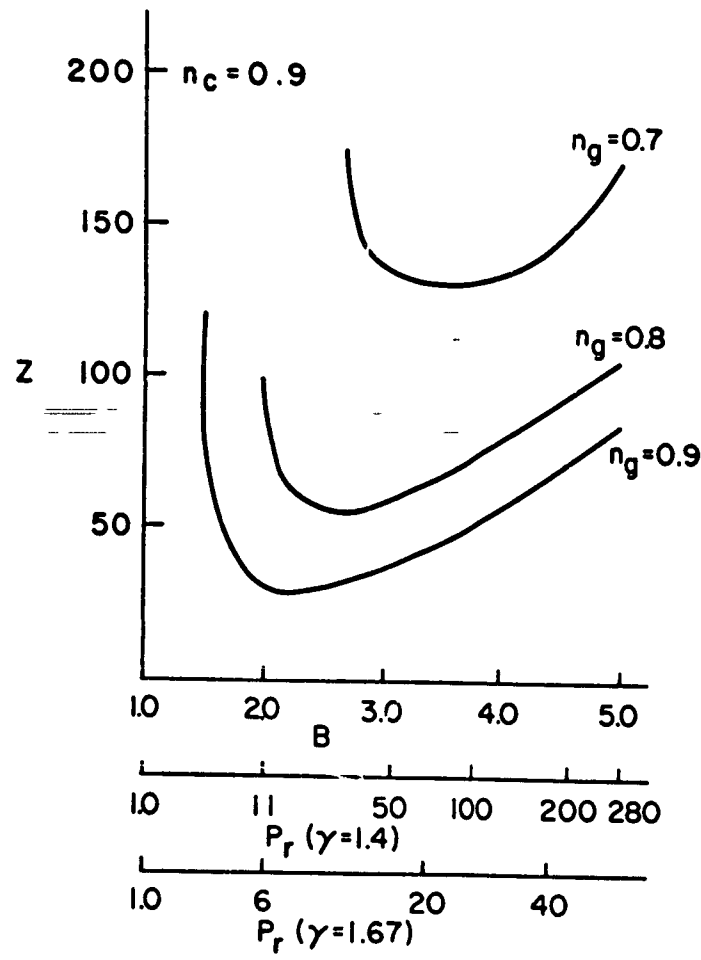


Figure 21. The efficiency of irreversible isothermal expansion tri-cycles as a function of the temperature and pressure ratios.

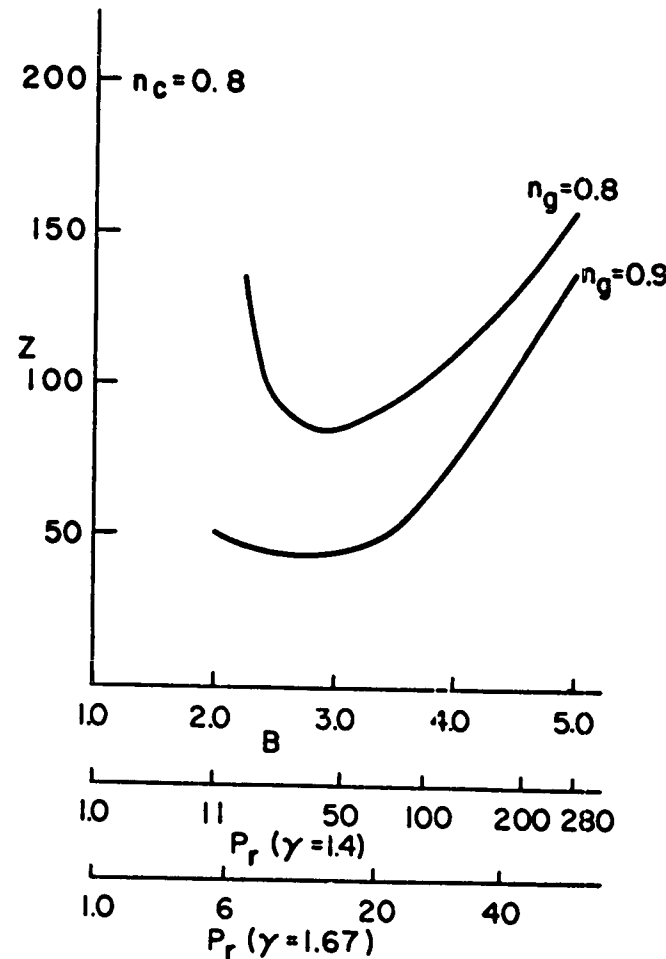


(g)

Figure 21. The efficiency of irreversible isothermal expansion tri-cycles as a function of the temperature and pressure ratios.

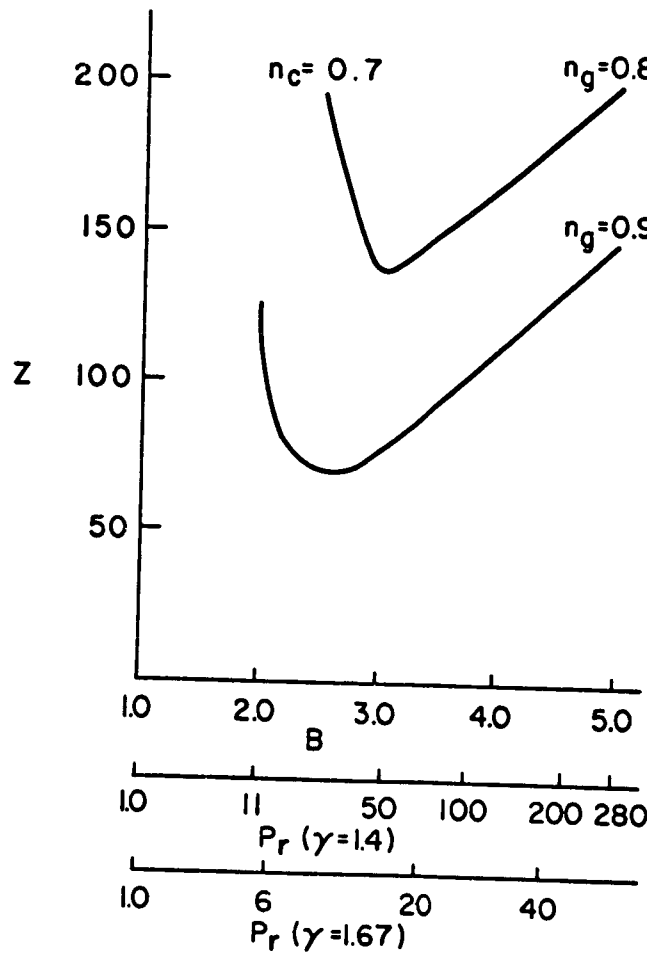


(a)

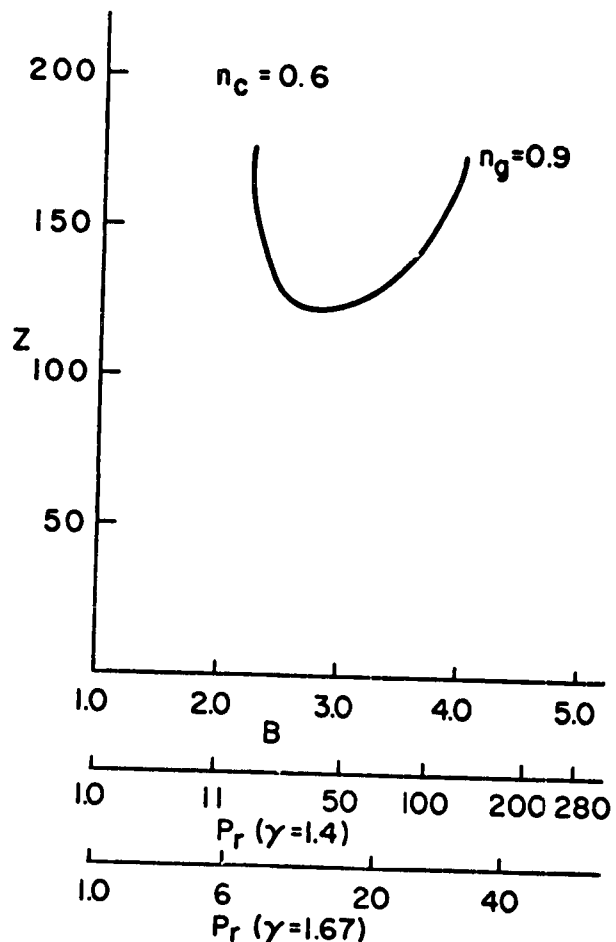


(b)

Figure 22. Radiator parameter of irreversible isothermal expansion tri-cycle as a function of the temperature and pressure ratios.

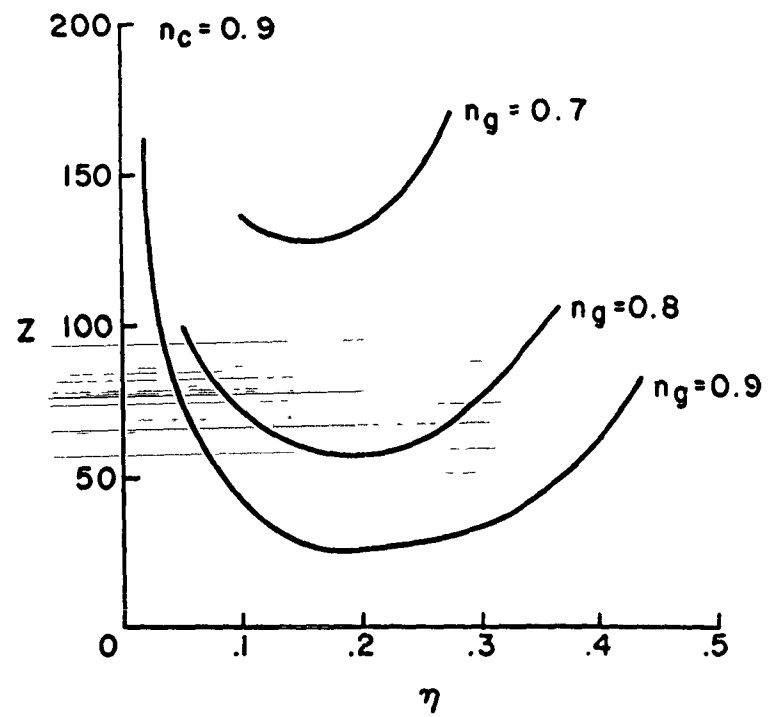


(c)

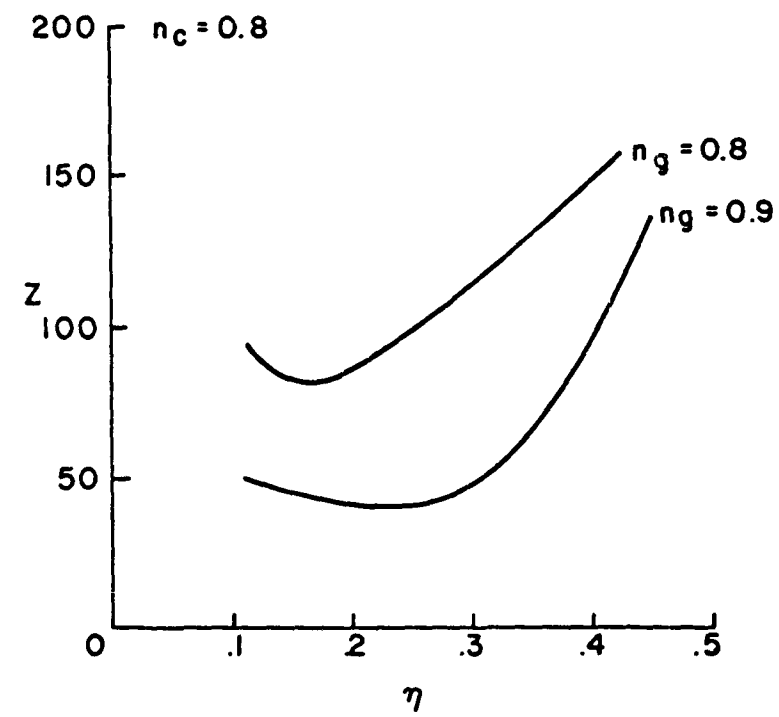


(d)

Figure 22. Radiator parameter of irreversible isothermal expansion tri-cycle as a function of the temperature and pressure ratios.

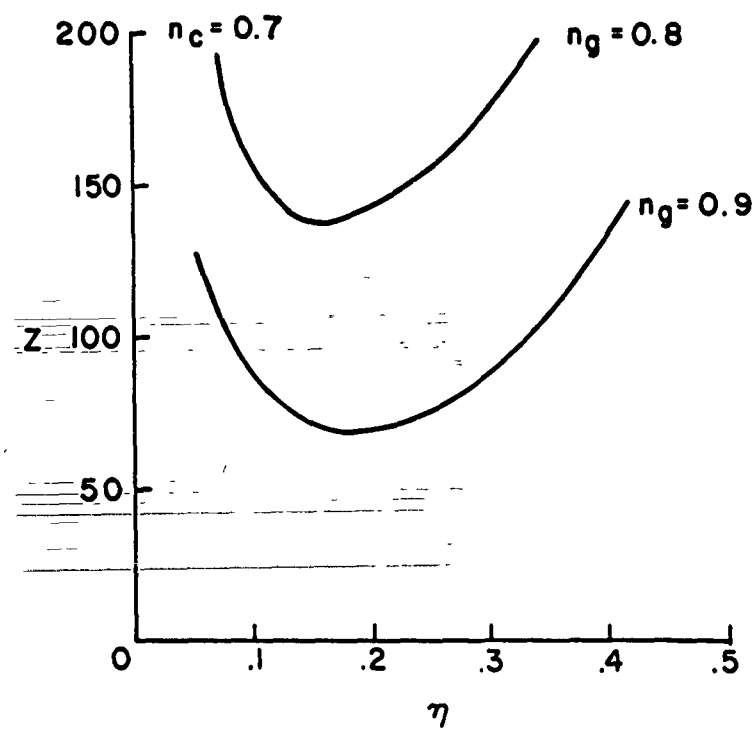


(a)

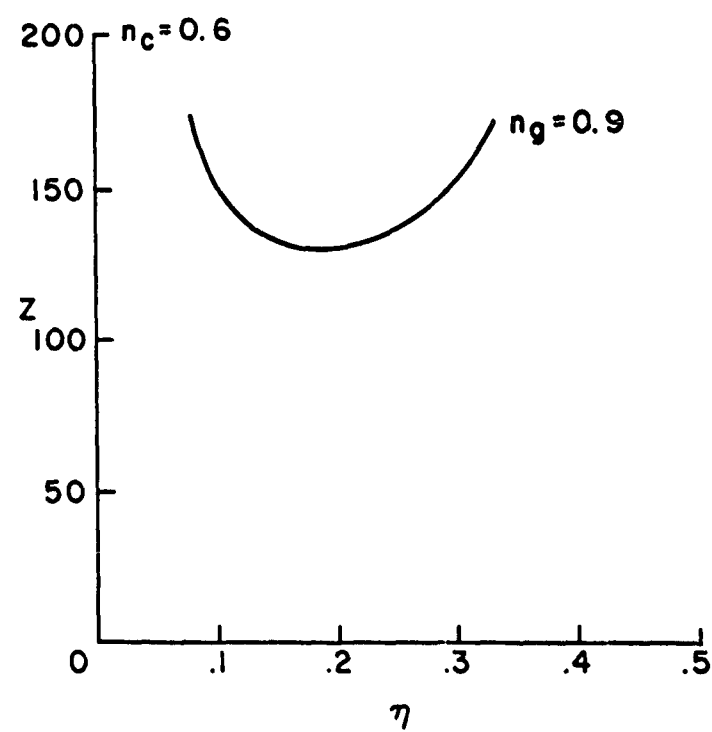


(b)

Figure 23. Radiator parameter of irreversible isothermal expansion tri-cycle as a function of the cycle efficiency.



(c)



(d)

Figure 23. Radiator parameter of irreversible isothermal expansion tri-cycle as a function of the cycle efficiency.

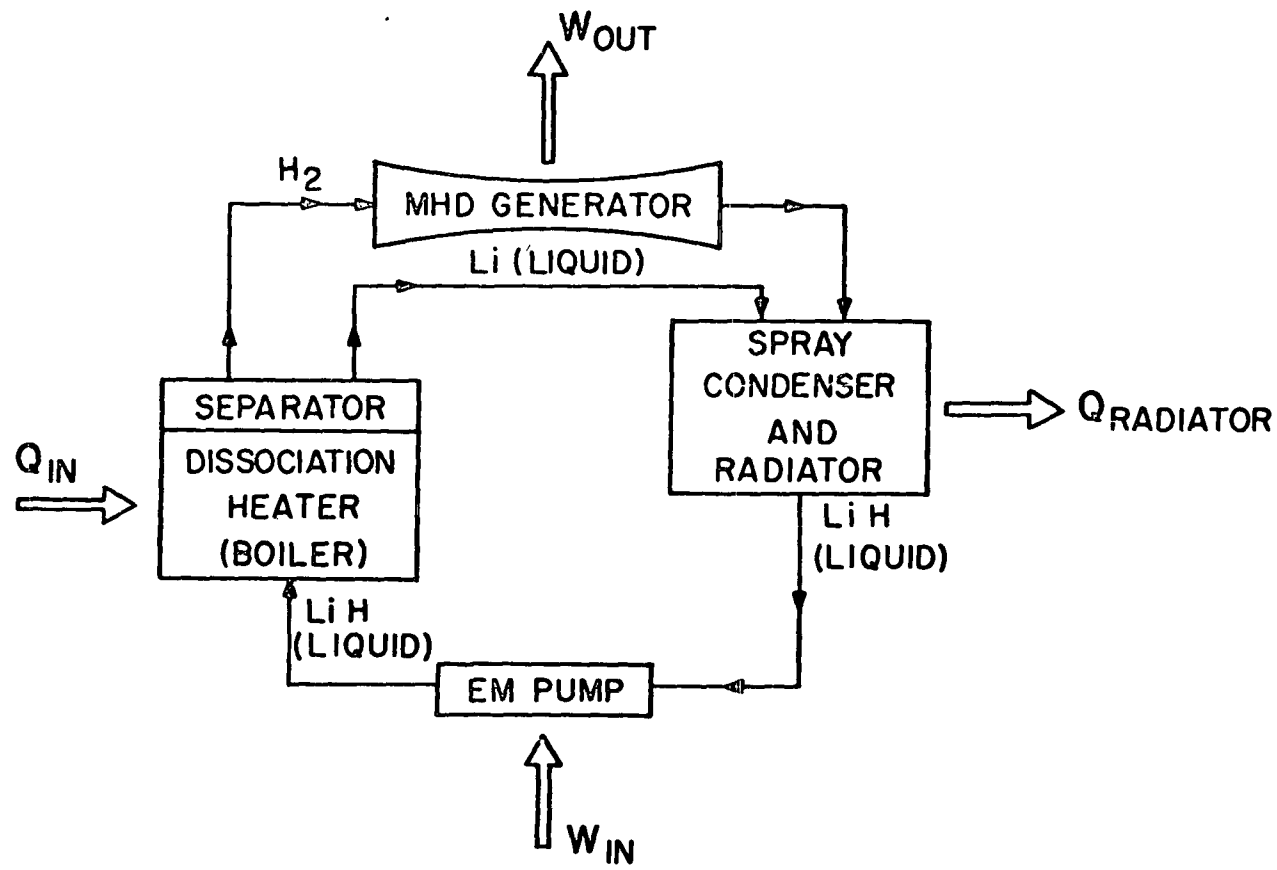
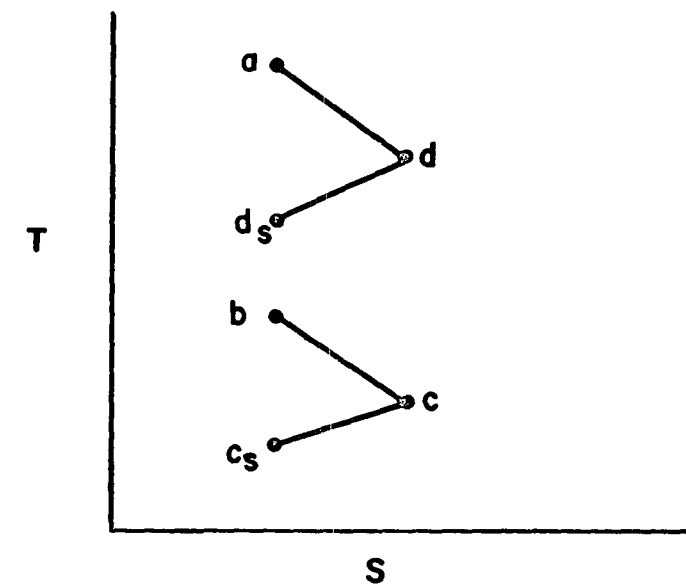


Figure 24. Li H Dissociation cycle.



**Figure 25.** Stagnation and local temperature described states in an MHD generator.

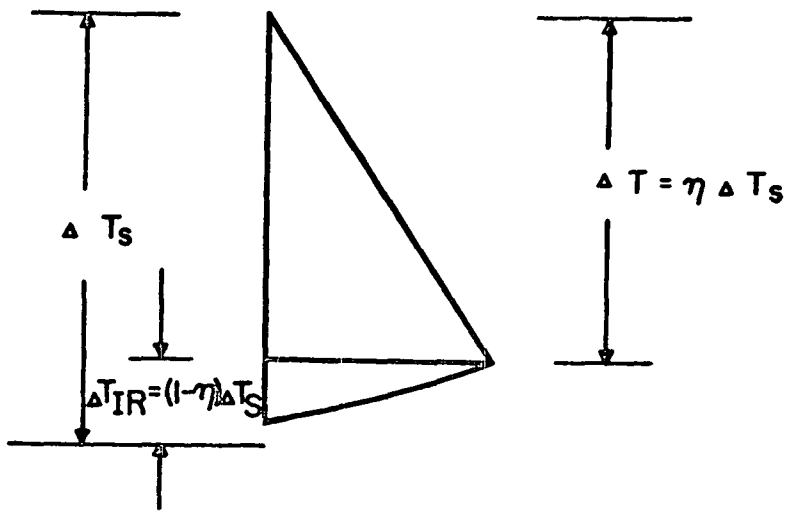


Figure 26. Temperature-entropy triangle.

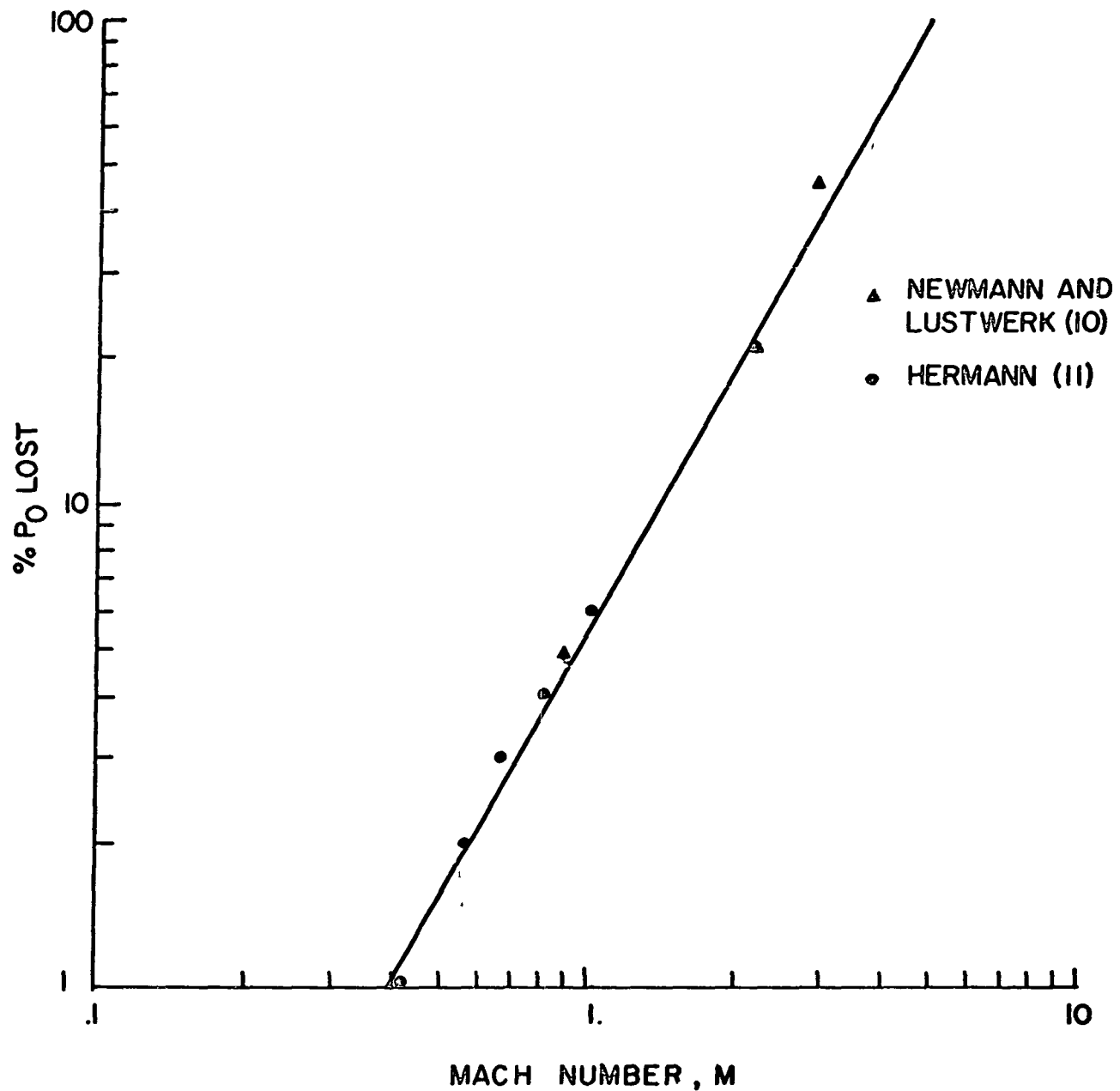


Figure 27. Percent of stagnation pressure lost in compressible flow diffusers as a function of the diffuser inlet mach number.

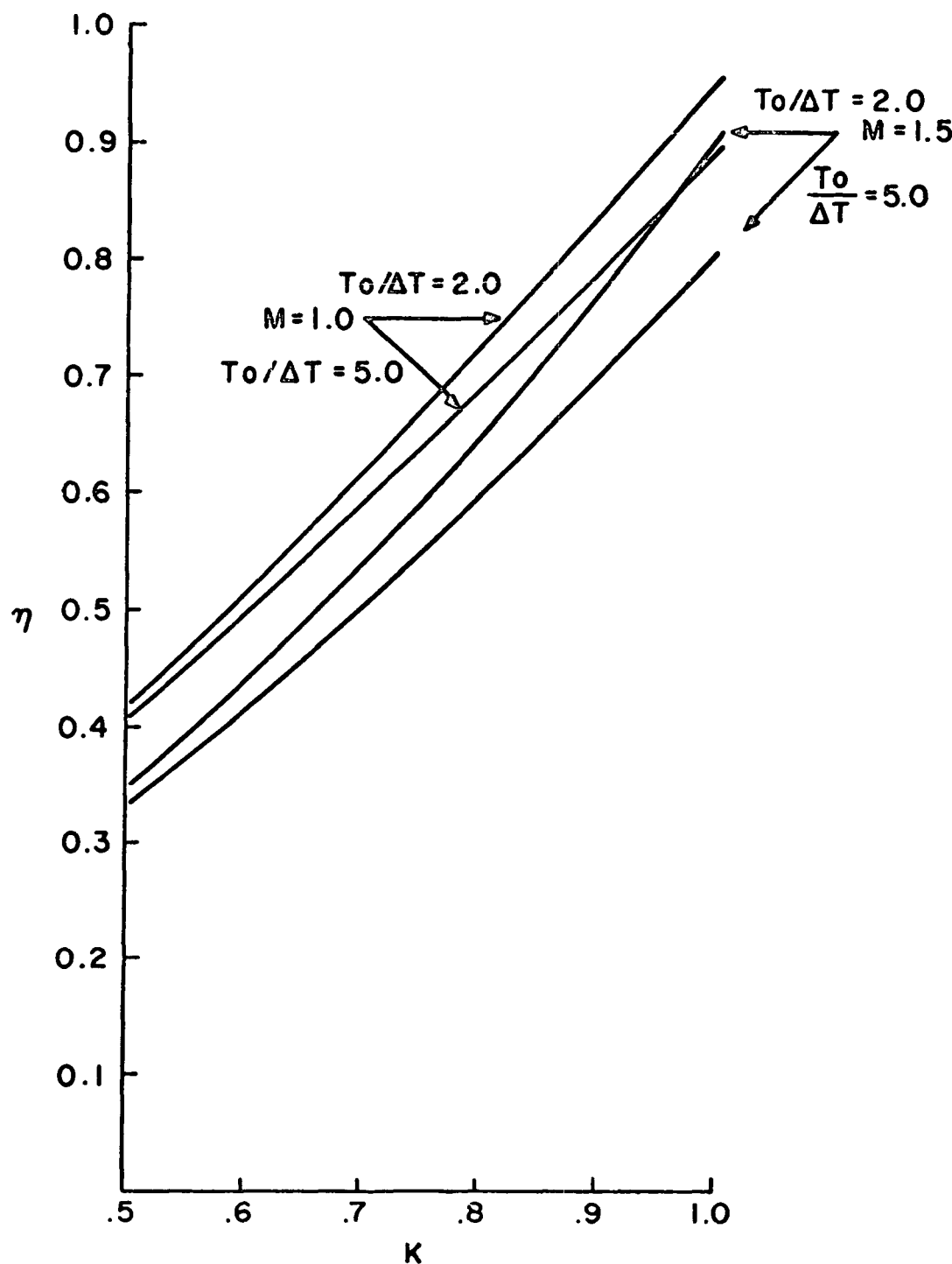


Figure 28. Over-all efficiency as a function of loading factor for various mach numbers and temperature ratios.

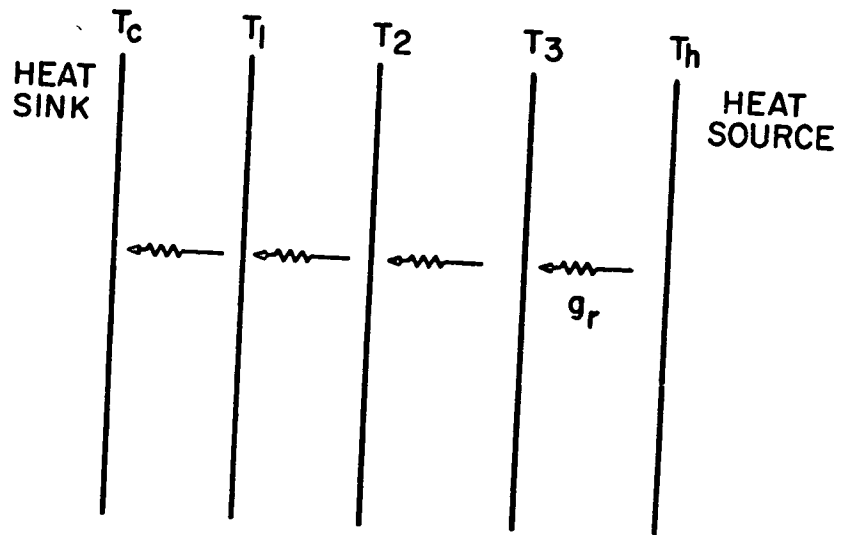


Figure 29. Radiative heat fluxes between parallel planes.

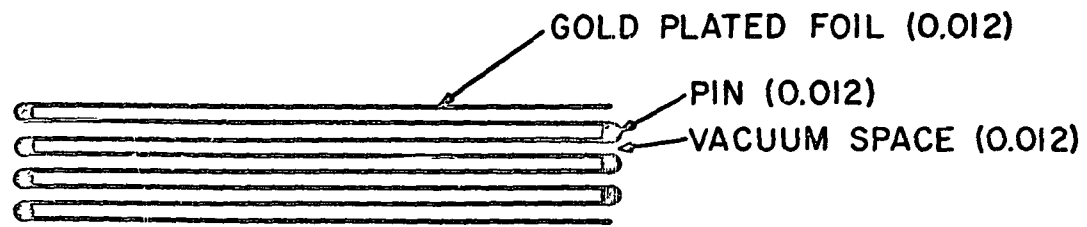


Figure 30. (a) Multiple radiation shield construction - ribbon wound on pins.

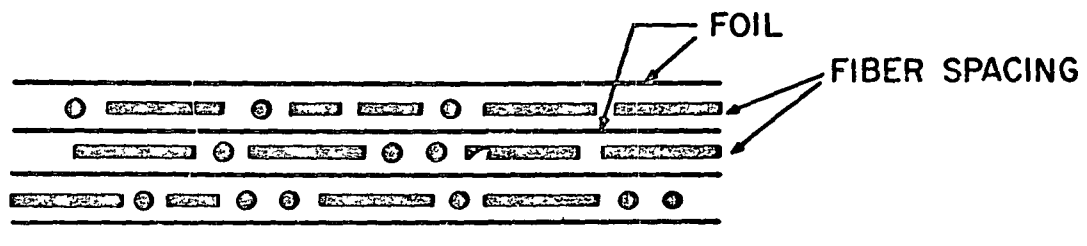


Figure 30. (b) Multiple radiation shield construction - fiber spacer.

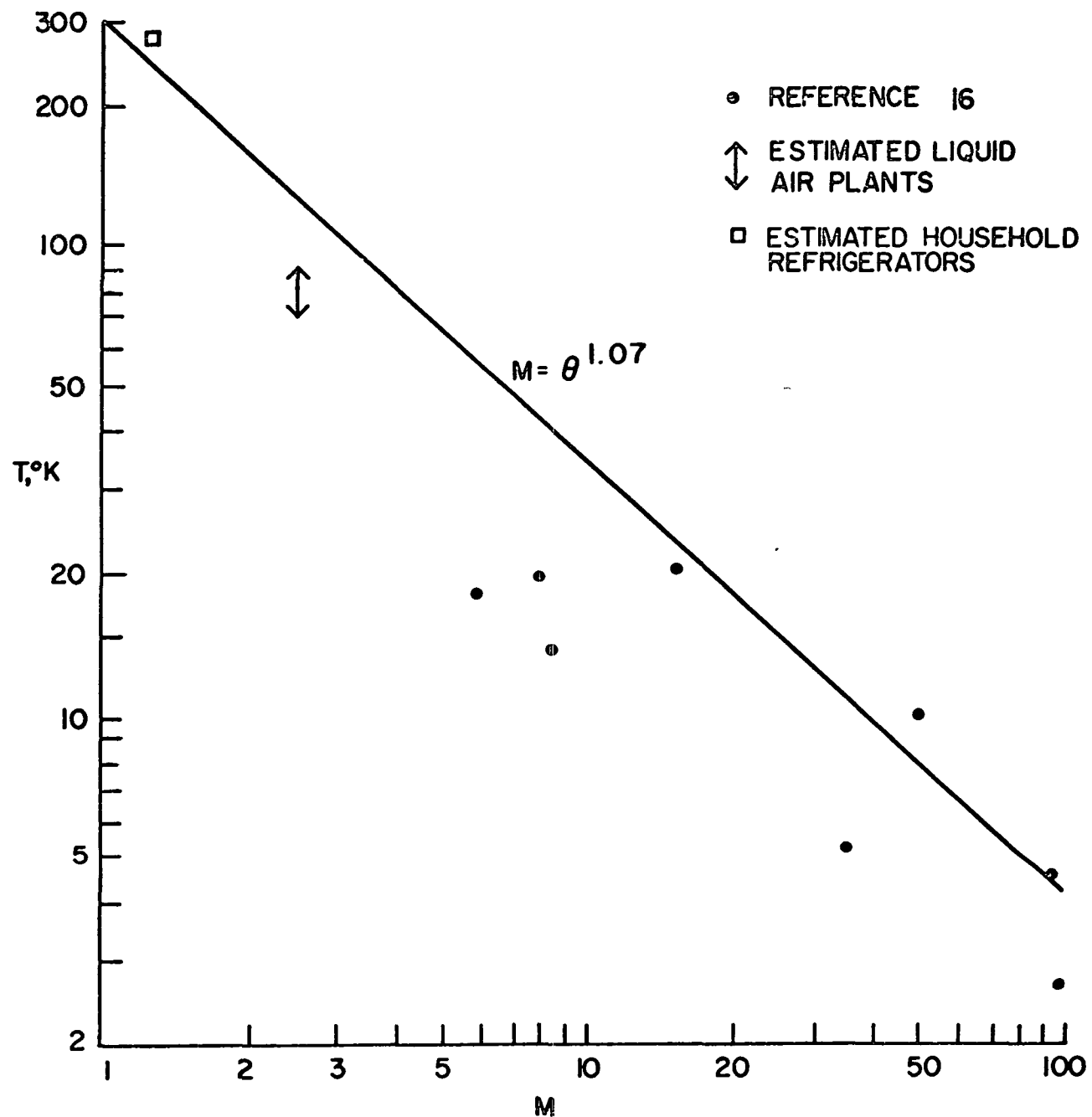


Figure 31. Mechanical refrigerator efficiency as a function of temperature.

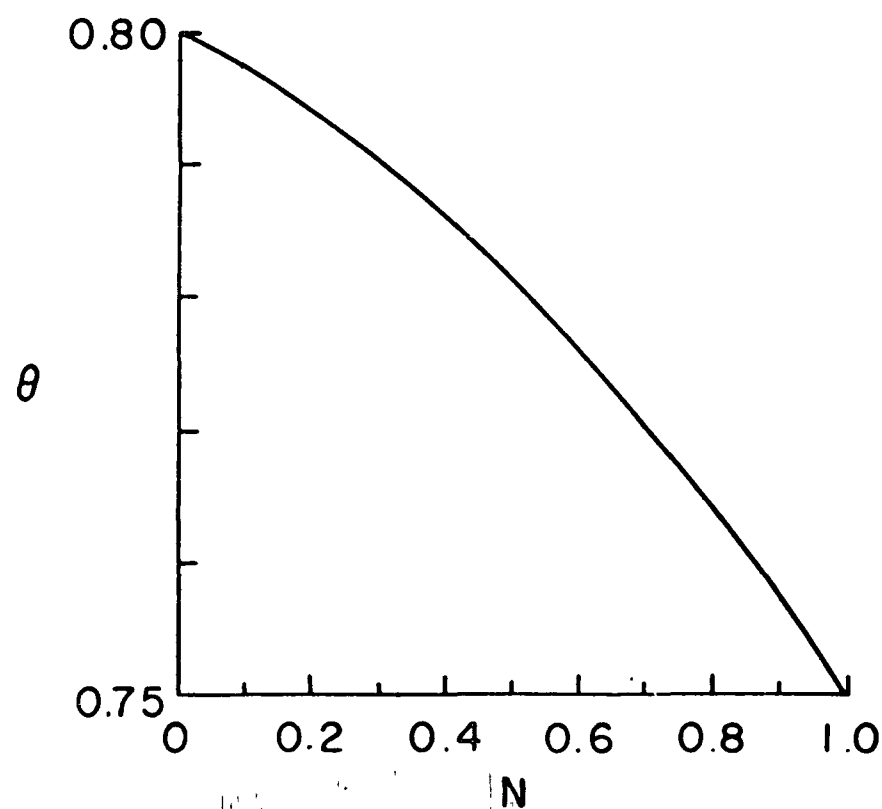


Figure 32. Temperature ratio for minimum area radiator as a function of the mechanical efficiency of the power converter.

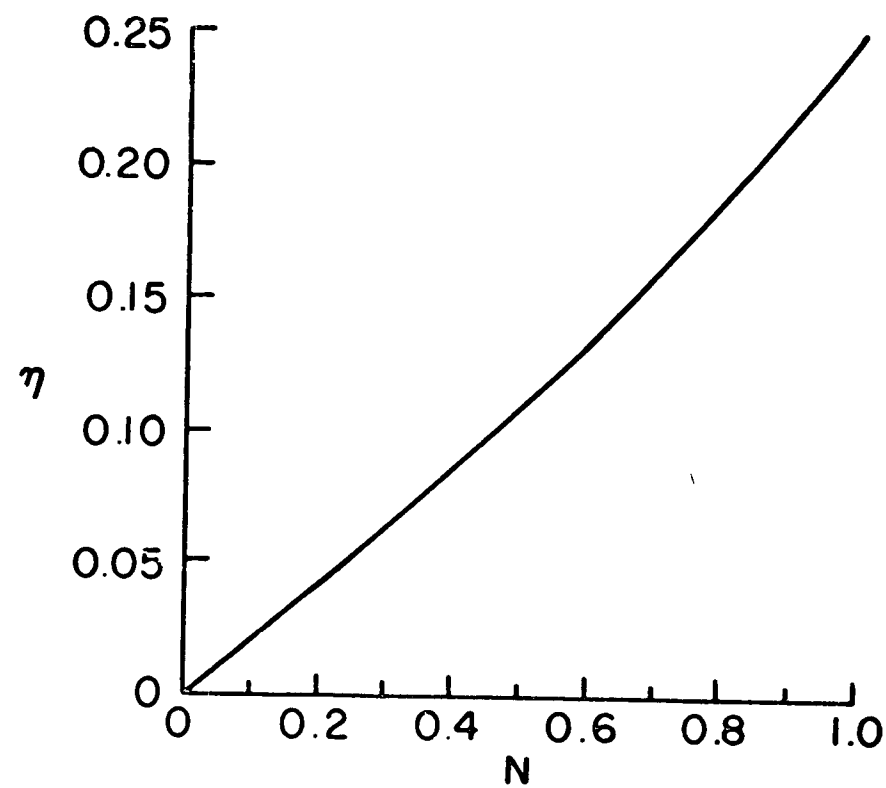


Figure 33. Thermodynamic efficiency of a power cycle for minimum radiator size as a function of mechanical efficiency.

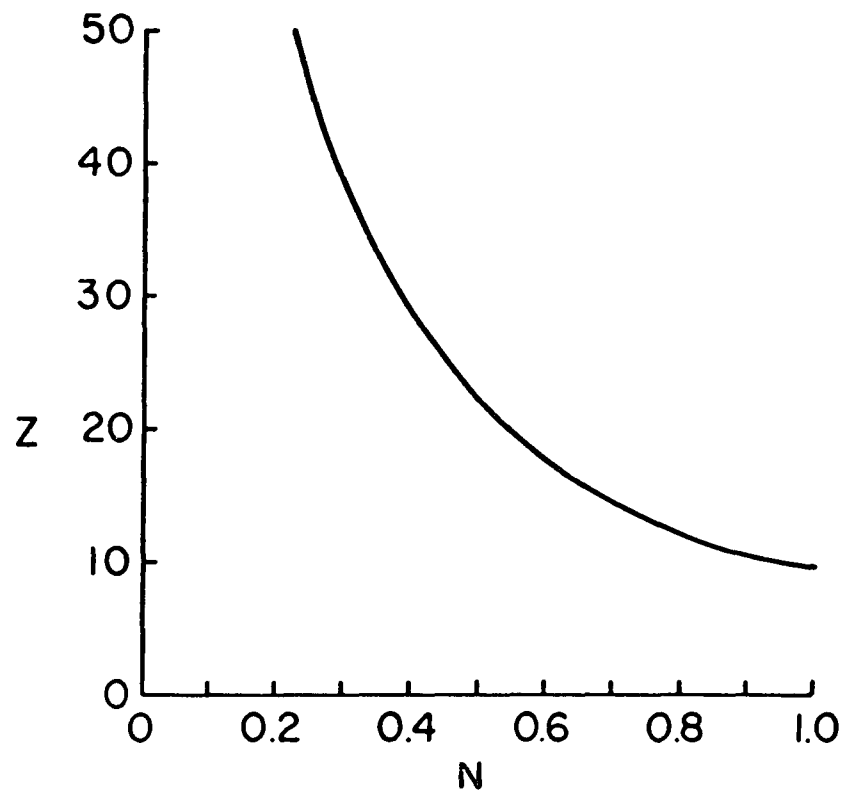


Figure 34. Radiator size parameter,  $Z = T_{\max}^4 \left( \frac{A}{P} \right)$ , for minimum radiator size as a function of mechanical efficiency  $N$ .

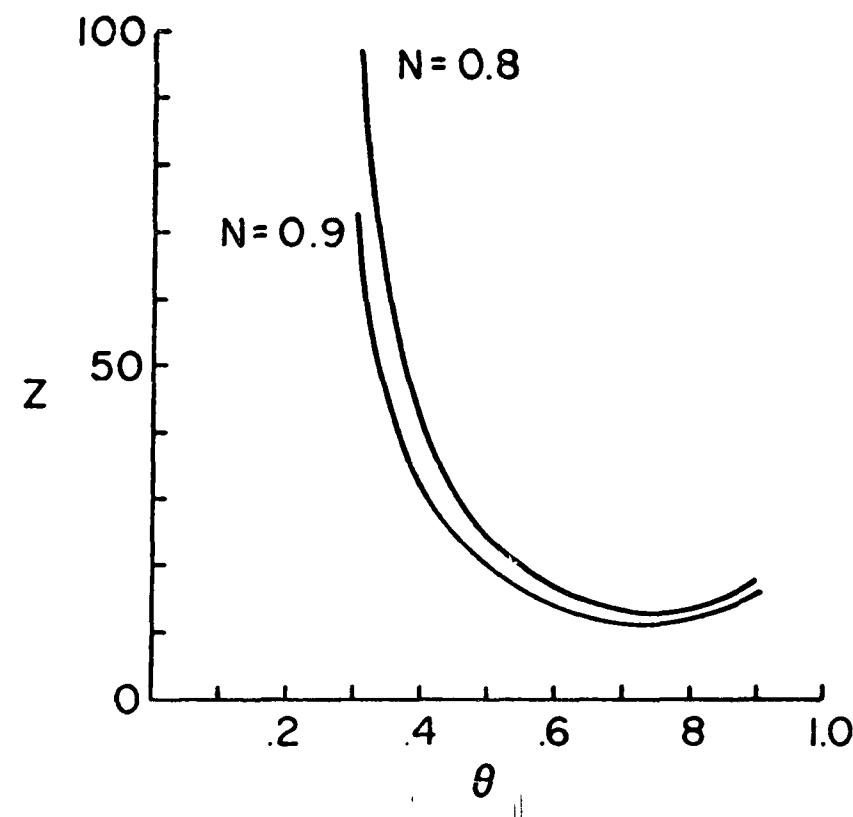


Figure 35. Radiator size as a function of  $\theta$  for two values of the mechanical efficiency.

SPACE SCIENCES LABORATORY  
MISSILE AND SPACE VEHICLE DEPARTMENT

## TECHNICAL INFORMATION SERIES

AUTHOR Freedman, S.	SUBJECT CLASSIFICATION MHD	NO. R62SD83
		DATE September, 1962
TITLE Thermodynamic Considerations for MHD Space Power Systems		
ABSTRACT Thermodynamic efficiencies and radiator sizes of Brayton Cycle MHD generator systems with and without regenerators, were obtained. A new gas cycle, the Tri-Cycle, was synthesized. The Tri-Cycle has a radiator size as small as the regenerative Brayton Cycle, but a higher pressure ratio. A new cycle was discovered which operates on a dissociating chemical reaction and combines		
G. E. CLASS I	REPRODUCIBLE COPY FILED AT G. E. TECHNICAL INFORMATION CENTER 3198 CHESTNUT STREET PHILADELPHIA, PENNA.	NO. PAGES 90
GOV. CLASS Unclassified		
Abstract (continued)		
the advantages of a dry gas expansion, a liquid compression, and a Rankine Cycle size radiator.		
Entropy generation in supersonic MHD generators was analyzed, the polytropic efficiency was related to the generator operating parameters.		
Transient boil-off and active refrigeration techniques were examined. Multiple radiation shield insulation thicknesses were computed. An optimum temperature ratio for heat rejection from an active refrigeration system was found.		

By cutting out this rectangle and folding on the center line, the above information can be fitted into a standard card file.

AUTHOR Steven I. Freedman / Steven I. Freedman  
 COUNTERSIGNED G. W. Sutton G. W. Sutton and Joseph Farber Joseph Farber,  
 Manager, MHD Power Generation Manager, Aerophysics Operation  
 DIVISION Space Sciences Laboratory, General Electric Missile & Space Division,  
Valley Forge, Pennsylvania

LOCATION \_\_\_\_\_